MECHANISMS OF THE STABLE AND VULNERABLE ARTERIAL PLAQUES AND THEIR ASSOCIATIONS WITH THE ARTERIAL WAVEFORMS

M A A ABDULSALAM

2021

MECHANISMS OF THE STABLE AND VULNERABLE ARTERIAL PLAQUES AND THEIR ASSOCIATIONS WITH THE ARTERIAL WAVEFORMS

MOHAMED ABDULSALAM A ABDULSALAM

A THESIS SUMBITTED IN PARTTIAL FULFILMENT OF THE REQUIREMENTS OF THE MANCHESTER METROPOLITAN UNIVERSITY FOR DEGREE OF DOCTOR OF PHILOSOPHY

DEPARMENT OF ENGINEERING

FACULTY OF SCIENCE AND ENGINEEERING

MANCHESTER METROPOLITAN UNIVERSITY

2021

ABSTRACT

Carotid plaque composition is a key factor of plaque stability and it carries a significant prognostic information. The carotid unstable plaques are characterized by thin fibrous cap ≤65μm with large lipid core (LC) while stable plaques have thicker fibrous cap and less LC. Identifying the percentage of plaque compositions is the clinical significant to predict the risk of cardiovascular events. This thesis aims to develop a non-invasive approach to distinguish stable and unstable plaques by defining the relationship between plaque composition and arterial waveform.

An in vitro arterial system, composed with Harvard pulsatile flow pump and artificial circulation system, was used to investigate the effect of the plaque compositions on the pulsatile arterial waveforms. Artificial plaques, characterised as human carotid arterial plaques, were fabricated and implemented into the artificial blood vessels, representing the diseased artery. The pulsatile pressure, velocity and arterial wall movement were measured simultaneously at the site proximal to the plaque. Non-invasive wave intensity analysis (Non-WIA) was used to separate the waves into forward and backward components. The correlation between the plaque compositions and the forward and backward waveforms were quantitatively analysed.

Five types of arterial plaques, composed of the LC, FC, Collagen (Col) and Calcium (Ca) with the percentage of compositions precisely same as the human carotid arterial plaques, were fabricated. The five typical artificial arterial plaques, classified by American Physiology Society, were implemented into the artificial carotid artery to represent the early stage of the diseased arterial system with 30% of blockage. Finally, two stable plaques (FC, FA), one unstable (PR) and one vulnerable plaque (TCFA) were tested with 75% blockage to investigate the effect of severe stenosis on arterial waveform and whether it is possible to characterise the vulnerable plaque or not at this stage.

The experimental results for early stage of stenosis and from the advanced stage of diseased artery observed a significant backward wave intensity associated with stable plaques, whereas no considerable backward wave intensity was detected in unstable plaques. The strong correlation between the compositions of the plaques with the backward waveforms observed in this study demonstrated that the components of the arterial plaques could be distinguished by the arterial waveforms. Moreover, the difference between vulnerable and stable plaques can be detected by the backward wave intensity. This could open a door to identify the plaque

vulnerability. These findings might lead to a potential novel non-invasive clinical tool to determine the compositions of the plaque and distinguish the stable and vulnerable arterial plaques at early and later stages.

Declaration

I Mohamed Abdulsalam A Abdulsalam hereby declare that the work referred to in this thesis submitted by me, under the guidance of Dr. Jiling Feng is my original work and has not been submitted to any other University or Institute or published earlier.

By:

Mohamed Abdulsalam A Abdulsalam

2021

ACKNOWLEDGEMENTS

Firstly, I would like to express my sincere gratitude to my Supervisor **Dr. Jiling Feng** for the continuous support of my Ph.D study and related research, for her patience, motivation, and immense knowledge. Her guidance helped me in all the time of research and writing of this thesis. I could not have imagined having a better Direct of Study (DoS) and mentor for my Ph.D study.

Besides my DoS, I would like to thank the rest of my thesis committee: Prof. Alhussien Albarbar and Dr. Fathalla Elnagi for their insightful comments and encouragement, but also for the hard question, which incanted me to widen my research from various perspectives.

My sincere thanks also goes to Mr Mike Green and Mr Toney Dickenson who gave access to the laboratory and research facilities. By their precious support, they provided me a good environment to conduct this research.

My wife, Hanan Idris, for consistently being there for support, but most of all she has been creating me a great environment during my PhD journey. This support has enabled me to develop the skills I possess today, I owe it all to her.

My close friend Dr Mohamed Naser for his support during our friend hood. He always supported me when I feel disappointed during my PhD. He is not only my best friend, but also he is my brother. I really appreciate your support.

The postgraduate students with whom I shared an office, for both helping me with my questions and problems, as well as providing me with an enjoyable and pleasant environment to work in.

Last but not the least, I would like to thank my family: my parents and to my brothers and sister for supporting me spiritually throughout writing this thesis and my life in general.

I dedicate this thesis to my wife
for her support and encouragement throughout my journey

Table of content

List of Figures

List of tables

List of abbreviations

Symbols	Meaning
LC	Lipid Core
Ca	Calcium
Col	Collagen
FA	Fibroatheroma plaque
FC	Fibro-calcified plaque
PE	Plaque erosion
PR	Plaque rupture
CN	Calcified nodule plaque
TCFA	Thin Cap Fibroatheroma plaque
CVDs	Cardiovascular Diseases
LDL	Low-density lipoprotein
ox-LDL	Oxidised low-density lipoprotein
ROS	Reactive oxygen species
SMCs	Smooth Muscle Cells
AHA	American Heart Association
IPH	Intraplaque haemorrhage
CMR	Cardiovascular Magnetic Resonance
MRI	Magnetic Resonance Imaging
CT	Computerized Tomography
IVUS	Intravascular ultra- sound
OCT	Optical coherence tomography
US	Ultrasound
MRA	MR angiographic

ID	Inside diameter
OD	Outside diameter
RPM	Revolution Per Minutes
WIA	Wave intensity analysis
Non-WIA	Non-invasive Wave Intensity Analysis
+	Forward wave
-	Backward wave
d*P*	Measured change in pressure
d*U*	Measured change in velocity
WI	Wave intensity
d*D*	Measured change in diameter
c	Local wave speed
$R_{\mp}$	Riemann variable
PU-loop	Pressure and Velocity loop
QA-loop	Flow rate and cross-sectional area loop
Ln*DU*-loop	Logarithm of Diameter and Velocity loop
D^2P-loop	Diameter and Pressure loop
BCPW	Backward Compression Plaque Wave,

CHAPTER 1
Introduction

1.1 Literature Review

Cardiovascular diseases (CVDs) such as strokes and heart attacks are the major cause of deaths and disabilities in Europe, and place a substantial burden on the health care systems and economies (Liu *et al.*, 2020). CVDs which are caused by disorders of the heart and arteries, such as the coronary and carotid arteries, leading to myocardial infarction or stroke, are now responsible for 30% of the total deaths in the world (Gaziano *et al*, 2010). Strokes are considered the third most common cause of death in developed countries. In the UK, for example, it has been reported that more than 100,000 stroke event occur each year and it is estimated this number will increase by 59% by 2035 (Stroke Association, 2018; Sasu *et al.*, 2016). It has been widely agreed that atherosclerosis in the arteries is the main cause of CVDs.

The atherosclerotic plaque process begins when low-density lipoprotein (LDL) accumulates abnormally within the artery wall at a rate determined by the plasma concentration of LDL and the condition of the endothelium (Brugaletta *et al.*, 2016). Elevated LDL levels are thought to promote atherosclerosis. LDL passes through endothelial cells and enters the intima, where it can undergo oxidation. Oxidised low-density lipoprotein (ox-LDL) is toxic, and this initiates an inflammatory process as shown in Figure 1.1. The damage to the endothelial cells is believed to be from Ox-LDL (Ross, 1999). This can induce so-called P-selectin, which behaves as an adhesion molecule for monocyte chemoattractant protein-1 and macrophages. Monocytes respond the inflammation by migrating from the blood stream into the artery wall where they mount an inflammatory response to become macrophages (Madamanchi *et al.*, 2005). They engulf the cholesterol-rich ox-LDL and become foam cells. When the foam cells die, they release their lipid content, which creates what is known as a lipid core (LC) below the fibrous

cap (Naim *et al.*, 2014). The fibrous cap represents an attempt by the body to heal the lesion, (Figure 1.1). Continued plaque growth caused by the accumulation of LDL within the intima causes the external elastic membrane to expand. This compensatory enlargement, known as arterial remodelling, allows the vessel to maintain adequate. However, as the plaque increases, the artery can no longer compensate by expanding outward and, consequently, plaque begins to protrude into the lumen. This generally occurs when plaque involvement reaches about 40% of the vessel circumference, which may be caused by biomechanical and haemodynamic stress, and disruption of the plaque can occur (Moll, 2008).

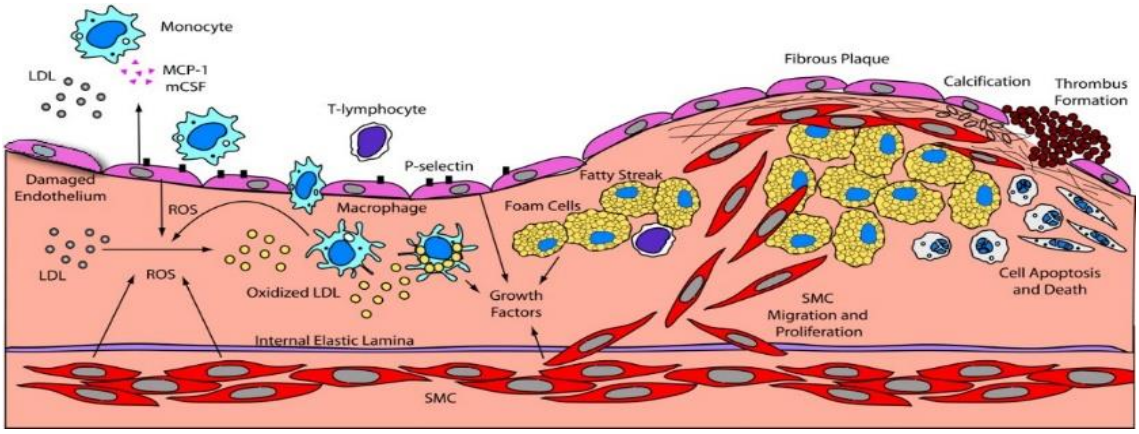

Figure 1.1 - The formation of atherosclerosis. Reactive oxygen species (ROS), generated by endothelial cells, Smooth Muscle Cells (SMCs), and macrophages oxidize the Low-density lipoprotein (LDL) in the subendothelial area in the endothelial damage positions, starting to accumulate the plaque formation. The consequences of plaque rupture, which is due to the collapse of fibrous cap, is the thrombus event and blood vessel occlusion. (Madamanchi et al., 2005)

1.1.1. Plaque Composition

Atherosclerotic plaque consists of various components, whose percentages can differ from one type of plaque to another. Most patients who have suffered a stroke event usually find that their plaques contain a lipid pool, necrotic core and/or haemorrhage. The percentage of calcium in the plaque could play a significant role in plaque stability (Tuenter *et al.*, 2016). The LC proportion is another indicator of plaque stability; the higher the LC percentage in plaque, the more likely it is to be unstable with a thin fibrous cap, and vice versa for stable plaque (Feng

et al., 2015; Meletta *et al.,* 2017). A fibrous cap, lipid-rich necrotic core, collagen and calcium could be the most significant components in arterial plaque.

1.1.1.1. Fibrous Cap

A fibrous cap is one of the most important factors of plaque stability. It consists largely of collagen and elastin, and forms over the LC (Finn *et al.,* 2010). The fibrous cap is located between the artery lumen and necrotic core and is shaped by the smooth muscle cells (SMCs) that transfer from the media to the intimal area generating cellular matrix proteins, (Figure 1.1) (Joshi *et al.,* 2012). The formation of fibrous cap starts when there is macrophages under the endothelium and maybe small pool of cholesterol are starting to accumulate, the macrophages which become foam cells pushing out its self through vascular endothelium to the lumen passing as blood cells(Anlamlert et al., 2017). Platelets will recognize the foam cells and start to get some aggregation, which will cause to release the platelets growth factor (Andrae, Gallini et al., 2008). Also, the macrophages themselves release cytokines, it is chemical messengers that go from one cell to another which signal the immune system to do its job (Fatkhullina et al., 2016). The cytokines and platelets growth factor affect the SMCs in the tunica media, which stimulate mitosis in the SMCs and the migration of SMCs over the plaque (Silverman-Gavrila et al., 2013). These SMCs will change to a different phenotype and they become different type of tissue to become non-stretchy and non-contractile forming a cap between the plaque and blood stream (Holdt and Teupser, 2013). These SMCs develop collagen cross the bridges that bind the SMCs with altered phenotype together and form the fibrous cap. The stable plaque contains plenty of SMCs with good number of collagen cross-linking stabilizing the roof of the plaque (Gomez and Owens, 2012). In the inflammatory processes, there will be inflammatory cells such as white blood cells. As the white blood cells are phagocytic, they ingest foreign material. In this stage, they will release the collagenase, enzymes, to digest the collagen. If there is a lot of inflammatory cells in the area of the plaque, the inflammatory processes is

going on, then some of the enzymes are going to be released and some of these enzymes are collagenases and proteases enzymes that will digits protein. These will dissolve the cross-linkages collagen and they also digest the SMCs. These enzymes are destroying the normal protective fibrous cap which reduce the stability of the plaque (Libby, 2013). Finally, fibrous cap is considered one of the most important factors in identifying plaque vulnerability. If the fibrous cap is thick, the plaque is more likely to be stable and vice versa. Plaque with a fibrous cap that is less than $65\mu m$ thick and has plenty of lipid core is considered unstable plaque (Joshi *et al.*, 2012; Camici *et al.*, 2012; van der Wal, 1999).

1.1.1.2. Lipid Core (LC)

Lipid core is another factor for identifying plaque vulnerability. The formation of LC begins when endothelial cells of the arterial wall become damage. This is caused by hypertension, smoking, high blood glucose and hypercholesterolemia, which increase the number of LDLs in the blood. When the endothelial cell damage, it increases the permeability of the arterial wall allowing the LDLs to enter the tunica intima then the monocytes normally move freely through the blood vessels and do not attach to the endothelial cells as a stream passed. However, when the endothelial cells are exposed to irritating stimuli or damage, they will express adhesion molecules that can capture nearby white blood cells. These white blood cells undergo morphological changes that allow them to flatten and squeezed between endothelial cells. This movement of white blood cells out of the bloodstream is called Diapedesis. White blood cells are capable of producing free radicals and when free radicals come in contact with LDLs, oxidation occurs oxidized LDL particles are especially effective at attracting and activating white blood cells. This white blood cells engulf the modified the LDL particles which stimulates them to produce even more oxygen free radicals. It becomes easy to imagine that an area of endothelial damage will lead to an accumulation of modified LDL particles and migrating. Macrophages in the tunica intima start to engulf modified LDL particles, ultimately

this leads to the production of a cell called a foam cell (Naim *et al.,* 2014). A foam cell is saturated with LDL particles and the excessive amount of lipid in the foam cell gives the cytoplasm of foamy appearance. Foam cell eventually die and release their contents which are then quickly engulfed by other nearby white blood cells. Finally, the accumulating lipid from the process just described and fragments of dead cells produce an area with the lipid core that begins to form a plaque (Figure 1.1).

Several studies indicate that the characteristics of plaque vulnerability include: thin layer of fibrous cap; infiltrating of macrophages and large amount of lipid core (Arroyo and Lee, 1999). In addition, the size of the LC is crucial for plaque stability, when the LC occupies more than 40 % of plaque volume and its fibrous cap less than 65µm thick, it is more likely to rupture and may be classified as vulnerable (Martinet, Schrijvers, & Meyer, 2011).

Vulnerable plaques such as thin cap fibroatheroma (TCFA) is known by large of LC area and its fibrous cap is less than 65µm with considerable amount of macrophages(Finn et al., 2010). This characteristics, particularly large LC and thin fibrous cap, indicate that the plaque is prone to rupture(Otsuka et al., 2016). The proportion of lipid core in the plaque is one of the most important key features to detect the degree of plaque vulnerability(Martinet et al., 2011). This has promoted several researchers to study the effect of LC on the plaque. Lindsay *et al.,* (2014) and Sun *et al.,* (2017) invesitgate the high risk of plaque caused by LC in the coratid artery by using a 3 Tesla Cardiovascular Magnetic Resonance (CMR) and multi-contrast carotid magnetic resonance imaging, respectively. Although these two studies contribute positively the risk of the plaque by identifying the feature of LC and detect the plaque vulnerability, the LC in the small arteries has not been detected yet. Another study attempted to distinguish between stable and vulnerable plaque based on the amount of LC using magnetic resonance imaging (MRI) and an ultrasound radiofrequency technique. This study succeeded to distinguish

between stable and vulnerable plaques by detecting the percentage of LC on the plaque, although fibrous cap, which is another main factor of plaque vulnerability, was not conducted. Therefore, detecting the amount of LC on the plaque is a vital factor for identifying the vulnerable of the plaque, which need an urgent non-invasive technique to reduce the risk of plaque rupture.

1.1.1.3. Calcium (Ca)

Ca is formed in plaque as part of atherosclerosis development due to chronic inflammation in the wall of the artery (Martinet et al., 2011). The accumulation of calcium could be form in any blood vessel type even in microvessels. Calcium can be found in the lumen in such a calcified plaque cap and it might enter the intima or media, which is prevalent in chronic kidney disease or type II diabetes (Ibrahimi et al., 2013). There is no clear differences between the calcification in intima and media as both of them generate inflammatory markers and cytokines (Saremi et al., 2009; Moe and Chen, 2005). Yet, osteogenic discrimination of metaplastic bone deposition has been rarely found in intimal calcification, while it has been oftentimes seen in medial calcification (Doherty et al., 2003). Imaging techniques such as non- invasive computerized tomography (CT), magnetic resonance imaging (MRI), intravascular ultra- sound (IVUS) and optical coherence tomography (OCT) can assess the plaque calcification, although the degree of plaque calcification cannot be detected accurately even if the standard B-mode US scan is used(Denzel et al., 2004). The stiffness in the blood vessel and the high pulse pressure are caused by the calcification in the media, whilst spotty calcifications in the intima are believed that one of the factors to destabilize the plaques (Nicoll and Henein, 2013; Ibrahimi et al., 2013). Presently, CT imaging cannot differentiate calcification between intimal and medial (Van Der Giessen et al., 2011). However, the invasive means such as OCT can distinguish between them (Cassar et al., 2013). Its percentage presence in the plaque could play an

important role in plaque stability, though there is no discernible relationship, so far, with the LC (Lafont, 2003).

1.1.2. Plaque Types

Several studies have found a link between the lesion category and threat of cardiovascular events. Particularly, plaque type 6, categorised by American Heart Association (AHA), as a large LC with a thin fibrous cap, thrombus development and intraplaque haemorrhage, which is highly related to myocardial infarctions or strokes (Table 1.1). Types 1, 2 and 3 are considered as stable plaques, whereas the degree of instability of the plaques increases from type 4 to 6. In addition, vulnerable plaques such as: the Rupture-prone, Ruptured, Erosion-prone, Eroded, Intraplaque haemorrhage (IPH), and Calcific and Chronically stenotic plaques are more likely to rupture than stable ones (Bentzon *et al.*, 2014; De Weert *et al.*, 2006; Sasu *et al.*, 2016). Distinguishing between stable and unstable plaque is important for vascular surgeons to avoid any sudden rupture of the plaque and a stroke event.

1.1.2.1. Stable vs. Unstable Plaques

A stable plaque is characterised as a thick fibrous cap with a small fatty core. Stable plaques are rich in collagen which makes the plaque more stable and the fibrous cap less likely to rupture (van der Wal, 1999; Virmani *et al.*, 2000). Unstable plaques are characterised as having a thin fibrous cap and containing a large quantity of LC (Figure 1.2). They grow in the presence of high levels of LDL in the blood, which increase the production of plaque. The fatty core increases and the fibrous cap starts to erode, while macrophages release enzymes which collapse the collagen in the fibrous cap (van der Wal, 1999).

The stable, unstable and vulnerable carotid plaques have recently been classified by several researches such as Butcovan *et al.* (2016) who investigated plaque composition to characterize plaques and identify plaque vulnerability. They categorised the carotid plaque into three types:

(i) stable plaques: fibroatheroma (FA) and fibro-calcified plaque (FC),

(ii) unstable plaques: plaque rupture (PR), plaque erosion (PE) and calcified nodule (CN), and

(iii) vulnerable plaques: thin-cap fibroatheroma (TCFA).

If the vulnerable plaque ruptures in the carotid artery, it will either block the flow of oxygenated blood to the brain or bleed, which will cause the brain cells to die (Li *et al.*, 2018). In this study, the three types of artificial plaques with the same features characterised by Butcovan *et al.*, (2016) were fabricated to investigate the correlation between the types/compositions of the plaques and arterial waveforms.

Table 1.1 - The classification of plaque according to the American Heart Association (Moridani, 2012)

Plaque type	**Description**
Type 1	Normal wall thickness (intima-media ratio up to 1) or minimal intimal thickening, some macrophages with few lipid deposits or foam cells.
Type 2	Type 1 lesion with additional smooth muscle cells with few lipid deposits (fatty streaks), T-lymphocytes, and and rare mast cells within or without the intimal thickness.
Type 3	Preatheroma: as type 2, with increased extracellular lipid deposits
Type 4	Atheroma: increase of intimal plaque with massive confluent lipid deposits (lipid core) covered mainly by the intima.
Type 5	As type 4, with increasing lipid deposits and a well-defined fibrous cap or with predominant calcifications.
Type 6	Complicated lesion: type 6 or 5 lesions in which disruptions of the lesion surface, haematoma or haemorrhage, and thrombotic deposits have developed.

The composition of plaque includes LC, calcium (Ca), collagen (Col) and intraplaque haemorrhage (IHP), as well as the fibrous cap. The plaque composition varies from one plaque type to another such as FA plaque has 57% LC, 0% Ca and 53% Col, while PE plaque has 71% LC, 18% Ca and 12% Col (Butcovan *et al.*, 2016).

Vulnerable plaques are indicated by a fibrous cap < 65µm and LC > 40 % of plaque volume. Stable plaques have a thick fibrous cap and contain a small amount of LC. In this regard, the plaque composition plays an important role in distinguishing between stable and vulnerable plaques. This needs urgent attention to develop techniques to detect vulnerable plaque.

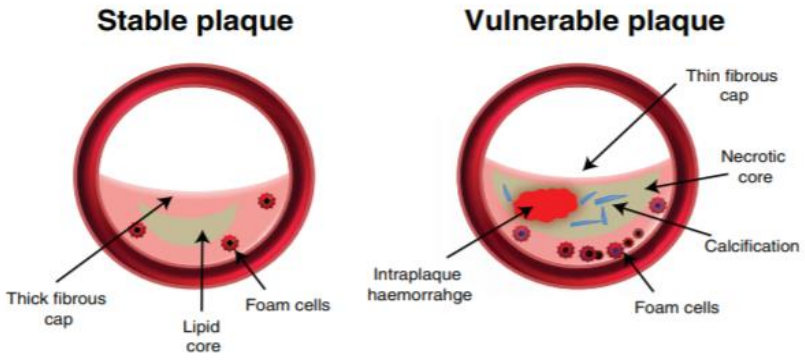

Figure 1.2 - The characteristics of stable and unstable plaques (Cuadrado *et al.,* 2016a). The stable plaque has thick fibrous cap and small amount of lipid core and foam cells, while the vulnerable plaque contains plenty of lipid and foam cells with haemorrhage abd thin fibrous cap.

1.1.3. Imaging Techniques Background

Advanced imaging techniques offer non–invasive means to describe and measure plaque volume, lumen diameter, stenosis, the presence of calcium and the presence of LC. For example, determining plaque composition, and hence its vulnerability, was achieved using ultrasound non-invasive vascular elastography (Naim *et al.,* 2013). Although this technique could identify the size of the LC of the plaque with high sensitivity, it failed to detect the calcium in the artery wall. The calcification was detected by using the Cone Beam Computed Tomography technique with ultrasound (Jashari *et al.,* 2015). It is true that this study identified the volume and the presence of calcification, but it did not detect either the progress of plaque or the LC in the early stages.

The high risk posed by a LC in the carotid plaque was investigated using a 3 Tesla Cardiovascular Magnetic Resonance (CMR) system to evaluate the components of frequently

occurring carotid artery disease and detect whether these changed after the first atherosclerotic plaque occurred (Lindsay *et al.*, 2014). This technique succeeded in detecting high risk LC, but could not evaluate small arteries such as the ones that extend around the brain (Klem *et al.*, 2006). The high risk features of LC were also investigated by Sun *et al.*, (2017) using multi-contrast carotid magnetic resonance imaging. This study presented novel indicators for plaque vulnerability in systemic atherothrombotic, but the patients were subjected to an intensive medical treatment before imaging, which may have reduced the accuracy of the results. Huang *et al.*, (2017) used magnetic resonance imaging (MRI) and an ultrasound radiofrequency technique to non-invasively differentiate between stable and vulnerable plaques. Their study provided important information for non-invasively discriminating between stable and vulnerable plaques based on a large LC and the presence or absence of IPH. However, this study did not take into consideration either the thickness of the fibrous cap nor calcification despite their being important factors for plaque stability.

An advantage of using MRI is that it allows the association between carotid plaque composition and carotid artery disease in patients to be determined (Hamada *et al.*, 2018). However, this study did not indicate the composition, proportion, or types of plaque. The MRI was utilized to evaluate the carotid plaque vulnerability using T1 and T2-weighted MRI techniques (Shimada *et al.*, 2018). This study may be an important indicator for plaque vulnerability, but its major limitation was that the pathological results of the plaques were not investigated in detail.

Majmudar *et al.*, (2013)studied the macrophages by using Polymeric Nanoparticle PET/MRI to detect atherosclerotic plaques. This study proved that this technique can be used as a non-invasive method to assess inflammation plaques and can play an important role in therapy. However, one of the limitations of the technique is that the data is not acquired simultaneously,

which may lead to generating erroneous results (Cuadrado *et al.*, 2016). Zhang *et al.*, (2019) applied Non-contrast Angiography to identify carotid plaque compositions and develop a machine learning algorithm to detect plaque composition. This study provided a tool for carotid plaque composition assessment but did not provide any information concerning discrimination between stable and vulnerable plaques.

Li *et al.*, (2018) applied a pulse wave imaging technique to investigate the effects of arterial narrowing on the properties of plaque when the degree of narrowing ranged from 50 percent to 80 percent. Even though this study opened the door to the possibility of distinguishing between stable and unstable plaques by determining the plaque composition, the results were insufficiently accurate because of complex waveforms (Li *et al.*, 2018). A recent study has used MRI to find the relationship between the risk of stroke and diseased blood vessels with or without IPH (Schindler *et al.*, 2020). This study indicated that identifying the proportion of IPH helps to detect the risk of a future stroke irrespective of the degree of blockage. The severity of carotid stenosis was investigated by Macharzina *et al.*, (2020) and Moradi *et al.*, (2020) using ultrasonographic colour-Doppler images and a contrast multidetector computed tomography technique, respectively. Both studies showed promise as a tool to assess the severity of stenosis of the carotid artery. However, plaque stenosis is not the main indicator of a stroke event because it can occur with a low level of stenosis, less than 30% (Li *et al.*, 2018).

Partovi *et al.*, (2012), Motoyama *et al.*, (2019) and Schinkel *et al.*, (2020) used a contrast-enhanced ultrasound technique to distinguish vulnerable plaques in the carotid artery. These studies aimed to evaluate the plaque vulnerability in order to reduce the risk of plaque rupture and introduced a new approach to detect vulnerable plaque. However, the ability of the contrast-enhanced ultrasound technique to determine the presence of carotid vulnerable plaques was questioned by D'Oria *et al.*, (2018). Although the imaging techniques successfully

measured plaque volume, lumen diameter, stenosis, the presence of calcium and LC, they suffered from limitations in terms of precisely distinguishing plaque composition. Therefore, other techniques which overcome these limitations are urgently needed to detect and identify the different types of plaques and determine the levels of vulnerability.

1.1.4. Wave Intensity Analysis Technique Background

Wave intensity analysis (WIA) is based on the method of characteristics that derives from the conservation of mass and momentum of flow in an elastic medium. In 1860, Riemann (a German mathematician) improved the method of characteristics to develop the hyperbolic partial differential equation. Riemann's method was used by Anliker *et al.,* (1971) to demonstrate the propagation of waves in an arterial system. Then Parker and Jones (1990) developed Riemann's analysis and introduced WIA, a method based on the time domain to analyse the behaviour of pressure and velocity waves in elastic tubes (Khir and Parker, 2002). The principal of this technique is to measure the pressure (invasive) and velocity simultaneously at particular points, in order to obtain the accumulated pressure and velocity. WIA separates the accumulated pressure and velocity into forward (+) and backward (-) waveforms, in order to provide information in relation to the elastic containing vessels based on the waveforms. The forward waves are mainly caused by the heart's contraction, while the backward waves are generated by reflections in the arterial system. The product of the difference in the measured pressure (dP) and difference in the measured velocity (dU) is called the net wave intensity (dP.dU). It is denoted by WI and its unit is energy flux per unit area.

Feng (2010) developed the WIA using the measured diameter of a blood vessel instead of measured pressure. This technique (non-WIA) allows the measured change in diameter (dD) of the blood vessel and velocity (dU) to separate the diameter, velocity and WI into forward and backward components non-invasively. The net non-WI is the product of the differences in the measured diameter (dD) and velocity (dU), (dD.dU). This technique has been used in

several *in-vivo* studies such as Biglino *et al.,* (2012) to assess the ascending and descending performance of the aorta; Pomella *et al.,* (2017) evaluated the reproducibility of non-WIA in the carotid artery; and Niki *et al.,* (2017) have explained the relationship between the increase in arterial stiffness with left ventricular performance. Both approaches require the local wave speed (c) in the arterial system, which is challenging in medical studies because the values change along arterial system (Parker, 2009).

1.1.4.1. Determination of Wave Speed

Although the determination of local wave speed (c) is important in the clinical field, it is notoriously difficult to determine because its value differs along the arterial system (Parker, 2009). It is widely known that the c can be used to estimate the arterial stuffiness, which can be used to predict and diagnose a stroke and other cardiovascular diseases (Pereira *et al.,* 2001). The first attempt to calculate c in *in-vivo* and in vitro was based on arterial elastic mechanical properties and blood density (Young, 1808; Weber and Weber, 1825; Weber, 1866). After theoretical development and experimental work, an equation for the local value of c was developed for thin-walled tube by Moens (1877) and Korteweg (1878). Young-Weber and Moens-Korteweg described their formula as (Eq. 1-1).

$$c = \sqrt{\frac{Eh}{\rho D}} \tag{1-1}$$

Where h is the arterial wall thickness, D is the arterial local diameter, E is the arterial Young's modulus and ρ is the local blood density.

However, estimating the local c from the elastic properties of the material requires invasive means to measure the properties of the wall, which clinically might be impossible. Another approach aimed to determine c depends on measurements of the time of transition of the wave from one point to another (so-called foot-to-foot). This latter method is the most common in clinical environments, as it does not need invasive measurements, only the measurement of the

pressure waveform at two different locations, where the distance between them is known. Then, the time lag between two waveforms is determined. Using the simple relationship *c* = (distance travelled/time taken), *c* can be estimated. Several studies have demonstrated that determining *c* in this way does not give an exact value because speed of the wave will differ depending on where in the human body the measurements are made (Parker, (2009); Alastruey, (2011)).

In 2001, Khir developed a PU-loop method that allows the localised wave speed to be determined through simultaneous measurements of pressure and velocity at single site. The local wave speed, c, has been found to be inversely related to the square root of the local distensibility (D_s) of the artery, as shown in Eq. (1-2)

$$c^2 = \frac{1}{\rho D_s} \tag{1-2}$$

Based on this relationship, a variety of techniques have been developed to determine the local value of *c* using measurements of pressure, velocity, diameter and area of the artery (Khir *et al., 2001*; Rabben *et al.,* 2004; Davies *et al.,* 2006; Feng and Khir 2010; Alastruey 2011). The simultaneous measurements of arterial wall movement and flow velocity can be obtained non-invasively in a clinical environment by using echo-tracking and Doppler ultrasound, respectively (Pomella *et al.,* 2017a). A summary of these techniques is given below:

1.1.4.1.1. PU-loop

The PU-loop technique, introduced by Khir *et al.,* (2001), can determine the local wave speed based on the simultaneous measurements of pressure and velocity at a single site. This technique assumes that in early systole period there is only a forward-travelling wave. Under this condition and using the water hammer equation (Eq. 1-3), the local *c* can be estimated as in Eq. (1-4). In the absent of reflections, the plot of pressure against velocity (Figure 1-3), should show a linear portion in the early systolic period and its value is equal to ρc.

$$dP = \rho c dU \tag{1-3}$$

$$\rho c = \frac{dP}{dU} \tag{1-4}$$

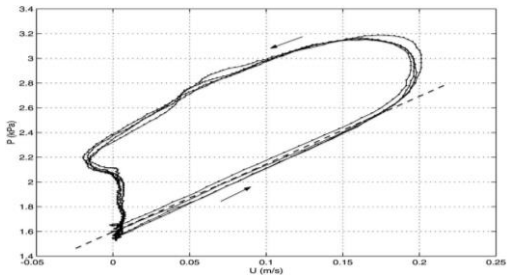

Figure 1.3 - The PU-loop as determined in the pulmonary artery by Khir *et al.*, (2001). (The dashed line represents the linear portion of the curve over the early systole period.)

1.1.4.1.2. QA-loop

QA-loop (Q represents flow rate and A is cross-sectional area of blood vessel) relies on the ratio of the measured cross sectional area of the blood vessel and blood flow rate simultaneously without the need for pressure measurements. Rabben *et al.*, (2004) used ultrasound to collect the measurements of flow and area of the left common carotid artery for young persons under controlled conditions to measure the local *c*, see Equation (1-5). This study found a linear relationship between the change of flow (dQ) and the change of cross sectional area (dA) in the early systolic period (friction-free), see Figure 1.4. The linear part of the curve is equal to the local *c*.

$$c = \frac{dQ}{dA} \tag{1-5}$$

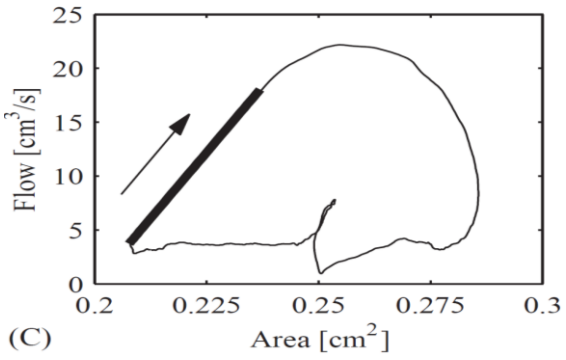

Figure 1.4 -The QA-loop of the left common carotid artery for a healthy young person as obtained by Rabben *et al.*, (2004). The thick line represents the early friction-free, cardiac cycle. The gradient of the linear equal to the local *c*.

1.1.4.1.3. Sum of Squares

This technique was introduced by Davies *et al.*, (2006) to overcome the strong reflections that may occur in the early systole. Using this method, the local value of *c* can be estimated by the simultaneous measurements of pressure and velocity. The local *c* can be determined from the summation of squares of *dP* divided by the summation of the squares of *dU* during one cardiac cycle, see (Eq. 1-6).

$$c = \frac{1}{\rho}\sqrt{\frac{\sum dP^2}{\sum dU^2}} \tag{1-6}$$

1.1.4.1.4. Ln*DU*-loop

Feng and Khir (2010) offered a novel algorithm for estimating the local *c* non-invasively. This technique was based on measuring the simultaneous wall movement (*D*) and flow velocity (*U*) at a particular position of the artery. The technique assumed that no reflected waves are present in the early systolic period. For this period, the relationship between ln*D* and *U* was shown to be linear. The gradient of this linear relationship corresponded to $\frac{1}{2}c$ (Eq. 1-7). Chapter 2 will give more details of this method.

$$c = \pm\frac{1}{2}\frac{dU_{\pm}}{d\ lnD_{\pm}} \tag{1-7}$$

1.1.4.1.5. D^2P-loop

Alastruey (2011) illustrated that the viscoelastic term increases constantly with time during the diastole. This elastic term creates an approximate linear relationship during the diastole between D^2 and P (Figure 1.5), which allows evaluation of the local *c* from the linear portion of the D^2P-loop in the diastolic period (Eq. 1-8).

$$c = D_o\sqrt{\frac{dP}{\rho\ d(D^2)}} \tag{1-8}$$

Where D_o is the mean arterial diameter.

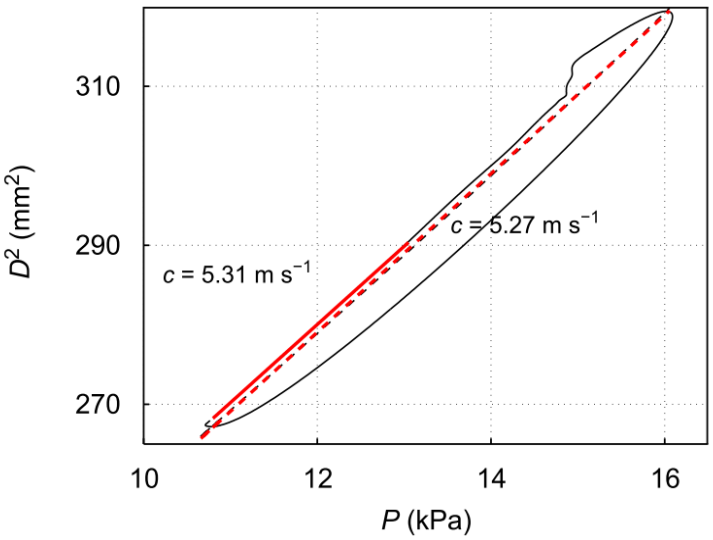

Figure 1.5 -The D^2P-loop from the midpoint of the thoracic aorta obtained by Alastruey (2011). The gradient of the linear portion of the curve is visible during the diastole.

1.1.4.1.6. Discussion of Wave Speed Determinations

The foot-to-foot method is one of the most common techniques for determining *c* in the medical field. The advantage of this method is that it does not require invasive measures but does need two locations in order to determine the value of *c*. Because the wave speed varies along the artery from one location to another, the estimated *c* is an average value for *c* over the distance between the two locations (Borlotti *et al.*, 2014a). As stated above Khir *et al.*, (2001) presented a *PU*-loop technique to estimate the local *c* at a single site instead of two sites using the water hammer equation (Eq. 1-3). Although the obtained value of the local *c* was in agreement with foot-to-foot technique (difference was less than 5%), the measurement of pressure requires invasive means, which is a major challenge. Rabben *et al.*, (2004) (*QA*-loop) and Feng and Khir (2010) (Ln*DU*-loop) found methods for *c* without using pressure.

Rabben *et al.*, (2004) extended the study of (Vulliémoz *et al.*, 2002) and found that the flow velocity is the function of cross sectional area. From this finding, they determined the local *c* as the ratio between the change of flow rate and the change of area, provided there are no reflections in the early systolic period. The value of *c* is the slope of the curve (*QA*-loop) that exist in this period. Feng and Khir (2010) developed an estimation of local *c* from loop

techniques by measuring the diameter and velocity of the carotid artery instead of computing flowrate and area. The local *c* here can be calculated as the ratio between the change of velocity and the change of logarithmic diameter (Eq. 1-7). In the early systole, if there is no reflection (backward wave), the plot will contain a linear portion that corresponds to $\frac{1}{2}c$. Determining the local *c* using the PU-, QA-, and LnDU- techniques depends on a linear portion of the relevant plot occurring during the early systolic period. However, Alastruey (2011) relied on finding a linear relationship between $D^2$and P in the late diastole. The major limitation of this technique is that it was developed using the Voigt- model.

Determination of local *c* in loop techniques relies heavily on the linear portion of plots obtained during the early systolic or late diastolic period when only a forward travelling wave exists. In the coronary case, however, a linear portion cannot exist because the blood flow is subjected to aortic and microcirculation effects (Sun *et al.*, 2000). In addition, the foot-to-foot method cannot be used to measure the local *c* in the coronary artery because its length is too short, though Davies *et al.*, (2006) did derive equation (Eq. 1-6), which can be used to estimate *c* in shorter arteries such as the coronary artery, with no consideration of wave reflection in the early systolic and to minimize the entire of forward and backward of WI in order to decrease the net energies in entire cardiac cycle.

To summarize, loop technique (that relies on the early systolic period) and the sum of squares technique for determining wave speed are directly influenced by positive and negative reflections of the pressure waves. Techniques that rely on pressure and flow velocity can overestimate the wave speed due to positive reflections and underestimate it because of negative reflections. In contrast, when using the diameter or area and flow velocity techniques, wave speed can be overestimated due to negative reflections and underestimated due to positive reflections (Borlotti *et al.*, 2014a). However, it has been observed that the D^2P-loop method is not significantly affected by reflections (Alastruey, 2011). Finally, the Ln*DU*-loop can be

performed on any part of the body and all types of patients and is relatively easy and fast to use and non-invasive, especially with modern methods of acquiring data such as ultrasound-based echo tracking (Borlotti *et al.,* 2014a). Thus, the Ln*DU*-loop is the simplest method to apply in the medical field, as will be explained in detail in Chapter 2.

1.1.4.2. Invasive Wave Intensity Analysis (WIA)

Wave intensity (WI) is a haemodynamic index, which can be used to assess the behaviour of the heart with its arterial system (Sugawara *et al.,* 2009). The invasive WIA technique was developed by Parker and Jones (1990). It is a method that is based on time domain analysis of the pressure and velocity waves in elastic tubes (Khir and Parker, 2002). Its origin and principles are described in Section 1.1.4 above. To date, invasive WIA has been used to analyse arterial waveform propagation in **in vitro** and *in-vivo* studies.

1.1.4.2.1. WIA in in vitro Studies

Khir and Parker (2002) studied the reflected waves generated by bifurcations in elastic tubes, decomposing the complex waveforms of the pressure and velocity into forward and backward components. This study demonstrated that wave reflections in the human arterial system travelling backward to the aortic root can be detected by the backward wave intensity. Using WIA, Feng and Khir, (2005) studied the effect of size and material properties on patterns of wave dissipation in the elastic tubes. This study demonstrated that the size of tube has a strong effect on the degree of wave dissipation, whereas the effect of material properties on the degree of wave dissipation is not significant. Feng and Khir (2007) also compared the propagation pattern of both "suction" and compression waves and found the degree of dissipation of expansion waves is greater than that of compression waves.

WIA was also used in in vitro by Li *et al.,* (2016) to determine the local reflection coefficient in flexible tubes. This study compared experimental results with theoretical values attained

from the mechanical properties of the tubes. This paper stated that the results could potentially be applied to medical cases to assess the health of blood vessel (Li *et al.,* 2016). Hacham and Khir, (2019) investigated the reflections generated by aneurysm and stenosis in in vitro. Their findings indicated that a backward compression wave was generated by a stenosis, while a backward expansion wave was generated by an aneurysm. The magnitude of the reflected waves increased the smaller the stenosis and the larger the aneurysm, while the value of *c* increased within the stenosis and decreased within the aneurysm. The change in the value of c was found to be inversely proportional to the size of the discontinuity, exponentially increasing with smaller stenosis and larger aneurysms, but always higher in the stenosis.

The findings of in vitro studies have motivated many researchers to apply the techniques used to *in-vivo* investigations of the behaviour of the blood vessel and its diseases.

1.1.4.2.2. WIA in *In-Vivo* Studies

WIA has been widely used in *in-vivo* studies. Khir and Parker (2005) studied the effect of arterial stenosis on pressure and velocity waveforms in the ascending aorta of dogs. They found that constrictions at some points in the aorta led to the increase in the magnitude of pressure, velocity, and intensity of backward waves. Another *in-vivo* study using WIA by Lu *et al.*, (2011) examined the strength of waves in the aorta and coronary arteries in four min-pigs to understand the counter-pulsatile of aorta and the complex interaction of proximal and distal effects. This study provided a mechanism to explain the increase of diastolic and the systolic unloading of an intra-aortic balloon pump on the left side of the heart. Alastruey *et al.,* (2013) investigated the effect of peripheral reflection on arterial pulse wave propagation in the arterial systems of rabbits. The waveforms of pressure and velocity were collected and a new application of WIA was used to study the effects of four parameters: the artery compliance and peripheral resistance, peripheral reflections, and cardiac cycle reflections.

Pulmonary hypertension disease was defined using WIA by investigating wave reflections in healthy and unhealthy cases (Quail *et al.,* 2015). This study distinguished the unhealthy state from normality and could be used as a biomarker to detect pulmonary hypertension and discriminate pulmonary hypertension subtypes. The effect of aortic flow and its wave reflection on the left ventricle function has been recently investigated by Park *et al.,* (2020) using WIA. This study shows that increased wave reflection decreased the left ventricle flow velocity in the contraction process, which might be clinically relevant to patients with hypertension and cardiovascular disease, if the reflection waves could be reduced.

Raphael *et al.,* (2016) applied WIA to investigate the mechanisms of hypertrophic cardiomyopathy in patients. Pressure and flow data were collected simultaneously at the nearest location of the left anterior descending artery using cardiac magnetic resonance. The results showed that patients with hypertrophic cardiomyopathy had less reserved flow than the control group, and it was concluded from this result that hypertrophic cardiomyopathy introduced a large backward systole compression wave, while the backward expansion wave was small (Raphael *et al.,* 2016). This work was expanded to investigate the coronary arteries using WIA. CMR was used to collect pressure and velocity measurements from an aortic distension and compared with invasive data obtained for the same patients. The results showed that CMR was acceptable only for selected participants (Raphael *et al.,* 2017), but might not be suitable for elderly patients and those who suffer from high pressure due to low aortic distension.

Lascio *et al.,* (2017) investigated the change of WIA parameters with the age of mice. The findings showed that the forward peaks of the WI signal decreased with advancing age, while the decrease of the backward WI signal could be due to the reduction of wave energy transferred from the heart to the arterial tree. Niki et al., (2017) using WI parameters compared 98 non-ischemic chronic patients before and after surgery, with 98 healthy participants, to clarify how the growth of arterial stiffness effected heart performance. Tamaru *et al.,* (2021)

recently investigated the mechanism of pressure drop in the left anterior descending and right coronary arteries using WIA based on the data measured using echocardiography. Twelve patients with stable chest pain were the subjects in this study. WIA showed that there is a gradual decrease in the dominant pushing and suction wave intensities proportional to the drop in pressure along the length of the controlled left anterior descending artery but not the right coronary artery. This result may help evaluate stenosis of the coronary artery (Tamaru *et al.*, 2021). Although the WIA has introduced several benefits as a diagnostic tool in the medical field, measuring pressure invasively remains the main drawback of this technique.

1.1.4.3. Non-invasive Wave Intensity Analysis Technique (Non-WIA)

Some 20 years after the introduction of WIA, Feng and Khir (2010) extended the technique by introducing a novel non-invasive algorithm that did not use pressure, to estimate *c*. Instead, by separating the measured waves into its forward and backward components using diameter and velocity, *c* could be determined non-invasively by plotting diameter against velocity (ln*DU*-loop) as has been explained in Section 1.1.4.1.4. The value of *c* and the shape of the ln*DU*-loop were very similar to the PU-loop (Feng and Khir, 2010). The non-WIA technique opened the door to many *in-vivo* and in vitro studies to investigate the behaviour of arterial systems non-invasively.

One *in-vivo* study conducted by Biglino *et al.*, (2012) studied the feasibility of implementing non-WIA in 15 healthy adults and 15 elderly patients who had coronary artery disease, in order to compare the ascending and descending aorta of healthy participants with those of the patients with a diseased coronary artery. Borlotti *et al.,* (2014) aimed to compare various techniques for estimating *c* in in vitro experiments and examining the precision when reflections were present. This study concluded that most techniques were affected by reflection, and that the non-WIA methods were the easiest to apply in clinical fields. Pomella *et al.*, (2017) used ultrasound for

WIA to determine the velocity and diameter of the common carotid artery of twelve young healthy volunteers under two conditions, at rest and cycling. The peak values of diameter and change of diameter; velocity and change of velocity were collected. The waveforms of diameter and wave velocity obtained by ultrasound were fairly reproducible using WI (Pomella *et al.,* 2017b). Non-WIA tests using ultrasound were conducted by Negoita, *et al.,* (2018) who aimed to present a technique for measuring local pulse wave velocity in the human ascending aorta using non-invasive ultrasound measurements for the diameter of the aorta and wave velocity. These results demonstrated that this non-invasive approach is easy to use, inexpensive, more accessible than MRI, and could be used to evaluate the mechanical properties of the aorta.

Abdulsalam and Feng, (2019) applied a non-WIA technique in in vitro to distinguish between stable and vulnerable plaques. This study indicated that the measured diameter for the artificial carotid artery of stable plaque is higher than unstable plaque, while the measured wave velocity in unstable plaque is slightly higher than stable plaque. These findings could assist in distinguishing between stable and vulnerable plaques and help vascular surgeons to make more precise decisions. However, this study investigated only fibro-calcified plaque (stable plaque) and thin-cap fibroatheroma (vulnerable plaque) and the conditions of this experiment generated further reflection, which produced unexpected results.

The mechanical properties of the internal carotid artery have been estimated by Ayadi *et al.,* (2020) using non-WIA to predict risk factor for cardiovascular events. Data was collected from twenty healthy young and old people using contrast magnetic resonance. This study shows that it is possible to determine arterial stiffness in clinical field trials using non-WIA techniques.

Finally, all previous in vitro and *in-vivo* studies, both WIA and non-WIA investigated the behaviour of the artery to study the wave dissipation, wave speed and wave reflection. To date, except for Abdulsalam and Feng (2019), these techniques have not been used to investigate the

composition of plaque in arteries to identify various plaque types. However, the work of Abdulsalam and Feng (2019) had several limitations. Therefore, non-invasive haemodynamic techniques need to be developed to identify plaque types and inform on vulnerability.

1.2. Contribution to Knowledge

Advanced imaging techniques offer non-invasive means to measure the extent of arterial plaques; however, current imaging techniques are unable to measure the thickness of the fibrous cap accurately due to limited resolution. In addition, a non-invasive technique to determine the composition of the plaque quantitatively is lacking. Furthermore, there is no clear evidence, so far, that imaging techniques can distinguish precisely between stable and unstable plaques, nor between the compositions of stable and vulnerable plaques. It has been proved that WIA and non-WIA are both efficient and reliable methods by which to study arterial wave propagation, with WI considered as the more important haemodynamic index to assess the condition of the arterial system. To date, neither WIA nor non-WIA have been used to study the compositions of arterial plaque and distinguish between stable and unstable plaques. Thus, the current study aims to fill this gap by applying non-invasive wave intensity analysis to study the differences between stable and vulnerable plaques, as well as their association with arterial waveforms, which is expected to vary with the change of plaque composition. This can lead to the identification of vulnerability.

1.3. The Main Aim of this Study.

The aim of this study is to determine the relationship that exists between plaque composition and arterial waveform. This relationship should distinguish between the arterial waveforms of stable, unstable and vulnerable plaques, informing on the vulnerability of plaques.

1.4. Objectives

In order to attain the aim of this project, the following objectives were undertaken:

Ob1: Initial test using in vitro experiments to demonstrate the hypothesis that arterial waveforms are associated with the plaque composition,

Ob2: Development of a variety of artificial plaques, which are characterised as real human carotid arterial plaque,

Ob3: An in vitro study of the effect of the different types of arterial plaques on arterial waveforms,

Ob4: Developing a Matlab code to separate the arterial waveforms into forward and backward components based on wave intensity theory,

Ob5: Determination of the correlation between the composition of the plaque and the arterial waveforms,

Ob6: Develop a non-invasive technique to quantify the vulnerabilities of plaque.

1.5. The Layout of This Thesis

Chapter 1 provides an introduction to cardiovascular diseases. The formation, composition and types of plaque are also illustrated in this chapter. The imaging techniques to detect plaque are reviewed. WIA and non-WIA techniques and their application to the cardiovascular system are also reviewed.

Chapter 2 demonstrates the theoretical background of the WIA technique. The method of characteristics is described. The key concepts of WIA including the wave speed, forward and backward wave components, and wave intensity are explained.

Chapter 3 presents the methodology used in this study: (i) experimental setup; (ii) fabrication of the artificial plaques; (iii) measurements and data collection; (iv) statistical analysis.

Chapter 4 demonstrates a pilot study to investigate the relationship between plaque compositions and arterial waveform in order to distinguish between stable and vulnerable plaques. Two types of plaques are tested, fibro-calcified plaque (stable plaque) and thin-cap fibroatheroma (vulnerable plaque). The healthy waveforms of diameter and velocity are

presented in order to be shown as a reference. Non-WIA is used to separate the arterial waveforms into forward and backward components. The results demonstrate that arterial waveforms are interrelated with the types and compositions of the arterial plaques.

Chapter 5 reports a study conducted to determine the quantitative correlation between the compositions of the plaque and the arterial waveforms. Six types of plaques were prepared with the degree of blockage 30% to establish the quantitative correlation between the different plaques and features of the arterial waveforms. A strong correlation between the percentage composition of the plaque with the amplitude of the backward diameter was observed. The results also imply that stable and unstable plaques could be distinguished by using net wave intensity.

Chapter 6 presents a study of the correlation between the compositions of the plaques and arterial waveforms for severe arterial stenosis (75% blockage). Four plaques (two stable, one unstable and two vulnerable) were used. The outcome of this study indicates that the measured diameter increases with plaque attached. A given diameter of an unstable plaque generates a higher amplitude than stable plaques. While the backward diameter of stable plaque generates a higher amplitude than unstable plaques. This chapter also shows that the identification between stable and unstable plaques could be detected by using ${}_{n}WI_{\pm}$.

Chapter 7 Discussion and Conclusions.

CHAPTER 2

Wave Intensity Analysis Background

2.1.Introduction

WIA, for dynamic cardiovascular investigation, based on the principals of conservation of mass and momentum, was introduced approximately three decades ago (Parker, 2009). In WIA, the waveforms of *P* and *U* are not represented as sinusoids but as successive wavefronts using the time domain rather than the frequency domain (Parker, 2009). Wave propagation problems in the flow domain were solved by Riemann using his 'method of characteristics'. In particular, arteries and their behaviour have been investigated by this method and, although they have complex shapes, they can be considered to be long and thin tubes (Parker, 2009).

2.2.The Governing Equations

WIA is the characteristic solution of laws of conservation of mass and momentum. It could be difficult to understand the development of WIA without understanding the principle of the method of characteristics. The mathematics may be complex, but the results are easy to understand. Inviscid and incompressible flows with no chemical reactions are assumed, and conservation of mass and momentum equations applied.

$$A_t + (UA)_x = 0 \tag{2.1}$$

The above equation represents the conversation of mass where: *A* is the tube (blood vessel) area; *U* is the average velocity of the flow through the area; *x* is distance along the tube (blood vessel or artery); and *t* is the partial derivative with respect to time. This means that the variation of volume in the element is related to the volume flow rates into and out of the element.

The fluid acceleration over the element in the conservation of momentum equation is the net sum of the rate of change of fluid flow and any applied force which acts on the element (invariably due to pressure).

$$U_t + UU_x = \frac{P_x}{\rho} \tag{2.2}$$

Where P_x is the average hydro-static pressure across A and ρ is the density of the blood, which is considered constant. Eqs (2.1) and (2.2) contain three variables: A, U and P, to be solved. The tube law, Eq. (2.3) provides the relationship between the tube local cross-sectional area and pressure, which can be expressed in the simple form (Parker, 2009):

$$A(x,t) = A(P(x,t); x) \tag{2.3}$$

Eq. (2.3) shows that the A is a function of P, where the pressure can differ from one location to another along the tube. The following equations derive the relationship between P and U in the mass and momentum equations by combining the tube law and the partial derivatives of the area:

$$\left(\frac{\partial A}{\partial x}\right)_t = A_P P_x + A_x \qquad \text{and} \qquad \left(\frac{\partial A}{\partial t}\right)_x = A_P P_t \tag{2.4}$$

$$\text{Where } A_P = \left(\frac{\partial A}{\partial P}\right)_x \qquad \text{and} \qquad A_x = \left(\frac{\partial A}{\partial x}\right)_P$$

A_P is the artery local compliance, which is caused by the variations of pressure. It is possible to arrange the final form of the mass and momentum conservation equations to be more convenient by substituting and rearranging the above equations.

$$P_t + UP_x + \frac{A}{A_P} U_x = -\frac{UA_x}{A_P} \tag{2.5}$$

$$U_t + \frac{1}{\rho} P_x + UU_x = 0 \tag{2.6}$$

The matrix form of the above two equations in terms of *x* can provide the eigenvalues, which will give the speed of the wave.

$$\begin{pmatrix} U & \frac{A}{A_P} \\ \frac{1}{\rho} & U \end{pmatrix} \tag{2.7}$$

Therefore, the eigenvalues will be,

$$\frac{dx}{dt} = \gamma_{\mp} = U \mp \left(\frac{A}{\rho A_P}\right)^{1/2} \tag{2.8}$$

The second term of the eigenvalue equation, $\left(\frac{A}{\rho A_P}\right)^{1/2}$, has the unit of velocity and can be considered as the speed of a wave which varies as it propagates along the tube. The distensibility of the blood vessel is $\frac{A_P}{A}$, so the wave speed, *c*, can be written as:

$$c = \left(\frac{A}{\rho A_P}\right)^{1/2} = \frac{1}{\sqrt{\rho D}} \tag{2.9}$$

The wave speed will, therefore, be a function of *P* and location in the blood vessel. However, the WIA assumes *c* is constant at any location in order to simplify the problem. It is important to draw attention to the fact that this method approximates the behaviour of real arteries.

$$c\,(x,t) = c\,(P(x,t);x) \tag{2.10}$$

2.3.Method of Characteristics Solution

Riemann observed that Eq. 2.8, is important in hyperbolic systems where Eq. 2.9 is real. Thus, the total derivative of Eq. 2.8 can be written as:

$$\frac{d}{dt} = \frac{\partial}{\partial t} + \frac{dx\partial}{dt\partial t} = \frac{\partial}{\partial t} + (U \mp c)\frac{\partial}{\partial t} \tag{2.11}$$

Substituting the above equation into the mass and momentum equations, we obtain:

$$\frac{dP}{dt} - (U \mp c)P_x + UP_x + \rho c^2 U_x = -\frac{UA_x}{A_P} \tag{2.12}$$

$$\frac{dU}{dt} - (U \mp c)U_x + \frac{1}{\rho}P_x + UU_x = 0 \tag{2.13}$$

Dividing Eq. 2.12 by ρc and combining with Eq. 2.13 an ordinary differential equation can be obtained:

$$\frac{dU}{dt} \mp \frac{1}{\rho c}\frac{dP}{dt} = -\frac{UcA_x}{A} \tag{2.14}$$

Eq. 2.14 can be written in terms of the Riemann variable $R_{\mp}$

$$\frac{dR_{\pm}}{dt} = \mp \frac{UcA_x}{A} \qquad where\ R_{\pm} \equiv U \pm \int \frac{1}{\rho c}\, dP \tag{2.15}$$

Eq. 2.15 is an ordinary differential equation in time and can be solved to obtain $R_{\pm}$. As the vessel is assumed uniform, $R_{\pm}$ will be constant in two cases: if $A_x = 0$ and with no velocity in the vessel, but if there is fluid flow with mean velocity *U*, and the value of *c* is greater than *U*, the waves propagate with speed *c* + *U* downstream and *c* - *U* upstream. On the other hand, if *c* is less than *U*, then there are no upstream waves, and both waves are in the downstream direction.

With the assumption that *c* is constant and *P* and *U* at (*x*,*t*), the pressure and velocity can be expressed as:

$$P = \frac{\rho c}{2}(R_+ - R_-) \tag{2.16}$$

$$U = \frac{1}{2}(R_+ + R_-) \tag{2.17}$$

The backward and forward characteristics at (*x*,*t*) are associated with $dR_{\pm}$ and also the boundary conditions of input and output of the blood vessel.

2.4.Wave Intensity Analysis

Understanding the method of characteristics leads to a better understanding of wave intensity (unit Wm^{-2}) and its application in arteries. The measurement of artery parameters, usually pressure and velocity, is typically accomplished at a particular position (*x*) and time (*t*). For $dR_{\pm}$, it is possible to write:

$$dR_{\pm} = dU \pm \frac{dP}{\rho c} \tag{2.18}$$

WI is . dU, and to obtain it, Eqs 2.16 and 2.17 should be expressed as a difference of measured pressure and velocity during the time dt:

$$dP = \frac{\rho c}{2} (R_{+} - R_{-}) \tag{2.19}$$

$$dU = \frac{1}{2} (R_{+} + R_{-}) \tag{2. 20}$$

$$dWI(t) = dP(t)dU(t) = \frac{\rho c}{4} (dR_{+}^{2} - dR_{-}^{2}) \tag{2.21}$$

The water hammer equation (Eq. (2.22)) which shows an important relationship between the change of pressure and wave velocity is a useful equation for arterial waves (Parker, 2009). The change of energy in the waves during wave propagation is due to the change in pressure and the stored potential energy in the arterial wall, and the difference of velocity is due to the kinetic energy due to movement of the blood. Therefore, the changes in pressure relate to the velocity waveforms and can be expressed simply by the water hammer equation:

$$dP_{\pm} = \pm \rho c dU_{\pm} \tag{2.22}$$

$$dP_{+} = \rho c dU_{+} \tag{2.23}$$

$$dP_{-} = -\rho c dU_{-} \tag{2.24}$$

Equations 2.23 and 2.24, respectively represent the forward and the backward directions of the wavefronts.

2.4.1. Wave Speed Determination

In the arterial system, it is difficult to measure the local speed of the waves, as it varies from site to site and from one artery type to another. To determine the local wave speed, several approaches have been applied. One relies on measuring the time taken for the wave to travel between two points, another depends on the dimension and the properties of blood vessel wall. The difference between them is that the first method provides the average value between two

sites and the second one requires measuring the wall properties invasively, which is difficult in the clinical field. However, several methods have been proposed more recently such as the *PU*-loop method. As described in Chapter 1, in the absence of reflections, the plot of pressure against velocity (Figure 1-3), should show a linear portion in the early systole, the gradient of which is equal to ρc. The measurement of the local wave speed is important in WIA calculation because its value is the key parameter for wave separation.

2.4.2. Wave Separations of Pressure and Velocity

Wave separation into forwards and backward travelling components depends on the value of the wave speed relative to U, as mentioned above. WIA was developed by Parker and Jones (1990) and allows the waveforms to be separated into forward and backward components based on the simultaneous of measurement of pressure and velocity at the same point. Figure 2.1 shows an example of the separated forward and backward wave components based on the measured aortic pressure and wave velocity in a dog. The forward and backward pressure and velocity changes could be determined by substituting Eq. (2.23) and Eq. (2.24) into Eq. (2.22).

$$dP_{\pm} = \frac{1}{2}\,(dP \pm \rho c dU) \tag{2.25}$$

$$dU_{\pm} = \frac{1}{2}\left(dU \pm \frac{dP}{\rho c}\right) \tag{2.26}$$

Eqs (2.25) and (2.26) are the changes in forward and backward pressure and velocity, the forward and backward pressure and velocity can be determined by the summation of $dP_{\pm}$ and $dU_{\pm}$.

$$P_{\pm}(t) = \sum_0^t dP_{\pm}(t) + P_0 \tag{2.27}$$

$$U_{\pm}(t) = \sum_0^t dU_{\pm}(t) + U_0 \tag{2.28}$$

Where P_0 is the initial static pressure, U_0 is the initial velocity and t is the time.

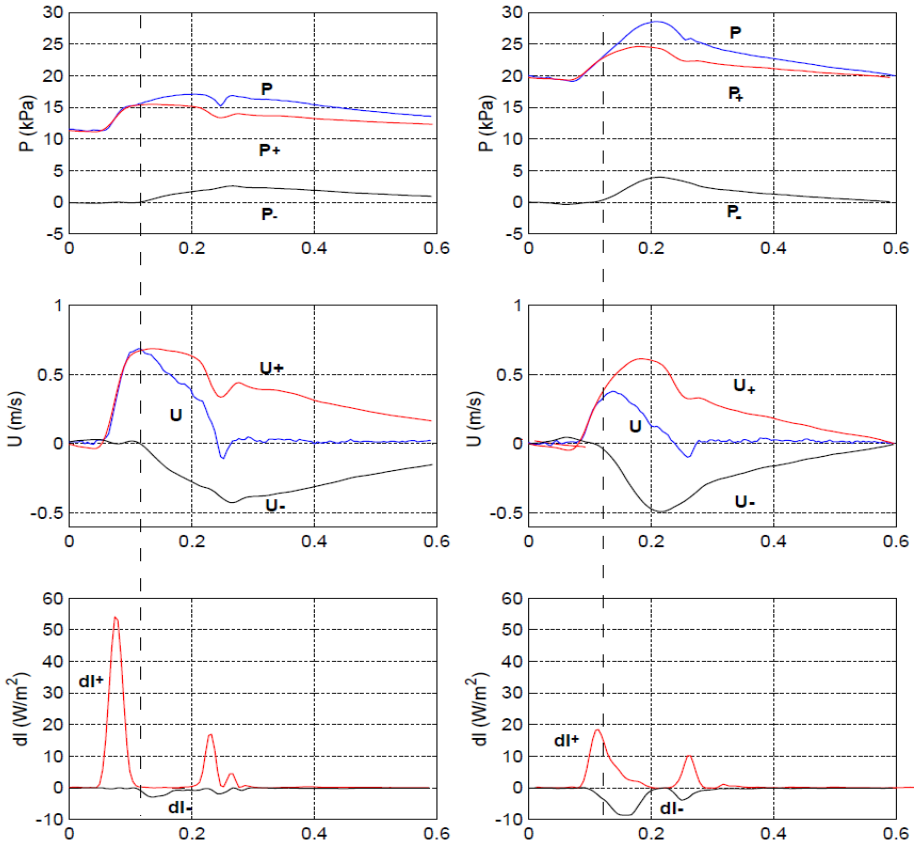

Figure 2.1 - Wave separation: pressure, velocity and wave intensity. The top panels represent pressure separation, the middle panels velocity separation and the bottom panels wave intensity separation (Parker, 2005)

2.4.3. Wave Intensity (WI)

Wave intensity is the energy flux transferred by the wave. The net wave intensity, WI, can be obtained by multiplying the changes in the measured pressure (dP) by the corresponding changes in velocity (dU), see Eqs (2.29) and (2.30). Waves, in general, can be categorized by the values of dP. If $dP > 0$, it refers to a compression wave, while if $dP < 0$ it indicates an expansion wave. The water hammer equation shows that the acceleration of the blood ($dU > 0$) could be caused by a compression wave (forward) and the deceleration would be caused by a forward travelling expansion wave ($dU<0$) (Khir *et al.*, 2001). Hence, if the sign of the instantaneous WI is positive, the magnitude of the forward travelling wave is greater than the backward travelling wave, and vice versa, as can be seen in Figure 2.1. From Figure 2.1, the

separation of pressure, velocity and wave intensity show that the amplitudes of P_{-}, U_{-} and WI_{-} through the occlusion are greater than those with controlled cases. This information could provide a clearer picture in terms of time and amplitude to help understand the behaviour of the arterial system. Therefore, this separation of pressure, velocity and intensity into two components can provide greater information about the mechanism of arterial systems particularly if large reflections occur in a blood vessel (Parker, 2009).

$$WI\,(t) = dP(t)\,.\,dU(t) \tag{2.29}$$

$$WI_{\pm} = \pm \frac{1}{4\rho c}\,(dP \pm \rho c dU)^2 \tag{2.30}$$

2.5. Non-invasive Wave Intensity Analysis (Non-WIA)

Two decades after the initial introduction of WIA, Feng and Khir, (2010) introduced a novel algorithm for estimating *c* by separating the measured waves into forward and backward components using arterial diameter and blood velocity measured non-invasively. In this technique, *c* was determined non-invasively by plotting ln(DU) against velocity in a so-called ln*DU*-loop. As explained in Chapter 1, the technique assumed that no reflected waves are present in the early systolic period and a linear plot is obtained in this early period, see Figure 2.2. The gradient of the slope of the linear portion of the curve provides a measure of *c*, see Eq. (2.31). When applied in the human carotid artery, the forward and backward components of the velocity are similar to the those obtained using the traditional WI approach, and the shape of the graph is very similar to that obtained using the PU loop. The separated forward and backward travelling wavefronts can be calculated using Eqs (2.32) and (2.33) as explained in Feng and Khir, (2010). This technique (non-WIA) has opened the door to many *in-vivo* and in vitro researchers to study the behaviour of arterial systems non-invasively.

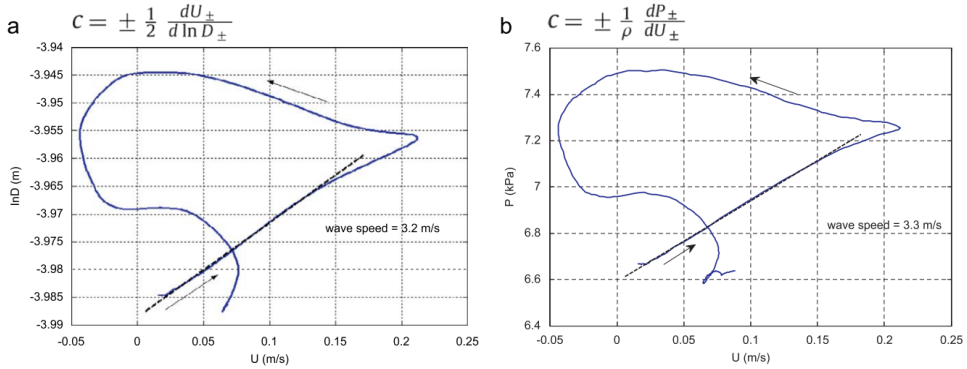

Figure 2.2 - The comparison between lnDU-loop and PU-loop (Feng and Khir, 2010)

$$c = \pm \frac{1}{2} \frac{dU_\pm}{d\ lnD_\pm} \tag{2.31}$$

$$dD_\pm = \frac{1}{2} \left(dD_\pm \frac{D}{2c}\ dU \right) \tag{2.32}$$

$$dU_\pm = \frac{1}{2} \left(dU_\pm \frac{2c}{D}\ dD \right) \tag{2.33}$$

Where: D is the initial diameter of the artery, $dD_\pm$ and $dU_\pm$ are the forward and the backward components of the diameter and velocity changes. The forward and the backward diameters and velocities can be calculated by the following equations:

$$D_\pm = \sum_{t=0}^{T} dD_\pm + D_0 \tag{2.34}$$

$$U_\pm = \sum_{t=0}^{T} dU_\pm + U_0 \tag{2.35}$$

Where T is the total time, D_0 and U_0 are the diameter and velocity at the given hydrostatic pressure, where the pump is off.

The non-invasive wave intensity, (non-WI), was defined in terms of D and U, and can also be obtained by the multiplication of the change of diameter (dD) and velocity (dU). The separated forward and backward non-WI, ${}_{n}dI_\pm$, can be calculated by Eq. (2.36),

$${}_{n}WI_\pm = \pm \frac{1}{4\,(D/2c)} \left(dD \pm \frac{D}{2c}\ dU \right)^2 \tag{2.36}$$

Finally, this study has utilized the non-WIA because it is a non-invasive technique; relatively easy and fast to use and in clinical situations. This technique is easy to use with ultrasound to obtain the necessary data non-invasively. Thus, it is possible to obtain the magnitude and

direction of the wave at any interval if c is known by taking measurements of D and U simultaneously. Because the forward and backward waves in arteries are caused by the pressure generated by the heart and reflections, respectively. Using this technique could give important information on arterial systems especially in the presence of plaque.

CHAPTER 3
Methodology

3.1. Experiment Setup

In this study, the correlation between the compositions of plaques and the corresponding arterial waveforms are investigated in vitro in the Physiological Fluid Dynamics Laboratory at Manchester Metropolitan University. Artificial arterial plaques, composed of the main components of arterial plaques, have been prepared and tested. The in vitro experimental apparatus consists of a Harvard Apparatus pulsatile pump, reservoirs and artificial blood vessels, see Figure 3.1. The measurement equipment includes Sonometric crystals (Sonometric Cooperation, ONT, Canada) for measurement of diameter, transonic flow probes (Transonic System, NY, USA) for flow rate, a tipped catheter pressure sensor (Gaeltec, UK) for pressure. The details of each of the components are given below.

3.1.1 Pulsatile Pump

The Pulsatile Blood Pump, see Figure 3.2, represents the left ventricle of the heart, which is used to generate pulsatile arterial waveforms. The shape and amplitude of arterial waveform are determined by the settings of the pump and the compliance of the arterial system. The three main settings of the pump are used to fix the percentage of the systolic and diastolic period, number of strokes per minute (RPM), and stroke volume, respectively. The systole and diastole percentages vary from $\frac{50}{50}$ to $\frac{25}{75}$, the RPM ranges from 10 to 100 RPM, and the stroke volume from 15 to 100 ml.

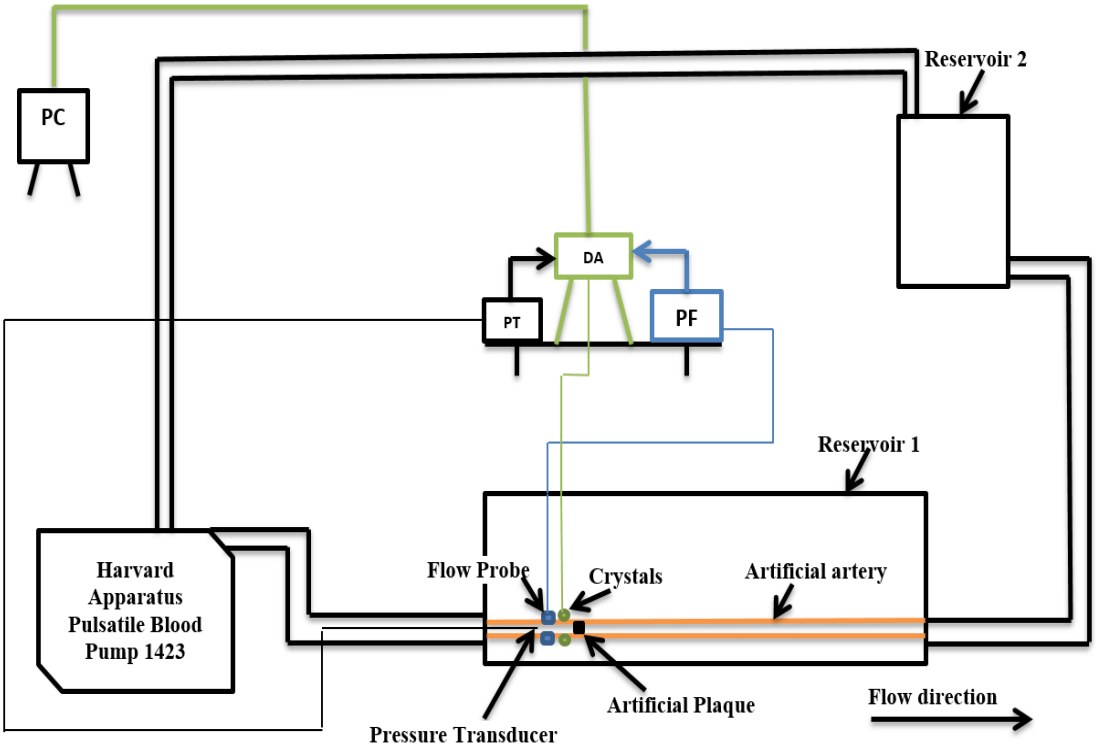

Figure 3.1 - Schematic diagram of artificial blood circulation system. PT is pressure transducer bridge amplifier; PF is Perivascular flow meter; DA is data acquisition and PC is personal computer.

Figure 3.2 - Harvard Apparatus Pulsatile Blood Pump 1423

3.1.2. Reservoirs

Two reservoirs are used in the system, see Figure 3.1. Reservoir one connects the outlet of the pump with the artificial blood vessel. Reservoir one is 500 mm long, 250 mm wide and 300 mm deep. Reservoir two is 200 mm long and wide, and 300 mm deep. Both reservoirs are made of stable, clear plastic, 8 mm thick. The altitude of water in the first tank is 30mm above the artificial blood vessel in all tests, in order to ensure that the flow probe and diameter crystals receive signals and also to avoid undesired reflections (Feng and Khir, 2010).

3.1.3. Artificial Blood Vessel

Latex penrose tubing (Kent Elastomer, UK) was employed to simulate blood vessels with a uniform shape along their length, see Figure 3.3 (Khir and Parker, 2002). To simulate the circulatory system, an artificial blood vessel was submerged in a tank of water (Reservoir one) and its inlet connected to the Pulsatile Blood pump and outlet to the top tank via PVC tube. PVC tubes (15 mm ID, 20 mm OD and 2.5 mm wall thickness), representing other arteries of the body, were used to connect the inlet and outlet of Reservoir one with the Pulsatile pump and with Reservoir two. From Reservoir two, PVC tubing connected with the pump to complete the circuit, (Figure 3.1).

Figure 3.3 - An example of artificial blood vessel made by Latex Penrose tubing

3.2. Artificial Plaque Fabrication

Based on a histological study of human carotid arterial plaque, Butcovan *et al.,* (2016) classified carotid atherosclerosis into three types: (i) stable plaques including fibroatheroma (FA) and fibro-calcified plaque (FC); (ii) unstable plaques such as plaque rupture (PR), plaque erosion (PE) and calcified nodule (CN); and (iii) vulnerable plaques such as thin-cap fibroatheroma (TCFA). The features of these types of plaques are presented in Table 3.1. In this study, artificial plaques with identical characteristics to those of human carotid atherosclerosis were fabricated manually (Figure 3.4).

The following components were used to form the artificial plaques: (i) calcium chloride hexahydrate and (ii) Collagen type III, (both obtained from Sigma – Aldrich, St. Louis, MO), and (iii) lipid core-soybean oil. Calcium chloride hexahydrate has been widely used in medical research such as composite living fibres for creating tissue constructs (Akbari et al., 2014) and phosphatidylthreonine and lipid-mediated control (Arroyo-Olarte *et al.,* 2015). Type III collagen was used to study the collagen chain in the human placenta in previous studies (Sage and Bornstein, 1979). In this study, this type of collagen was used to fabricate the fibrous cap and the collagen part of the plaque, and soybean oil was used to form the lipid core of the artificial plaque.

Gelatine from bovine skin, type B, and collagen from human placenta, type III, (both obtained from, Sigma – Aldrich, St. Louis, MO) were mixed using deionized water to form the material of the fibrous cap (Guo *et al.*, 2013). The fibrous cap in this study was formed by two methods. The first (Study 1 and 2) was by brushing the liquid mix of collagen and gelatine onto the mould to give it the shape of fibrous cap with specific thicknesses. The second method (Study 3) used the bovine skin shaped by the same mould with various thicknesses. The in vitro study by Teng (Teng et al., 2014) was referred to for the size and shape of the artificial plaque components.

As the main components of the plaque is Ca, LC, Col and fibrous cap, the first component that was prepared is the fibrous cap. This fibrous cap was fabricated by two methods, as mentioned above, and both methods gave the same result (Abdulsalam and Feng, 2019; Abdulsalam and Feng, 2021). The procedure of the first and the second methods are explained below.

3.2.1. Plaque Preparation First Method

1- The mould of the fibrous cap which met the dimensions of Teng et al., (2014) (The length was 21.5 mm and the width 6.5 mm) and occupied the 30% blockage of the inner diameter of the artificial artery was fabricated using 3D-Printing machine at Manchester Metropolitan University Printing City workshop. The material of the mould was flexible plastic in order to be easy to remove the fibrous cap from the mould.

2- As the fibrous cap contains mostly of collagen, the Collagen type III (powder), (Sigma – Aldrich, St. Louis, MO) and gelatine from bovine skin type B (powder) (Sigma – Aldrich, St. Louis, MO) were mixed with deionized water. The amount of collagen, gelatine and water were 0.6g, 0.2g and 0.2g, respectively. The deionized water was boiled at 100C^{o} and 0.2g was poured into 0.6 of collagen and 0.2g of gelatine. Then, all

of them were blended by using small spoon to dissolve the collagen and gelatine with deionized water.

3- This fluid, dissolved collagen and gelatine, were used to form the fibrous cap by using the moulds. This was done by using small painting brush, where it was immersed in the fluid and brushing the fluid on the mould based on the fibrous cap thickness required. The thickness of fibrous cap for each type of the plaque was achieving by try and error. For example, the fibrous cap thickness of the fibroatheroma (FA) plaque was 0.35mm and for thin-cap fibroatheroma (TCFA) plaque was 0.022mm (Table 3.1). In order to achieve the fibrous cap thickness of FA plaque, plenty amount of fluid on the brush was required to brush it in the mould because the thickness of the fibrous cap was thicker than that in TCFA, which required small amount of fluid. The exact thickness was hardly to achieve at the first time so that each type of fibrous cap plaque was made at least 10 times in order to obtain three fibrous cap with thickness close to the one that we needed it. Those 10 fibrous caps, which were on the moulds, were left 24 hours to become dry and easy to remove them from the moulds. Finally, those 10 fibrous caps of each type of plaque were measured by micrometre to obtain the closest three fibrous caps of the required thickness.

4- Plaques that require calcium or collagen were prepared and mounted in the fibrous cap (Figure 3.4 A&B). For instance, the composition of fibro-calcified plaque (FC) includes 47% lipid core, 6.2 calcium and 47% collagen (Table 3.1). The percentage of collagen was firstly fabricated and mounted in its location on the fibrous cap and left it for 24 hours to ensure that the load of collagen did not break the fibrous cap. In the second day, if the fibrous cap bore the load of the collagen, the percentage of calcium would be the second preparation. The preparation of calcium was made by mixing the

deionized water with calcium until to become thicker. Then its percentage was mounted on its location on the fibrous cap and left it for 24 hours to guarantee that the calcium would not collapse the fibrous cap.

5- In the third day, if the fibrous cap sustained the load of calcium and collagen, the bottom part of the fibrous cap was covered by the same material of the artificial artery (Figure 3.4C). The coverage process was done by cutting the latex tube, which is the same material of the artificial artery, in the form of fibrous cap to become a piece of latex; then putting a little glue in the bottom end edge of the fibrous cap and mounted on the latex piece. After closing the bottom of fibrous cap, the lipid core percentage was inserted in the small medical syringe and injected from the base side on its location of the lipid core (Figure 3.4D). Then the small hole that caused by syringe was closed by silicone and left it for 24 hours to ensure there was no leak and the fibrous cap afforded the collagen, calcium and lipid core in order to be the whole plaque. In the fourth day, if there were no leak, no break of fibrous cap and no distention in the bottom of the plaque due to the lipid core, the whole plaque would be ready to implement in the experiment.

3.2.2. Plaque Preparation Second Method

1- The fabrication of the fibrous cap mould was the same as the first method by printing them in 3D-Printing machine. However, the dimensions were different to the 30% blockage. The dimensions here were as follows: 15 mm in length and 4 mm in width (Teng *et al.,* 2014; Almuhanna *et al.*, 2015) with 75% stenosis.

2- The fibrous cap in this method was made by bovine skin. This skin was stretched manually by pulling the piece of skin in each end side and measure its thickness by micrometre to reach the thickness less than required one. The reason why we need less

thickness than the required one is because the skin could shrink slightly when we put it in the mould for 24 hours. Once the thicknesses were achieved to be less than the required one, they would mounted on the mould and left for 24 hours to become dry and easy to remove them from the moulds. Then, they removed from the moulds and measured again to ensure that the thickness was as we required.

3- Step 4 and 5 from method one is then the same in method 2 except the process of covering the bottom side of the fibrous cap as the latex material was used to cover the bottom side in first method, whereas in the second method, the bovine skin was used to cover the bottom side.

Finally, the artificial plaque was ready for use in the in vitro experiment. The stages of the fabrication procedure are shown in Figure 3.4. This artificial plaque was mounted in the artificial artery at its location (100mm, 266mm and 300mm from the inlet for study one, two and three, respectively.) by putting small amount of glue on the bottom end edge of the plaque then inserted into the artificial artery using lab scoop spoon (Figure 3.5A). Then, it would leave for 24 hours to make sure that the plaque was glued properly on the artificial artery and there was no leak and crack on the fibrous cap or distention on the bottom of the plaque. Thereafter, as the plaque mounted inside the artificial artery and at its location, it could be installed in the artificial arterial system for testing (Figure 3.1).

Table.3.1 - Compositions of three types of plaque: stable (fibroatheroma (FA) and fibro-calcified plaque (FC)); vulnerable plaques (thin-cap fibroatheroma (TCFA)) and unstable (plaque rupture (PR) and plaque erosion (PE)). LC, Ca and Col are Lipid Core, Calcium and Collagen, respectively

Plaque type	**Fibrous cap (mm)**	**LC %**	**Ca%**	**Col%**
FA (Stable)	0.35	57 %	0 %	43 %
FC (Stable)	0.27	47 %	6.2 %	47 %
TCFA (vulnerable)	0.022	26 %	0 %	74 %
PR (Unstable)	0.017	22 %	0 %	78 %
PE (Unstable)	0.013	71 %	18 %	12 %
CN (Unstable)	0.022	0%	100%	0%

These characteristics obtained by (Butcovan *et al.*, 2016)

3.3 . Measurements

In this study, the effect of plaque composition between stable plaque (FC) and vulnerable plaque (TCFA) was firstly investigated. The length of the plaque was 21.5 mm, width 6.5 mm (Teng *et al.,* 2014) and the artificial artery diameter was 9.5 mm (Park *et al.,* 2001). The composition of the two plaques was based on Table 3.1. The main aim of experiment one was to distinguish between stable and vulnerable plaques by investigating the effect of plaque composition on the arterial waveform. The degree of blockage in this experiment was 30% ($\pm$ 5 %). The shape and amplitude of arterial waveform, which are similar to those for human carotid arteries, were determined by the settings of the pump and the compliance of the arterial system. The heart rate of a healthy human is between 60 to 100 beats per minutes. In the experiment, the pump rate was set at 70 RPM and stroke rate at 17 cc. Regarding the main settings, the simulated ventricle on the pump was connected by PVC tubing to receive and pump the circulating fluid. The output of the pump is connected to Reservoir one, where the artificial carotid artery was installed. Reservoir two is connected to the suction element of the simulated ventricle in the pump to complete the circuit. Water (density is 998.2 kg/m^3 and viscosity is 1.002×10^{-3} kg/m.s at 20 ^{0}C) was used to mimic blood travelling in the circulation system (Feng *et al.,* 2007). The artificial artery was of length 400 mm and simultaneous diameter, flow rate and pressure measurements were taken proximal to the artificial plaque. The two artificial plaques, Figure 4.1, were mounted 100 mm away from the inlet injection. The distance between pressure transducer, flow probe and crystals was less than 5 mm, and the artificial blood vessel was straight and its diameter was 9.5 mm. The base of the plaque had a small amount of glue added and was inserted into by using small medical spoon and placed 100 mm into the artificial artery, away from the inlet. The healthy pressure was between 127 mmHg and 75 mmHg, and the velocity ranged between 0.5152 m/s and -0.033 m/s. Sonosoft software was used to collect and convert the data to a form suitable for inputting to the

computer. Matlab R 2018a was used for analysing the data. The measurements, plaques, positions and setting up of this experiment are illustrated in Figure 3.5.

In addition, the measurements and the settings of the second experiment were similar to the first experiment, including artery diameter, pump setting, degree of blockage, and size of the artificial arterial plaque. However, the difference was that the position of the plaques was shifted to 266 mm from the inlet injection. The reason for this was to avoid wave reflections and re-reflection from the inlet injection that had been observed in the previous experiment, and which produced some unexpected results (Abdulsalam and Feng, 2019). Moreover, various types of plaques were used in experiment two including FC and FA stable plaques; PE, PR and CN unstable plaques and TCFA vulnerable plaque, see Section 1.1.2.1, in order to investigate the effect of plaque composition, apart from their fibrous caps, on the arterial waveform and identify plaque vulnerability. All plaques used are shown in Figure 5.1.

Furthermore, the correlation between plaque composition and arterial waveforms for severe arterial stenosis was investigated in experiment three. The composition of the plaques used were based on Table 3.1. But the relative dimensions of the plaque were different from experiments one and two, it was 15 mm in length and 4 mm in width (Teng *et al.,* 2014; Almuhanna *et al.,* 2015). The blockage degree in this experiment was larger than in the first two experiments, 75% ± 5%, see Figure 3.6. Additionally, the diameter of the artificial artery was changed to 6.35 mm (Krejza *et al.,* 2006).

The shape and amplitude of arterial waveforms, which are again similar to those for the human carotid arteries, were determined by the settings of the pump and the compliance of the arterial system. The pump rate was set at 74 RPM and stroke at 17 cc. The artificial artery length was 400 mm and again, as in the first two experiments, simultaneous diameter, flow rate and pressure measurements were taken proximal to the artificial plaque. The artificial plaques were

mounted 300 mm away from inlet injection to avoid reflections and re-reflections from the inlet injection. The distance between pressure transducer, flow probe and crystals was also less than 5 mm. The healthy pressure was between 135 mmHg and 70 mmHg and the velocity ranged from 0.6396 m/s to -0.1108 m/s.

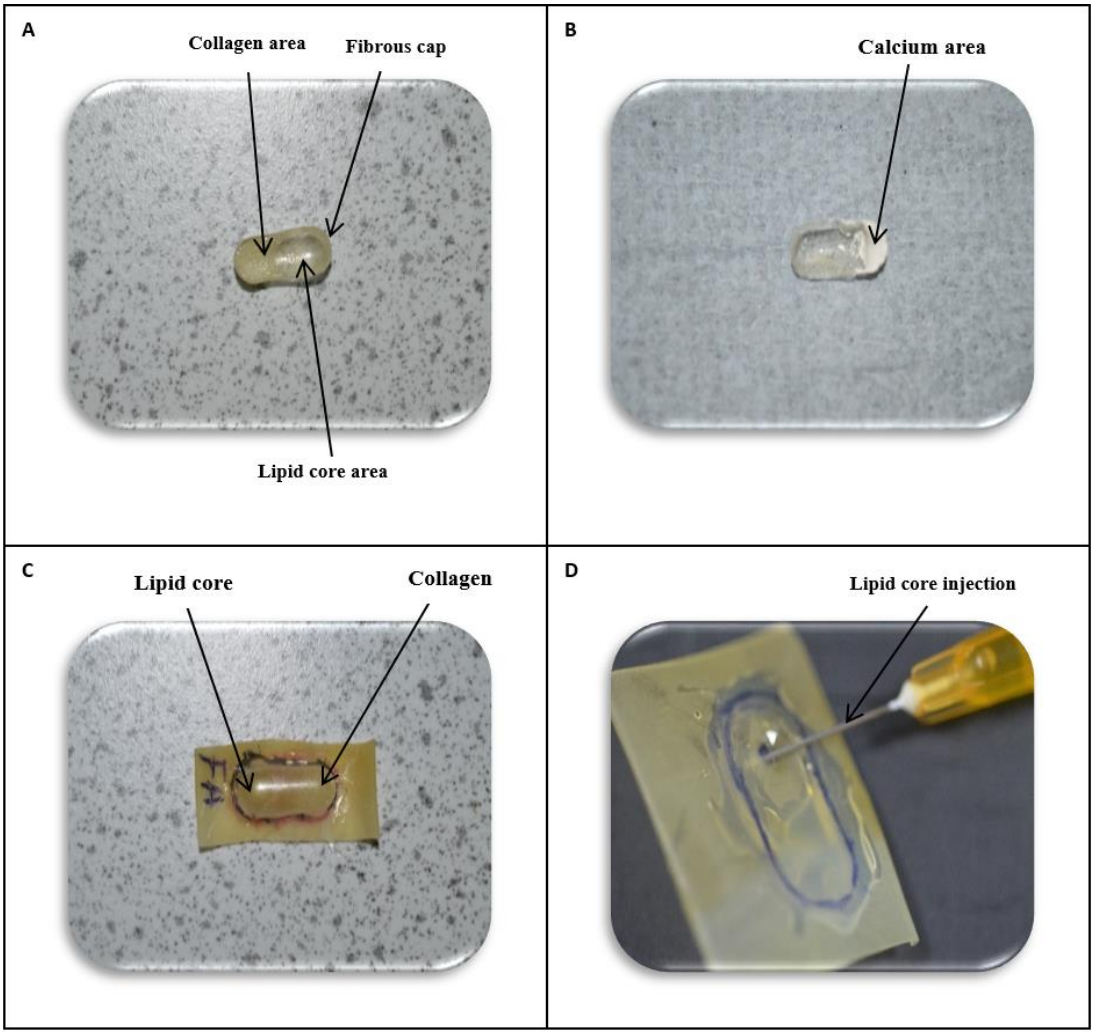

Figure 3.4 - Artificial plaque preparation procedures. (A) Example of inserting collagen into FA type plaque. (B) Example of inserting calcium into FC type plaque. (C) Example of the whole plaque that was used in the experiment. (D) Shows how the artificial lipid core was injected into the plaque. The blue dot shows where the lipid core should be injected.

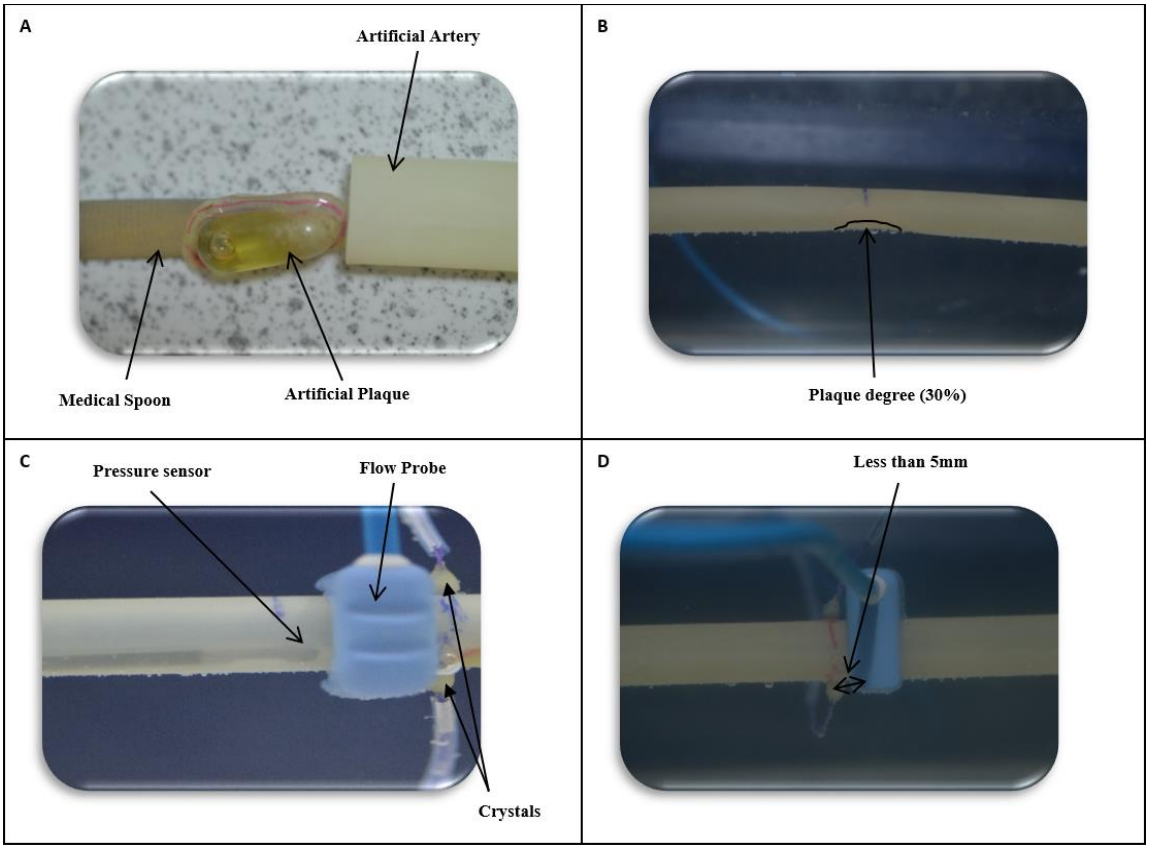

Figure 3.5 - Plaque position and measurement locations. (A) Illustrates how the plaque was inserted into the artificial artery and located 100 mm away from the inlet. (B) Shows the degree to which the plaque blocked the artery (30% blockage). (C) Shows the measurement sensors located before the plaque. (D) Illustrates the distance between flow probe and crystals which was less than 5 mm.

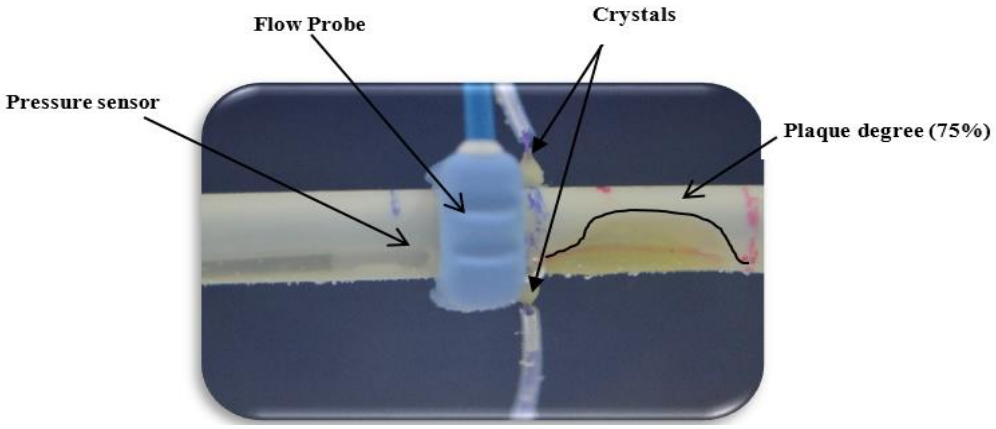

Figure 3.6 – Illustrating the plaque degree and the position of the plaque was close to the measurement sensors. The distance between the measurement sensors was less than 5mm.

3.4 . Statistical Analysis

3.4.1. Correlation

A measure of association is a statistical association used to indicate the strength of the relationship between two variables and can be either positive or negative ranging from -1.0 to +1.0. Pearson Product-Moment Correlation Coefficient (*r*) is the most popular correlation coefficient used to describe the strength of the linear association between two variables.

In the second and third experiment, the relationship between arterial backward diameter with the percentage of collagen, lipid core and calcium on the plaque were determined by Pearson Product-Moment Correlation Coefficient (*r*). Each type of plaque were tested three times. Two times the same compositions and one time with different compositions in the experiment and their backward amplitudes and compositions are illustrated in Table 3.2.

3.4.2. Significant association

The data in second experiment indicated that, there is a positive strong correlation between backward diameter amplitude and collagen percentage with P-value 0.005, where *r* value was 0.74 (Figure 5.8A). However, a strong negative correlation was found between backward diameter amplitude and the percentage of lipid core with again P-value 0.005, where r value was 0.82 (Figure 5.8B), while a weak negative correlation was observed between calcium and backward amplitude with r value equal 0.3 (Figure 5.8C).

In the third experiment, however, the results were opposite to the second experiment as the correlation between LC with backward diameter amplitude was significantly positive at r = 0.76 (Figure 6.6A), whereas the correlation between Col and backward diameter amplitude was significantly negative with r = 0.85 (Figure 6.6B).

Table 3.2 – The backward diameter amplitude of the three tests with plaque composition for 30% and 75% stenosis including lipid core (LC), calcium (Ca) and collagen (Col). This data was used to determine the correlation between backward diameter with LC, Ca and Col.

30% Stenosis Test 1					**75% Stenosis Test 1**			
Plaque type	**Amplitude**	**LC**	**Ca**	**Col**	**Amplitude**	**LC**	**Ca**	**Col**
FC	0.51	47.00	6.23	46.86	0.512	47.00	6.23	46.86
FA	0.49	56.99	0.00	43.00	0.44	56.99	0.00	43.00
PE	0.53	70.29	17.85	12.00	-	-	-	-
PR	0.70	22.03	0.00	78.00	0.38	22.03	0.00	78.00
TCFA	0.60	25.90	0.00	74.00	0.38	25.90	0.00	74.00
30% Stenosis Test 2					**75% Stenosis Test 2**			
Plaque type	**Amplitude**	**LC**	**Ca**	**Col**	**Amplitude**	**LC**	**Ca**	**Col**
FC	0.63	30.00	15.00	55.00	0.54	50.00	6.00	44.00
FA	0.47	60.00	5.00	35.00	0.49	50.00	0.00	50.00
PE	0.47	60.00	20.00	20.00	-	-	-	-
PR	0.65	25.00	0.00	75.00	0.42	28.00	0.00	72.00
TCFA	0.55	45.00	0.00	55.00	0.41	30.00	0.00	70.00
30% Stenosis Test 3					**75% Stenosis Test 3**			
Plaque type	**Amplitude**	**LC**	**Ca**	**Col**	**Amplitude**	**LC**	**Ca**	**Col**
FC	0.61	47.00	6.23	46.86	0.51	47.00	6.23	46.86
FA	0.48	56.99	0.00	43.00	0.41	56.99	0.00	43.00
PE	0.53	70.29	17.85	12.00	-	-	-	-
PR	0.69	22.03	0.00	78.00	0.38	22.03	0.00	78.00
TCFA	0.57	25.90	0.00	74.00	0.36	25.90	0.00	74.00

CHAPTER 4

Pilot Study of the Effects of Stable and Vulnerable Plaques on Arterial Waveforms

4.1. Introduction

Atherosclerosis plaque in the carotid arteries is considered the main cause of stroke, which are initiated by inflammatory processes in the endothelial cells of the artery, which are associated with retained low-density lipoprotein (LDL) particles. LDL passes through the endothelium, and builds up as the so-called '*Plaque*'(Johri *et al.,* 2017). To date, a novel technique, able to distinguish the composition of the plaque and provide accurate information to the vascular surgeon to identify the type of plaque, is still lacking. The aim of this chapter is to use the non-invasive wave intensity analysis (non-WIA) technique to separate the arterial waveform into its forward and backward components to differentiate between stable and unstable plaques.

4.3. Results

4.3.1 The FC and TCFA Plaques

The stable (FC) and the vulnerable (TCFA) plaques are illustrated in Figure 4.1 A and B, respectively. The composition of FC plaque is 47% collagen, 6.2% calcium and 47% lipid core with 0.27mm fibrous cap. The calcium part was mounted on the side edge of the plaque, then the collagen part was following to it and the rest of the plaque was the lipid core. While the TCFA plaque, which its component proportion was 74% collagen, 0% calcium and 26% lipid core with 0.022mm fibrous cap. The 74% of collagen was placed on the side edge and the 26% of lipid core was next to it. The flow direction was facing the stable part (Calcium and Collagen) of the FC plaque, whereas the soft part (Lipid core) of the TCFA plaque was facing the follow direction in order to study the effect of the stable and vulnerable plaque on the arterial waveform.

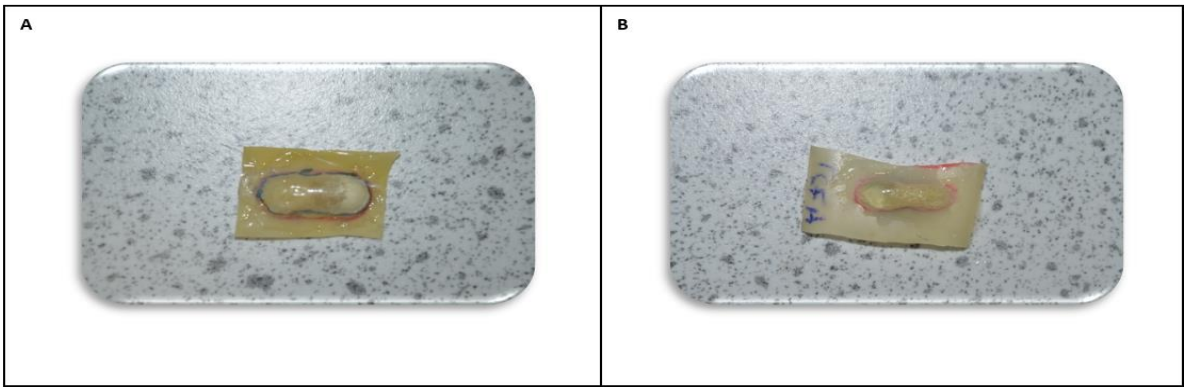

Figure 4.1 Examples of stable and vulnerable plaques used in experiment 1. (A) is the FC *stable* plaque and (B) is the TCFA vulnerable plaque.

4.3.2 The Measured Diameter and Velocity

The measured waveforms of the arterial velocities and diameters are shown in Figure 4.2 A and B, respectively, for the healthy condition (no plaque), with vulnerable plaque and with stable plaque. It is clear that the lowest value of the peak arterial diameter occurred for the healthy condition. The peak arterial diameter, and maximum change in arterial diameter, increased when the plaques were attached. As was expected, the stable plaque generated the highest peak amplitude, and the peak amplitude for the vulnerable plaque is less than that with the stable plaque. A somewhat similar pattern was found for the waveforms of the arterial velocity, but the differences between the three waveforms was not significant.

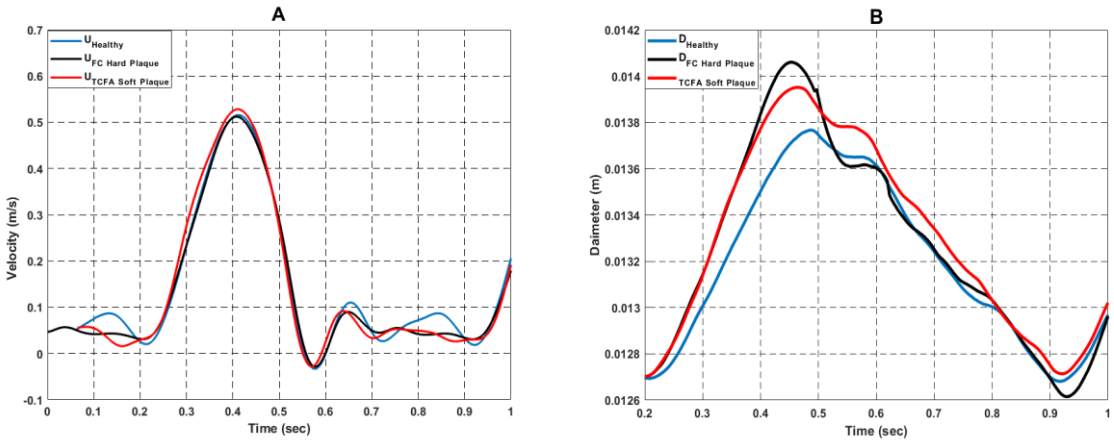

Figure 4.2 - The measured velocity (A) and diameter (B) waveforms in three types of the arterial system: healthy (blue), and with stable plaque (black) (FC), and with vulnerable plaque (TCFA) (red). The FC stable plaque generate higher amplitude than TCFA vulnerable plaque due to its stiffness, whereas its velocity amplitude is lower than TCFA plaque.

4.3.2. The Forward Diameter and Velocity

WIA is used to separate the measured pressure, velocity and diameter into the forward and backward components for the two types of arterial-plaques used (Figure 4.2).

The peak change in amplitude of the forward velocity generated by the heart (ventricle) in the presence of stable plaque (0.553 ms^{-1}) is slightly higher than for vulnerable plaque (0.533 ms^{-1}) and more higher than for the healthy condition (0.461 ms^{-1}). Similarly, the peak change in amplitude of the forward diameter for stable plaque (1.04 mm) is slightly higher than that of vulnerable plaque (0.96 mm) and much higher than for the healthy condition (0.84 mm).

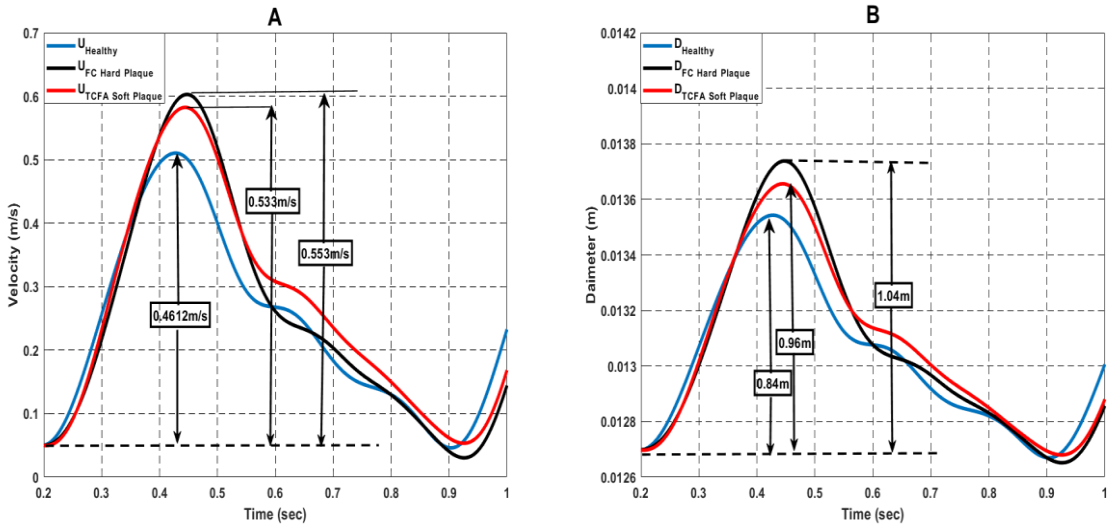

Figure 4.3 - (A) & (B) The forward velocity and diameter for healthy condition (blue), stable plaque (black) (FC), and vulnerable plaque (TCFA) (red), measured proximally to the plaque. The double-arrow lines demonstrate how the amplitude is measured. The forward velocity and diameter amplitude of stable plaque is higher than unstable plaques due to the increase of the ventricle flow to overcome the increase of reflected waves that arrive before closing the aortic valve.

4.3.3. The Backward Diameter and Velocity

The waveforms for velocity and arterial diameter due to the backward waves produced from reflections are shown in Figure 4.4 A, B, respectively. It can be seen that the peak change in backward velocity for the vulnerable plaque is larger than for either the stable plaque or the no plaque condition. Interestingly, the peak-peak values of the arterial velocity waveform showed little difference between the vulnerable plaque (0.193 ms^{-1}) and healthy (0.189 ms^{-1}) conditions. But both were much larger than for stable plaque (0.248 ms^{-1}).

The arterial peak diameter for the healthy condition (0.56 mm) was not significant different from the peak diameter in the presence of vulnerable plaque (0.55), and both were much greater than for stable plaque (0.44). This phenomenon is opposite to the prediction that stable plaque should have greater backward reflection than vulnerable plaque because of its relative stiffness. These results are not expected, and further investigations are needed.

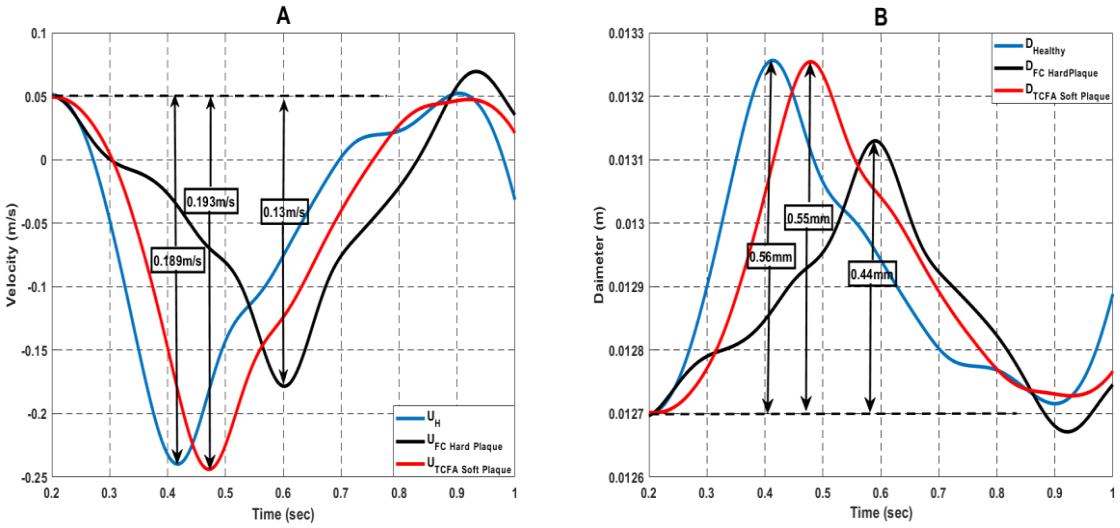

Figure 4.4 – The backward velocity and diameter for healthy, stable plaque (FC) and vulnerable plaque (TCFA). (A) The backward velocity for healthy (blue), stable plaque (black) (FC) and vulnerable plaque (TCFA) (red). (B) The backward diameter for healthy, stable and vulnerable plaques. The backward velocity and diameter amplitude of TCFA plaque is higher than FC plaque. This result is out of our expectation because the stable plaque should produce higher reflection leading to higher amplitude. This phenomenon might be from the refelctions and re-reflections in the inlet injection.

4.4. Discussion

This study investigated two types of plaques: the FC stable and TCFA vulnerable plaques. Configuration of these two artificial plaques were derived from previous studies regarding plaque characteristics and properties by Guo *et al.,* (2013), Teng *et al.,* (2014) and Butcovan *et al.,* (2016).

The data was collected five minutes after starting the experiment. Each plaque was tested three times to ensure the reproducibility. As expected, see Figure 4.2, the stable plaque with the higher proportion of Ca gave the greatest measured peak diameter, whereas the vulnerable plaque with a higher percentage of lipid core gave a lower amplitude for the measured diameter. Both were much larger than the peak measured diameter for the healthy condition. Looking closely at the measured arterial velocity waveforms, shown in Figure 4.2 A, we see the peak velocity for the stable plaque is slightly smaller than the vulnerable plaque indicating that the stable plaque generated a stronger reflected wave which led to a greater value for the amplitude of the peak value of the arterial diameter waveform and lower amplitude for the peak velocity.

Figure 4.3A shows that the forward velocity in the presence of stable plaque is slightly higher than with vulnerable plaque. This observation could be explained as due to the presence of a reflected wave occurring at the inlet of the system, which led to the increase of the velocity. Likewise, the forward diameter amplitude (Figure 4.3B) in stable plaque is slightly higher than in vulnerable plaque with the same reason.

The amplitude of backward waveform in the arterial system in the presence of stable plaque was expected to be higher than vulnerable plaque because the stiffness of arterial stable plaque is higher than for vulnerable plaque, and thus should produce a greater higher reflection. It was observed that the backward reflection amplitude for vulnerable plaque in velocity and diameter is higher than for stable plaque (Figure 4.4 A and B). These results did not meet our

expectations. The reason for this phenomenon could be re-reflections from the inlet tube or because the material properties of the artificial artery for the stable plaque was different from the one used with vulnerable plaque. This needs further investigations. As this study is a pilot study, which aims to examine whether the stable and vulnerable plaque could effect on the arterial waveforms and the number of plaques implemented were only two types, the statistics analysis was not undertaken in this chapter, which will be conducted in Chapter 5.

4.5. Conclusions

This study confirms that the arterial waveform can provide useful information about different types of plaques. The compositions of the plaque are related to the waveform properties, which could lead to being able to characterise stable and vulnerable plaques. Using WIA to separate the waves into forward and backward waves has the potential to distinguish between stable and vulnerable plaques. These findings indicate that the forward velocity and diameter amplitude with stable plaques is higher than with vulnerable plaques. However, the observation that the backward velocity and diameter amplitude in the presence of vulnerable plaque is higher than for stable plaque needs further investigation.

The outcome of this study could assist in distinguishing between stable and vulnerable plaques, but the study had several limitations that need to be addressed. Firstly, other types of plaque should be investigated, which may increase the capability of using this technique. Secondly, the shape of the plaque was uniform, which is different from the human carotid arterial plaques observed from clinical studies. Finally, the position of the plaques should be shifted further from the inlet injection to reduce the effect of reflections and re-reflection.

CHAPTER 5

The Composition of Vulnerable Plaque and Effects on Arterial Waveforms

5.1. Introduction

Plaque advancement prediction is essential to cardiovascular studies and disease diagnosis, prohibition, and treatment. Atherosclerotic plaque is an arterial disease which builds up in the arterial wall and can be identified by the composition of the plaque which includes lipid core (LC), calcium (Ca), collagen (Col) and other substances from the blood (Libby *et al.,* 2011). Atherosclerosis causes narrowing of the carotid lumen leading to either occlusion of the blood flow to the brain cells or plaque rupture causing a stroke event (Li *et al.,* 2018). Strokes cause around 4.1 million deaths per year, including 46% of all deaths in Europe (Nichols *et al.,* 2013). Globally, almost 17.5 million die annually because of cardiovascular diseases and this figure is expecting to increase to around 24 million by 2030 (Stroke Association, 2018). The Stroke Association also expects that people over 45, who have a first time stroke, will increase by 59 % within the next 20 years. A number of studies such as Li *et al.,* (2018) have indicated that most ischemic strokes are correlated with carotid plaque.

Carotid plaques can be classified into mainly stable and vulnerable (Finn *et al.,* 2010). Vulnerable plaques are often identified by a thin fibrous cap with a large LC and interstitial Col (Van Den Oord *et al.,* 2014), which increase the rupture risk. Stable plaques can be characterized by a dense, thick fibrous cap including smooth muscle cells in an extracellular matrix rich in type I and III Col, and tend to be asymptomatic (Finn *et al.,* 2010). The appearance of calcification in atherosclerotic plaque is prevalent in late-stage carotid plaque and grows with age (Bentzon *et al.,* 2014). The existence of Col and Ca in the plaque could increase its stiffness leading to more stable plaque (Li *et al.,* 2018). Although recent clinical practices such as carotid endarterectomy rely heavily on the degree of stenosis (Chan *et al.,*

2014a), most stroke events that occurred were not due to the lumen itself narrowing (Ammirati *et al.,* 2015). Moreover, histopathological research has found that stroke events can happen with plaques stenosis less than 30% and without any other detectible causal reason (Wasserman *et al.,s* 2005).

Non-invasive imaging techniques to evaluate the relationship between the behaviour of the plaque and the possibility of a stroke event have been improved by applying MRI, multi-detector computer tomography and ultrasound (Underhill *et al.,* 2010; Chan *et al.,* 2014). To date, however, an effective non-invasive imaging technique to distinguish vulnerable plaques in the carotid artery is still lacking.

Several researchers have attempted to study diseased blood vessels non-invasively. For instance, distinguishing between diseased and healthy coronary arteries was investigated by Biglino *et al.,* (2012) using arterial waveforms. The effect on the measured arterial waveform of Ca and LC in carotid plaque was studied by Feng *et al.,* (2015) using WIA. These studies demonstrated that plaque properties could be identified using the arterial waveform, but no evidence has been presented on how to discriminate between vulnerable and stable plaques.

Recent research findings, based on the physical testing of human carotid arterial plaques, indicated that vulnerable plaques may possess unique mechanical properties associated with their specific structures and sub-components (Cunnane *et al.,* 2016; Kobielarz *et al.,* 2020). This finding inspired a new non-invasive approach to assessing vulnerability to atherosclerosis. Specifically, the clinical significance of the arterial pulse waveform to the local physical properties of the cardiovascular system has been recognized for several decades (Xiao *et al.,* 2019). For instance, the pulsatile wave velocity, which is a function of the stiffness of the arterial wall, has been used as a clinical index to assess cardiovascular disease (Bogatu *et al.,* 2020). The behaviour of the arterial waveform interrelates with the components and mechanical

properties of arterial plaque. Here, we propose that the specific properties of vulnerable plaque should lead to unique arterial blood waveforms, which will provide an alternative route to the detection of vulnerable arterial plaques non-invasively. Recently, this author has reported the results of in vitro experiments which found a significant difference of arterial waveforms between arterial systems with vulnerable plaque (thin-cap fibroatheroma) and stable plaque (fibro-calcified) (Abdulsalam and Feng, 2019). This finding leads to the hypothesis that a unique correlation might exist between the arterial waveforms and the composition of the arterial plaque. The purpose of this chapter is to distinguish between various kinds of plaque at an early stage, 30% blockage, and inform on vulnerability of plaques by defining a relationship between the composition and arterial waveform. This was done by constructing different types of plaques, FC, FA, PR, PE, CN and TCFA, which categorized from America Cardiovascular Association and testing them in in vitro experiment in order to increase the capability of using the Non-WIA technique. In addition, the position of the plaques was shifted further from the inlet injection to reduce the effect of reflections and re-reflection that occurred in Chapter 4.

5.3. Results

5.3.1. The FC, FA, PE, PR and TCFA Plaques

The stable plaques FA and FC are illustrated in Figure 5.1 A and B, respectively. The 43% of collagen was mounted in the end side edge of the plaque and the 57% of the lipid core was placed next to it. The location of calcium, collagen and lipid of FC plaque was mounted as the same way in Chapter 4 study. The unstable plaques, however, PE, PR and CN plaques are shown in Figure 5.1 C, D and E, respectively. The calcium part of PE plaque was placed on the side edge end of the plaque and the lipid core was next to it, while the lipid core of PR plaque was mounted between the collagen, where the collagen was placed in the both edge side end of the plaque. The CN plaque was mostly calcium but the data was not collected because the fibrous cap did not bear the load of calcium although it was prepared several times but all trials

went to fail. In addition, the TCFA vulnerable plaque is illustrated in Figure 5.1 F. The 74% of collagen of TCFA plaque was mounted in the side edge and the rest of the plaque was only lipid core. The flow direction was facing the hard part of the FC and PR plaques, whereas the soft part of the FA, PE and TCFA plaque was facing the follow direction in order to study how the hard and the soft position of the plaques effect of the stable, unstable and vulnerable plaques on the arterial waveform.

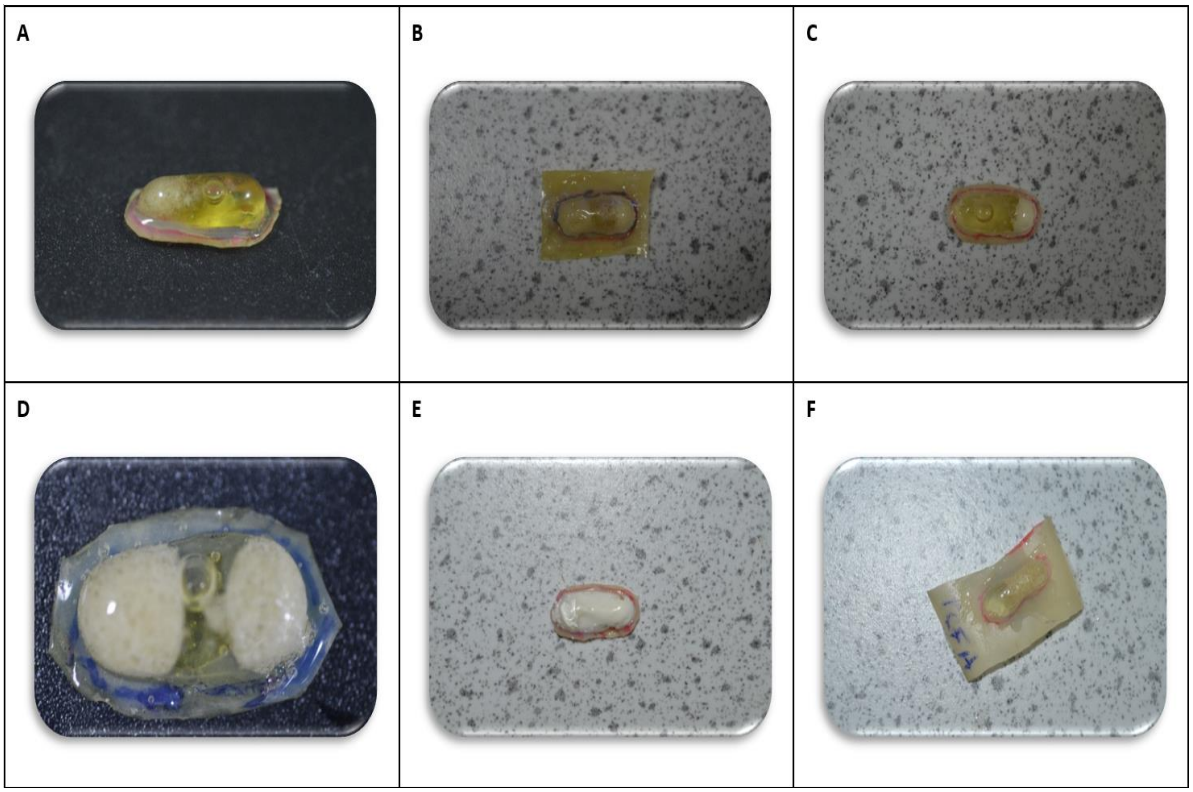

Figure 5.1 - An example of the artificial plaques that were used in Experiment 2. (A) FA stable plaque. (B) FC stable plaque. (C) PE unstable plaque. (D) PR unstable plaque. (E) CN unstable plaque and (F) TCFA vulnerable plaque.

5.3.1. The Measured Diameter and Velocity

Figure 5.2A shows the diameter of the artificial artery measured at 5 mm from the unstable (PE, TCFA) and stable (FC) plaques. The diameter measured at the same position with no plaque (healthy) is also plotted on the same graph. In this figure, the peak value of the diameter waveform was observed for the case with FC plaque, which is 42% higher than the diameter measured at the same position for healthy one. The presence of the unstable plaques also caused a slight increase of the measured peak diameter waveform by 30% for TCFA and 39% for PE plaque, respectively. The exceptional results were shown in Figure 5.2B, indicating that PR (unstable) plaque generated the highest measured diameter amplitude with 77% increase by comparing with healthy case and the lowest amplitude of diameter was found with FA plaques implemented.

The measured pulsatile velocity waveforms in the artificial artery with TCFA, FC, and PE plaques attached are presented in Figure 5.2 C. The lowest peak amplitude of the velocity waveform was observed in the system with FC plaque. Compared with the healthy condition, FC plaque caused 3.8% decrease in peak velocity. In contrast, the velocity waveforms measured with TCFA and PE plaques present are very similar to that measured for the healthy system. Figure 5.2 D shows the velocity waveform measured in the system with FA (stable), PR (unstable) plaques and healthy artery (no plaque). Here, the highest peak velocity was observed with FA (stable) plaque, while the lowest peak velocity occurred with PR (unstable) plaque. The presence of PR plaque caused an approximately 8% decrease of peak velocity compared with the healthy case.

5.3.2. Separated Forward and Backward Diameters

5.3.2.1. Wave Speed Determination (No Plaque)

Figure 5.3 shows how the wave speed was determined using the non-invasive ln(DU)-loop technique. The artificial artery diameter was 9.5 mm, which responded to the single pulse from the pulsatile blood pump. The early systolic period (initial part of the loop) is visibly linear from the beginning of injection. The linearity of the early systolic period means that forward waves only exist along the straight line whose gradient corresponds to 1/2 c. The indicated line corresponded to c = 3.5 ms^{-1} and this value was used to separate the measured velocities and diameters of no plaque, FC, TCFA, PE, FA and PR plaques.

5.3.2.2. The Separated Waveforms with FC, TCFA and PE Plaques

The separation of the diameter for three types of the plaques are illustrated in Figure 5.4 A-D. Compared with the healthy condition, an increase in the backward diameter was observed for all three types of plaque. FC plaque with components consisting of LC (47%), Ca (6%) and Col (47%), causes +39% of increase of diameter (from 0.44 mm to 0.61 mm), the TCFA plaque was composed of LC (26%) and Col (74%) and resulted in a 30% of increase in diameter (from 0.44 mm to 0.57 mm). PE plaque composed of LC (70%), Ca (18%) and Col (12%) resulted in an increase in diameter compared to the healthy case of 23% (from 0.44 mm to 0.55 mm). We see the plaque with the highest LC content corresponded to the lowest value of diameter.

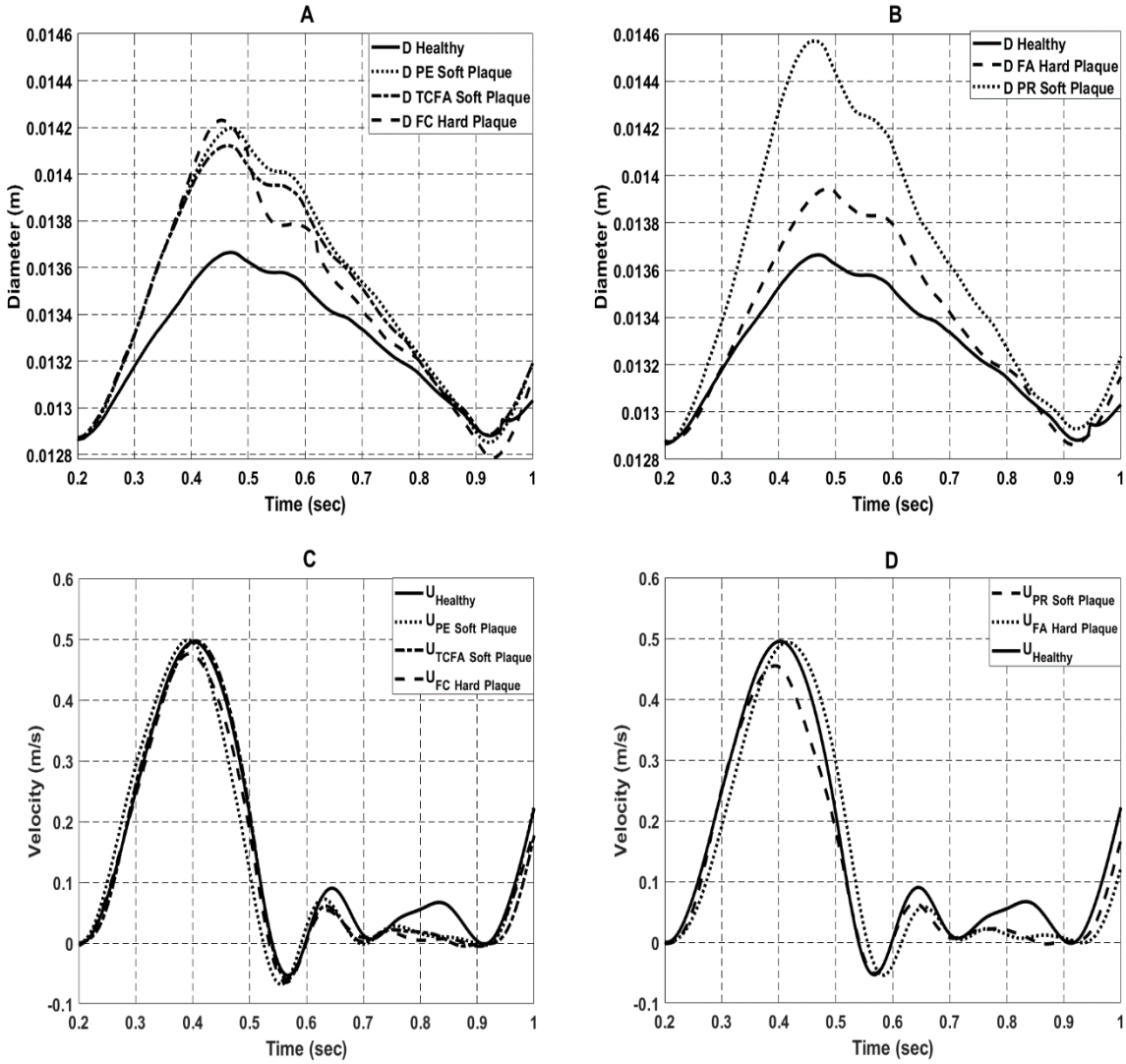

Figure 5.2 - (A) The measured diameter for stable plaque (FC), unstable plaque (PE) and vulnerable plaque (TCFA) and healthy case; (B) the measured diameter for stable (FA) and unstable (PR) plaques, and the healthy case; (C) the measured velocities for stable plaque (FC), unstable plaques (PE) and vulnerable plaque (TCFA) and the healthy case; (D) the measured velocities for stable (FA) and unstable (PR) plaques and the healthy case. (A), higher measured diameter is observed for FC stable plaque, following the PE unstable plaque and then the TCFA vulnerable plaque. The plaque composition here is the main cause of this differences because the flow direction was facing the stable part of FC and PE plaques, while in TCFA plaque, the soft part was facing the flow direction. (B), the PR plaque generate higher amplitude than FA plaque because the flow direction was encountering the stable part of PR plaque which is 78% of collagen, whereas the soft part of the FA plaque (57% LC) was facing the flow direction.

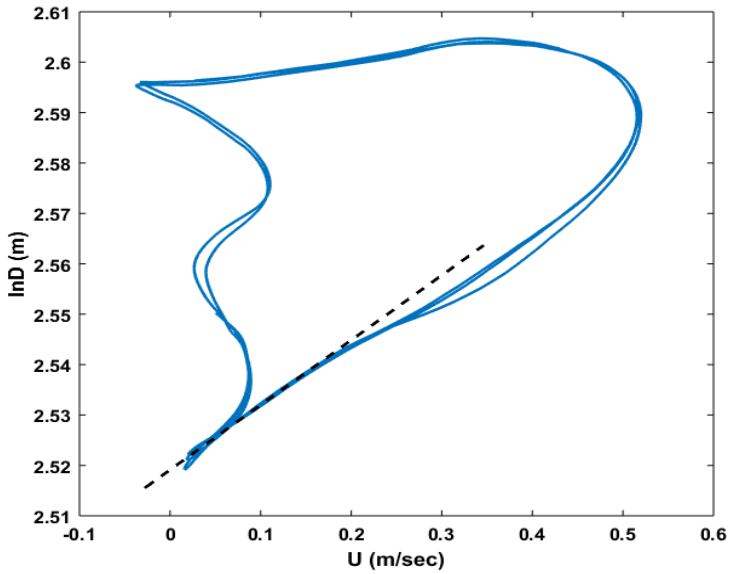

Figure 5.3 - The wave speed determined by the non-invasive ln(DU)-loop technique from experiment. The linear portion, dashed line, is visible and its gradient corresponds to 0.5c. The value of c is 3.5 m/s.

5.3.2.3. The Separated Waveform with PR and FA Plaques

Figure 5.5 shows the results of waveforms associated with the PR and FA plaques. The composition of PR unstable plaque in this study, including 22% of LC, 0% of Ca and 78% of Col, generated 0.61mm backward diameter amplitude. By comparing with those observed in healthy condition, PR plaque causes 57% of increase in diameter. The backward diameter of FA plaque, which contained of 57% of LC, 0% of Ca and 43% of Col, increased slightly at 9% compared with healthy case.

The results for the measured and separated waveforms related to the PR and FA plaques are out of our expectation. We expected that FA (stable) plaque caused the stronger reflection, accordingly, leading to the higher diameter waveform. While, the lower diameter waveform is expected with PR plaque due to the potential less strong reflection to be generated by the unstable plaque. The phenomena opposite to our expectation with higher diameter related to PR plaque and the lower diameter linking with FA plaque, was observed among all of the tests.

Therefore, it is speculated that the underpinning mechanism lies in the compositions of the plaques, particular the percentage of typical components.

5.3.2.4. Non-invasive Wave Intensity (WI)

The WI of the healthy (no plaque) and stable plaques are illustrated in Figure 5.6. Figure 5.6A and 5.6A$^{/}$ illustrate the healthy WI and its early systolic period magnification. The stable plaques, FA and FC, with their enlargements are exhibited in Figures 5.6B & 5.6B$^{/}$ and Figures 5.6C & 5.6C$^{/}$, respectively. Figure 5.7 illustrates the PR and PE unstable plaques and TCFA vulnerable plaque. Figures 5.7A, 5.7B and 5.7C represent the PR, PE and TCFA plaques with their magnifications. From these results, a strong evidence was found at the early systolic period between the arterial stable and unstable plaques compared with healthy case. As can be seen in no plaque and unstable plaques, no reflection was observed in this period, Figures 5.6A$^{/}$, 5.7A, 5.7B and 5.7C. However, Figures 5.6B and 5.6C show a significant reflection in the early systolic period for FA and FC plaques (stable plaques). It is also noted that the FA plaque produced higher reflection than FC plaque. Therefore, the arterial stable plaques (FA and FC) generated a significant backward WI reflection at early systolic period, whereas the unstable plaques produced insignificant backward WI reflection or much lower reflection than that in stable plaques.

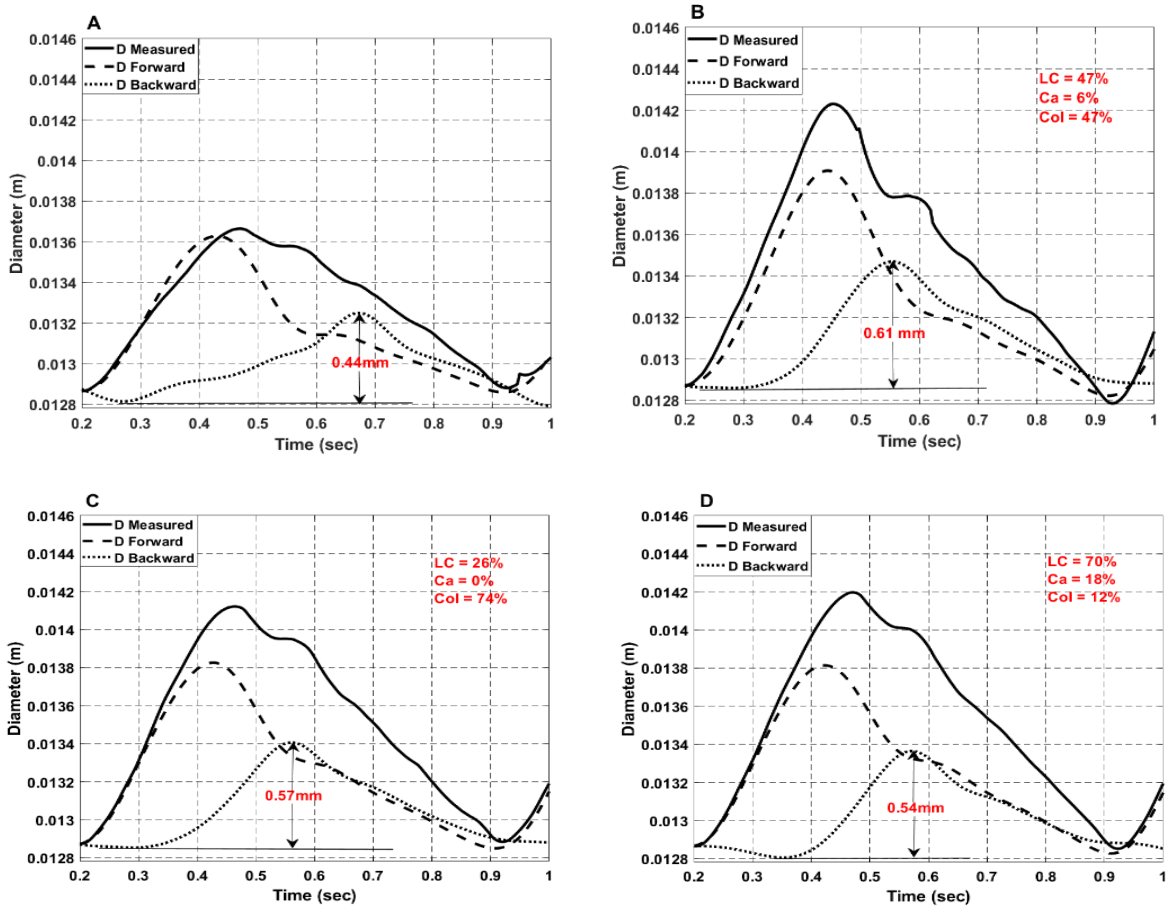

Figure 5.4 - Measured, forward and backward arterial diameters in (A) the healthy tube, (B) tube with stable plaque (FC), (C) vulnerable plaque (TCFA) and (D) unstable plaque (PE). The solid, dashed and dotted lines represent the measured, forward and backward waves, respectively. The backward amplitude of FC plaque in (B) is the highest because the FC plaque was stiffest, while the backward diameter of the healthy one (A) is the lowest due to no plaque implemented. Although the PE plaque (D) has 12% collagen and 18% calcium, which consider as one of the stability factors, its backward amplitude is less than TCFA plaque (C). This is because the PE plaque has plenty of lipid core (70%), while TCFA plaque has only 26% of lipid core and 74% of collagen.

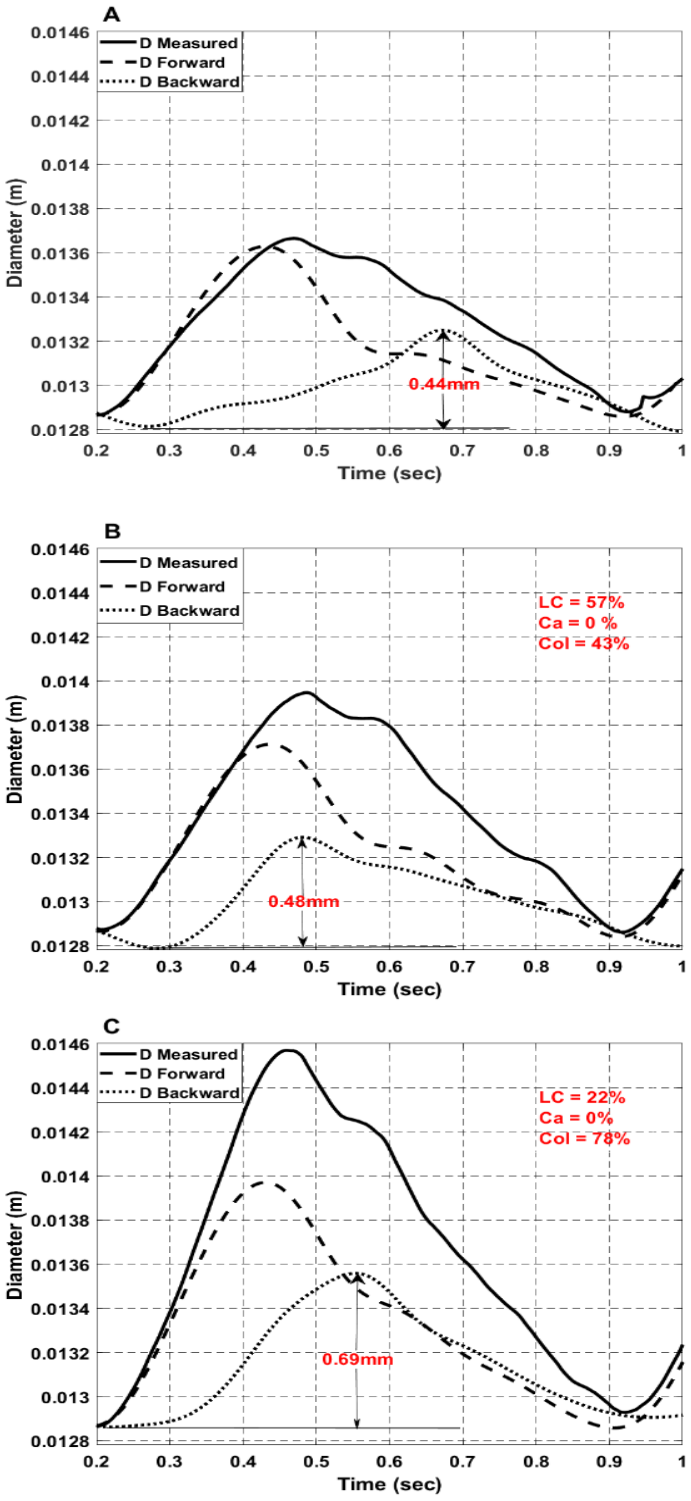

Figure 5.5 - The measured, forward, and backward diameter waveforms for (A) the no plaque condition, (B) stable plaque (FA), and (C) unstable plaque (PR). The solid line on the three plots represents the measured diameter, the dashed line the forward wave and the dotted line the backward wave. Figure 5.5 B and C show PR unstable plaque generated higher peak backward diameter amplitudes than FA stable plaque. The reason of this is because the PR plaque has 78% of collagen which was facing the flow direction, while the FA plaque has higher lipid core than PR plaque and lower proportion of collagen than PR plaque.

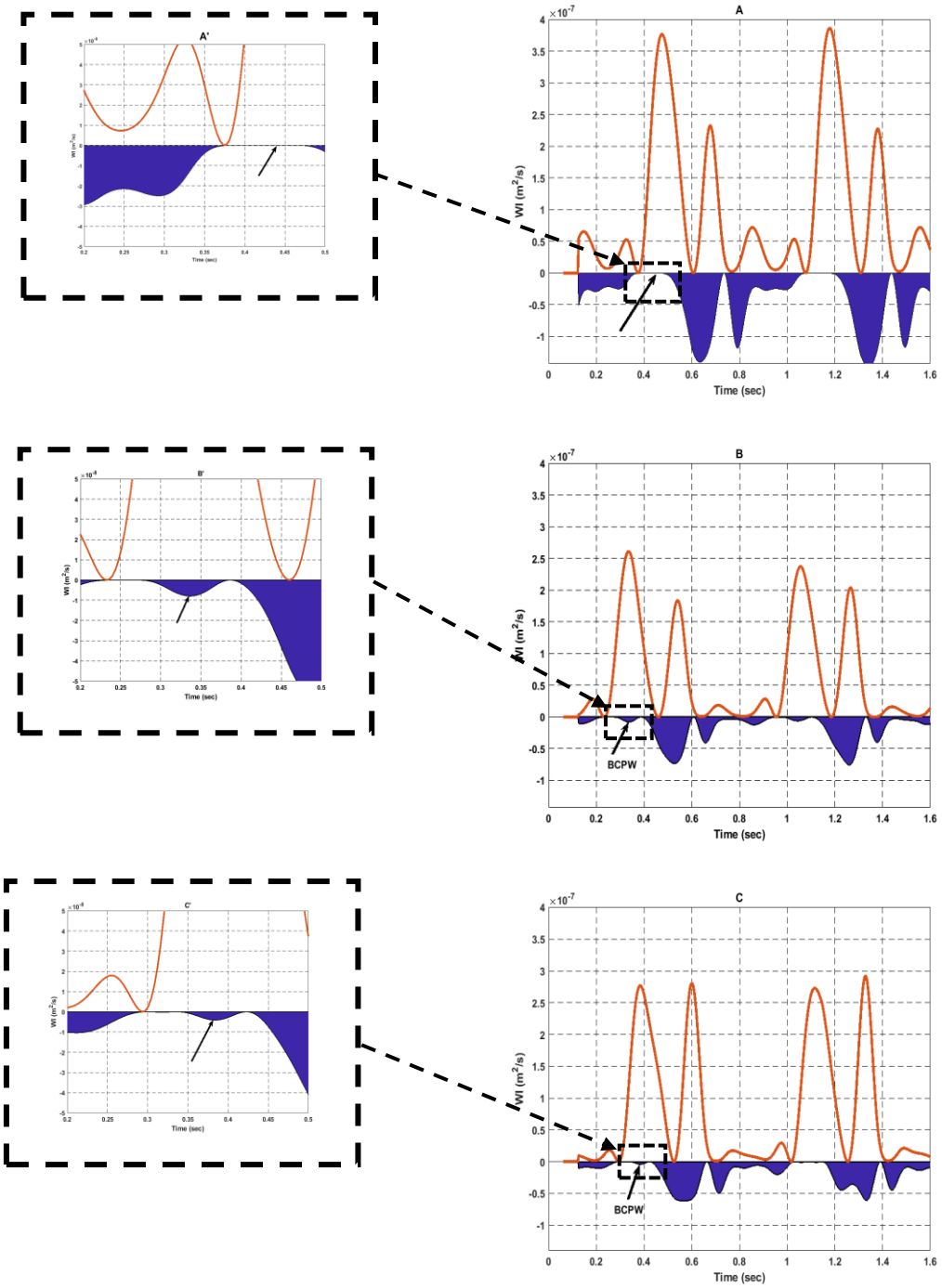

Figure 5.6 - The separation of non-invasive wave intensity (WI) into forward and backward for three scenarios: (A and A/) healthy with no plaque, (B and B/) $_{n}WI$ for stable plaque (FA), and (C and C/) WI for stable plaque (FC). The orange line represents the forward WI and the blue area represents the backward WI. These results indicate that the stable plaques caused considerable backward reflections in the early systolic period with the FA plaque producing greater reflection than FC plaque. This might be from their fibrous cap thickness as the fibrous cap thickness of FA plaque was thicker than FC plaque. No reflection in the early systolic period was observed in the healthy case because no plaque was implemented.

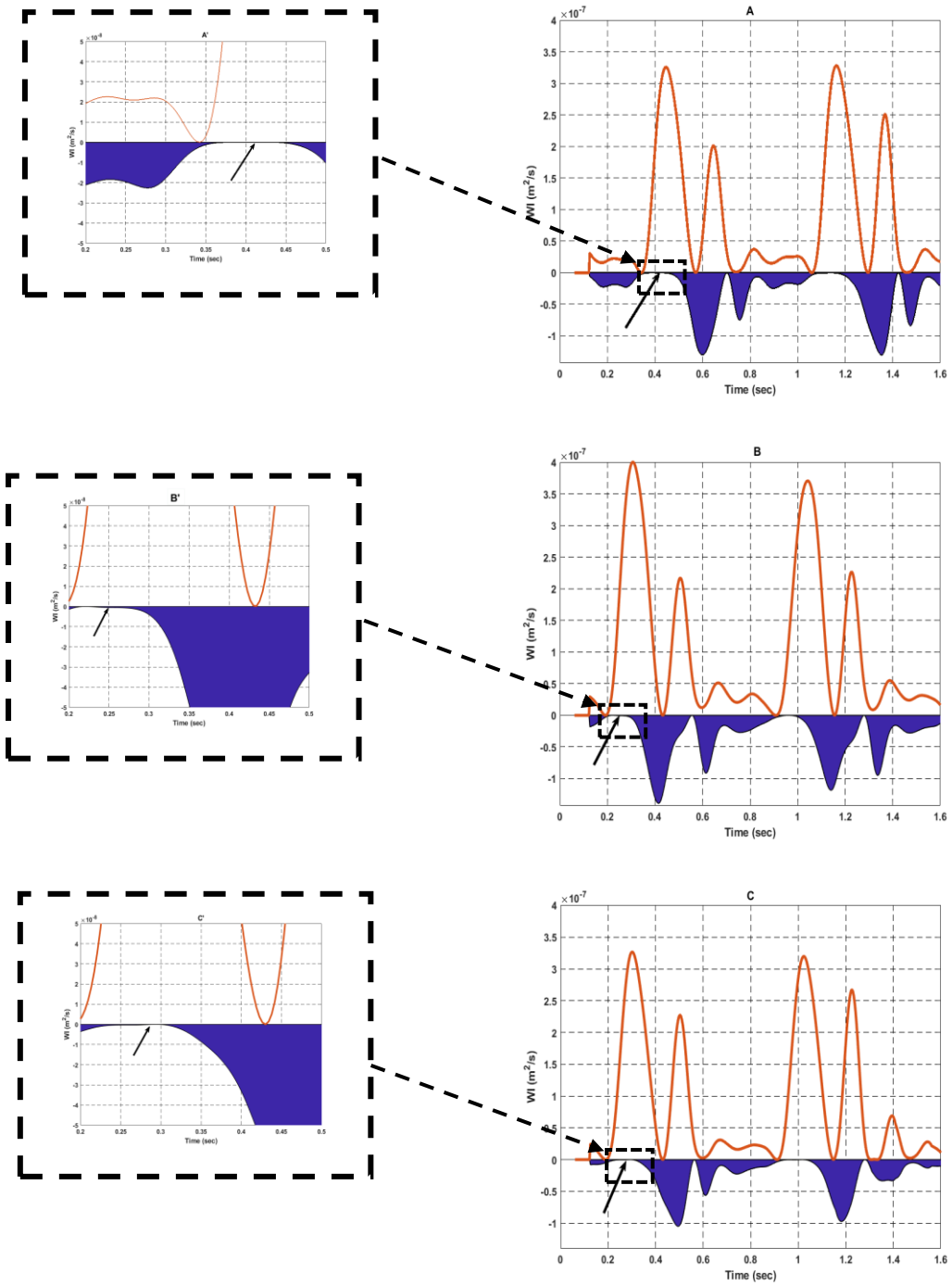

Figure 5.7 - The separation of non-invasive wave intensity ($_{n}$WI) into forward WI and backward WI for three scenarios for two unstable plaques; (A and A$^{/}$) for PR plaque, (B and B$^{/}$) for PE plaque and one vulnerable plaque (C and C$^{/}$) for TCFA plaque. The orange line represents the forward WI and the blue area represents the backward WI. We see that these plaques did not cause any substantial backward reflection in the early systolic period. In (C) the, WI for TCFA plaque shows little reflection occurred in the early systolic period. The absent or the insignificant reflection of the unstable and vulnerable plaques could be from their fibrous cap thickness as their fibrous cap thicknesses were too thin.

5.3.3. Statistical Analysis Results

The results of the correlations between backward diameter amplitude with Col, LC and Ca are presented in Figure 5.8. In Figure 5.8 A, we see a strong positive correlation (R = 0.75) between backward diameter amplitude and Col. In addition, a strong negative correlation (R = -0.82) was found between backward diameter and LC, see Figure 5.8 B. However, Figure 5.8 C reveals no significant correlation between Ca and backward diameter (R =- 0.3). These results indicate that the higher the percentage of Col in the plaque the greater the backward diameter reflection, while the higher the percentage of LC the lower the backward diameter reflection.

5.4. Discussion

The arterial system in the human body is very complex and its properties change from one place to another, particularly at bifurcations which can cause reflections that affect the propagation of pressure pulses and change the arterial diameter during the cardiac cycle (Parker, 2009). The existence of arterial plaque could increase the number of reflections and make the waveform more complex. It is therefore very important to understand wave behaviour in the arterial system in order to understand how arteries transmit pressure pulses. This can be done by separating the measured waves into forward and backward travelling waves to extract more information from the measured waveforms. The forward waves (positive direction) are mostly caused by the heart, while the backward waves (negative direction) are mostly due to reflections (Parker, 2009). To separate these waves, a knowledge of wave speed is required to use in the non-WIA technique. There is growing evidence that the composition of arterial plaque could be characterized by the arterial waveform which may lead to identifying plaque vulnerability, (Biglino *et al.*, 2012; Feng *et al.*, 2015; Li *et al.*, 2018; Abdulsalam and Feng, 2019). This study attempts to investigate the effect of plaque composition on arterial waveform using different types of plaques (FA, FC, PR, PE and TCFA) (Butcovan *et al.*, 2016) in in vitro experiments, see Figure 3.1 in Chapter 3.

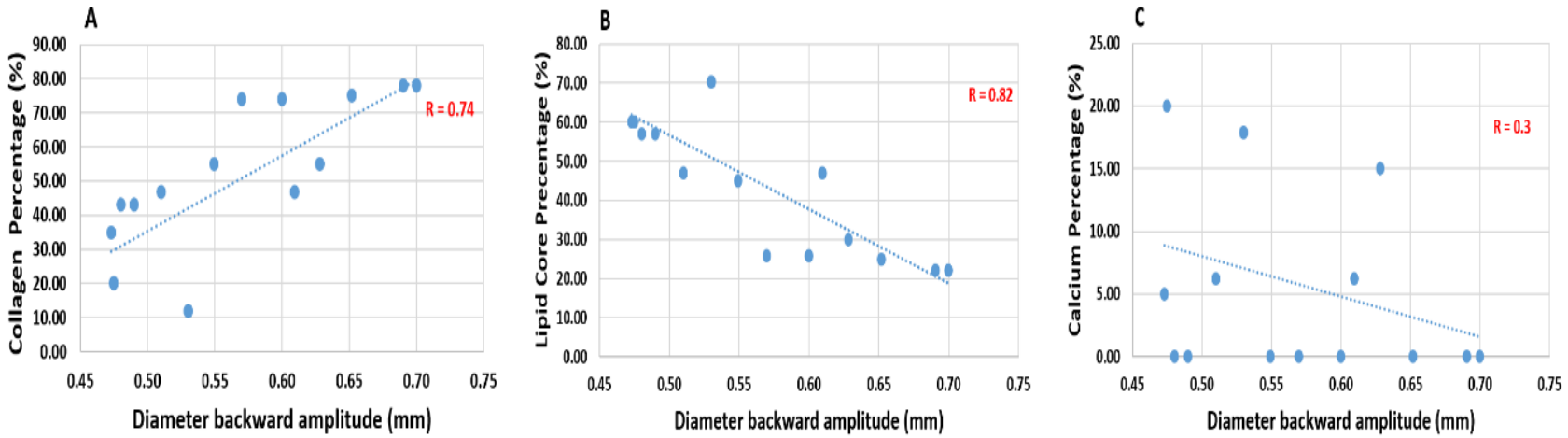

Figure 5.8 - The effect of arterial plaque, Col, LC and Ca on arterial backward wall movement. (A) Shows a significant positive correlation (R=0.74) between Col% and backward diameter amplitude. (B) illustrates a negative correlation (R=-0.82) between the LC% and amplitude of the backward diameter. (C) Demonstrate that the effect of Ca% on arterial backward diameter had a small and not very significant negative correlation. This indicate that plaques with higher percentage of collagen generate higher backward reflection, while plaques with higher percentage of lipid core generate lower backward reflection leading to predict that the higher collagen percentage the more plaque stability and the more plenty of lipid core the less plaque stability.

One observation of this study is that the measured diameter in the presence of stable plaque was larger than for unstable plaques. For example, the presence of FC stable plaque produced a larger value of the diameter than PE and TCFA unstable and vulnerable plaques, respectively, see Figure 5.2A. However, the measured pulsatile velocity in the presence of unstable plaques was greater than for stable plaques.

A possible explanation is that the mechanical properties of the plaques, particularly arterial plaque stiffness. Stable plaques contain greater proportions of Ca and Col than unstable plaques. As can be seen from Table 3.1, FC plaque contains 47% Col and 6% Ca, whereas PE has 12% Col and 18% Ca, and TCFA plaque contains 74% Col and 0% Ca. The strong reflection generated by FC led to a higher peak amplitude of the diameter compared with PE and TCFA plaques. However, we observed that PR, a unstable plaque, generated higher amplitude than FA, a stable plaque (Figure 5.1 B). The unstable and stable classifications of PR and FA are due to (Narula *et al.*, 2013). This unexpected finding could be attributed to their compositions.

The separated forward and backward diameters for the stable and vulnerable plaques with different components are shown in Figure 5.4 and Figure 5.5. The correlations between the percentages of each component and the amplitude of the backward diameter are plotted in Figure 5.8. A significant positive correlation was found between Col% and the backward diameter amplitude, and a significant negative correlation between LC% and amplitude of the backward diameter. This implies that the higher the percentage of collagen in PR plaque the larger the amplitude of the backward diameter, while the higher the percentage of lipid core in the plaque the lower the amplitude of the backward diameter. Therefore, plaque composition, particularly LC% and Col%, has a direct effect on the amplitude of the backward diameter.

The findings from this study indicate the possibility of using arterial waveforms to detect the compositions of stable and vulnerable plaques in clinical settings. Currently, in clinical practice, the narrowing of blood vessels is measured using ultrasound echo tracking and Doppler sonography, which allow measurement of the diameter of arterial wall and velocity of the blood non-invasively. It has been demonstrated that non-WIA is a reliable approach to analyse the carotid arterial waveforms using ultrasound echo and a Doppler system (Pomella *et al.,* 2017a). Thus, the approach to detect the compositions of stable and vulnerable plaques developed in this study has clinical significance. The approach can be employed by cardiovascular/vascular clinicians to distinguish stable and vulnerable plaques, providing guidance for stratification of the victims of atherosclerosis for surgery.

Wave Intensity in Figure 5.6 A demonstrates that the forward compression wave, produced by ventricular contraction (Raphael *et al.,* 2016), appears as the first positive peak of the early systolic period. Then a backward compression wave, negative peak, caused by a reflection that occurs mid-systole when $dD > 0$ and $dU < 0$. Finally, the forward expansion wave, the second positive peak, correlates with the relaxation of the left ventricle at the end of the systole (Feng and Khir, 2010; Pomella *et al.,* 2017).

By using the non-WIA technique, we found stable plaques generated four main waves in the systolic period, as shown in Figure 5.6 B and 5.6 C. Two of them appear in the early systole including: the first positive peak from the contraction of the heart and the first backward negative peak caused by reflection from the stable plaque (Backward Compression Plaque Wave, BCPW). The other two peaks are the second backward negative peak, which is due to circulation reflections located mid systole and the second positive peak, caused by the deceleration of the heart at the end of the systole. However, the existence of unstable plaques indicated that no significant BCPW were observed in the early systolic period. This may

indicate that the fibrous cap thickness may be the cause of the BCPW because the BCPW of FA plaque, which has a fibrous cap thickness of 0.35mm, was greater than the 0.27 mm thickness for FC plaque.

5.5. Conclusion

This chapter investigated the effect of artificial plaque composition on arterial waveforms. The results show that plaques with low LC% and higher values of Col% and Ca% generate higher backward diameter amplitudes. A strong positive correlation was found between Col% and backward diameter amplitude, and an even stronger negative correlation between LC% and backward diameter amplitude. The strong correlation between the composition of the plaques with the backward waveforms observed in this study demonstrated that the components of the arterial plaques could be distinguished by the arterial waveforms. In addition, stable plaques generated a significant backward wave intensity, while no significant backward wave intensity was observed in unstable and vulnerable plaques. This finding might lead to a potential novel non-invasive clinical tool to determine the compositions of the plaque and distinguish stable and vulnerable arterial plaques at an early stage. However, severe plaque stenosis (between 50 and 90%) should be performed for further investigation about the effect of plaque composition on the arterial waveform

In addition, further investigation and experimentation into the effect of Ca% together with Col is strongly recommended in order to give a clearer picture of its effect on arterial backward amplitude.

CHAPTER 6

The Correlation between Plaque Composition and Arterial Waveforms for Severe Arterial Stenosis

6.1. Introduction

Cardiovascular disease considers the most common reason for fatalities in developed countries (Taylor and Figueroa, 2009), which causes a narrowing in the blood vessel because of the deposit of fat carried through the blood stream on the inner face of the artery (Razavi *et al.,* 2011). This fatty substance increases the degree of stenosis of the artery, causing a decrease of the fibrous cap thickness leading to plaque rupture (Weber and Noels, 2011). The rupture of the plaque in the coronary artery could cause a myocardial infarction, while a similar incident in the carotid artery would cause a stroke (Weber and Noels, 2011).

Several investigations, regarding plaque features, have found that the unstable plaques are more likely to rupture and cause a stroke than stable plaques (Butcovan *et al.,* 2016). Recently, numerous studies have found that plaque composition could give a more predictable biomarker of a stroke event than the degree of stenosis, which may reduce the risk of a stroke incident (Naghavi *et al.,* 2003; Saba *et al.,* 2014). For example, the percentage of LC and the thickness of the fibrous cap when the degree of stenosis was between 50% and 79%, as identified using MRI carotid scans, were found to predict the likelihood of high-risk stroke (Xu *et al.,* 2014). Although this study improved the classification of future stroke risk beyond artery stenosis, the effect of Ca on the plaque was not conducted in this study. MR angiographic (MRA) is widely used to identify the ulcerations in lumens with a degree of stenosis between 50% and 90% (Underhill *et al.,* 2010). However, MRA cannot depict the plaque burden, which reduces the likelihood of detection of high-risk plaque composition (Kerwin *et al.,* 2013). A multi-contrast MRI technique was utilized by Fayad and Fuster, (2001) to characterize vulnerable plaques in

terms of LC, fibrous cap and Ca. The main limitation of this technique was the inhomogeneity of the intensity in the tissue due to imaging artifacts (Ziegler *et al.*, 2020). Although minimizing the risk of plaque rupture was investigated by detecting the carotid vulnerable plaques Contrast-Enhanced Ultrasound technique (Partovi *et al.,* (2012), Motoyama *et al.,* (2019) and Schinkel *et al.,* (2020)), using Contrast-Enhanced Ultrasound technique to detect the carotid vulnerable plaque was questioned by D'Oria *et al.,* (2018).

In terms of surgical intervention, a common clinical practice used for severe carotid stenosis is endarterectomy which helps to decrease the danger of stroke(Ozawa *et al.,* 2016). This surgical intervention relies heavily on symptomatology and the degree of blockage (Chan *et al.,* 2014b). However, some cerebrovascular events have been found with degree of stenosis less than 30% without any symptoms (Li *et al.*, 2018). Thus, a severe degree of stenosis of the arterial plaque may not always be the key factor in detecting the risk of a stroke (Xu *et al.,* 2014). Therefore, detecting high risk carotid plaque remains elusive, but is necessary to prevent a patient from a stroke event. However, identifying plaque features in the severe stenosis stage could reduce stroke risk and help to determine the right measures to avoid a stroke event. The main aim of this chapter is to investigate the severe blockage of the vessel (75%) in order to find the correlation between the compositions of plaques and arterial waveforms. In addition, the plaques and measurements were shifted to reduce the reflection and re-reflection that occurred in the previous study (Chapter 5) at 300mm for the inlet injection.

6.3. Results

6.3.1. FC, FA, PE and TCFA Plaques

Figure 6.1 A shows the different types of fibrous caps of the used plaques. Figure 6.1 B, C, D and E shows the procedure of preparing the FC stable plaque and the position of calcium, collagen and lipid core. Figure 6.1 F shows the four types of plaques that were used in the experiment. The CN plaque was tested again in this study, but we could not collect the data

from it because again the fibrous cap could not bear the load of calcium. The flow direction was facing the collagen part of the TCFA and PR plaques, whereas the soft part of the FA plaque and the calcium part of FC plaque was facing the follow direction in order to study how the collagen, calcium and the soft position of the plaques effect on the arterial waveform.

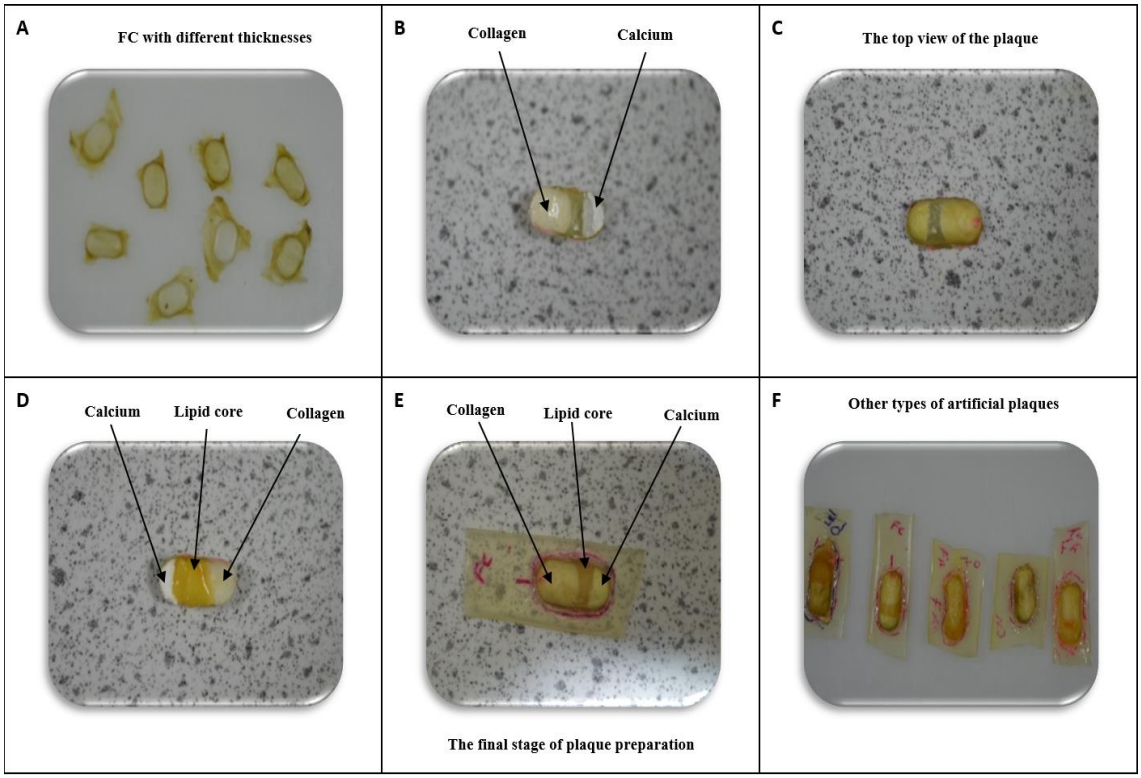

Figure 6.1 - An example of fabrication of one of the artificial plaques prepared in experiment 3. (A) Shows the final stage of fibrous cap preparation. (B) Shows the collagen and calcium mounted in the FC. (C) Presents the top view of plaque without the LC. (D) Shows the LC three days after inserting the collagen and calcium. (E) Illustrates the whole plaque with its main components LC, Ca and Col. (F) Displays some of the plaques used in the experiment

6.3.2. Measured Pressure, Diameter and Velocity with No Plaque Present

Figures 6.2A and B show the pressure and arterial wall movement measured with the 6.35 mm artificial blood vessel with no plaque present. It is clear that the shape of the pressure wave is very close to that for the diameter, indicating a linear relationship existed between pressure and diameter, as found by Niki *et al.*, (1999) in a study to derive the pressure waveform of the carotid artery by scaling the waveform to artery diameter. The velocity profile was measured simultaneously at the same location (Figure. 6.2C). The healthy pressure ranges between 70 to 135 mmHg, while the diameter changes from 7.5 mm to 8.28 mm within one cardiac cycle. The velocity of the pulsatile flow ranges from -0.11 to 0.64 ms^{-1}.

6.3.3. Measured Diameters and Velocities with Plaques

Figure 6.3A shows the measured diameter of the artificial blood vessel for four types of plaques, PR (unstable, dotted line), TCFA (vulnerable, solid line), FA (stable, centre line) and FC (stable, dashed line). The measurements for these plaques were collected at the same location as for the healthy scenario. This figure shows that the measured peak diameter waveform of PR and TCFA plaques have nearly the same shape. In addition, they are higher than the FC and FA plaques, (Table 6.1). The highest peak velocity waveform was observed in PR and TCFA unstable and vulnerable plaques, respectively and their trend shapes were very similar.

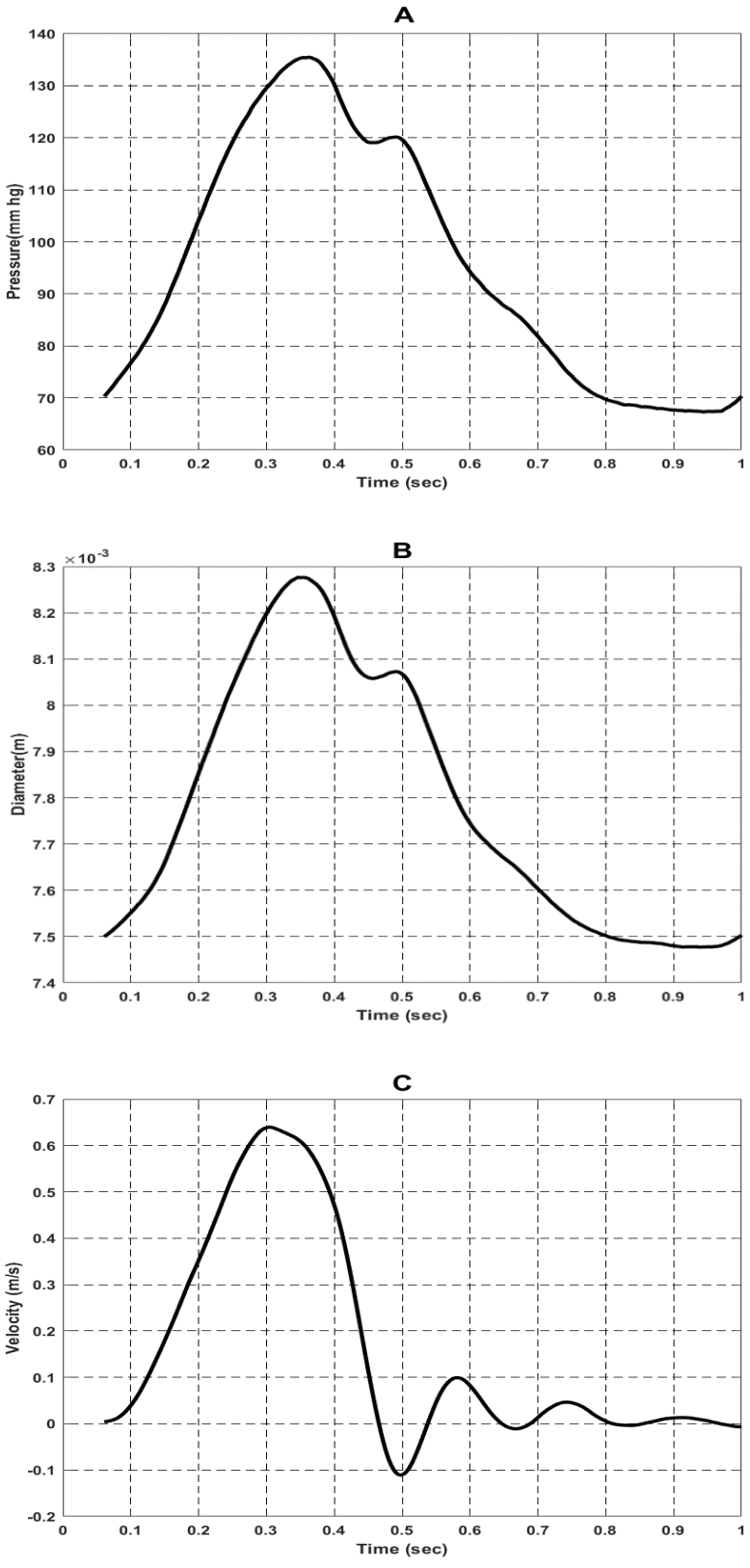

Figure 6.2. Pressure, diameter and velocity measured 30 cm away from the inlet with no plaque present. (A) The measured pressure ranges between 70 to 137 mm Hg, while (B) the measured diameter starts at 7.5 mm and increases to 8.28 mm. (C) The shape of velocity waveform is similar to the waveform in a human carotid artery with the peak velocity at 0.62 ms^{-1}(Masuda *et al.,* 2013).

In comparison with the no plaque case, the PR and TCFA plaques caused a noticeable increase in the measured diameter and velocity waveforms, while the FA and FC plaques generated only a very slight increase in diameter and velocity waveforms compared with the no plaque case. These results indicate that PR and TCFA plaques generated higher measured diameter and velocity amplitudes than the FA and FC plaques.

6.3.4. Wave Separation

6.3.4.1.Diameter Separation (Healthy, Stable and Unstable Plaques)

Figure 6.4A-E illustrates the separation of the measured diameter into its forward and backward components for the healthy case and all plaque types. It was observed that there is an increase of the backward diameter for all plaque types compared with the healthy scenario. A significant increase in the amplitude of the backward diameter was observed in the case of stable plaques with 58.5% and 36.5% increase for FC and FA, respectively (Table 6.1). PR and TCFA vulnerable plaques caused 18% increase in backward diameter. The backward amplitude of unstable plaques are lower than stable plaques, which agrees with Abdulsalam and Feng (2021) results although their blockage degree was 30%.

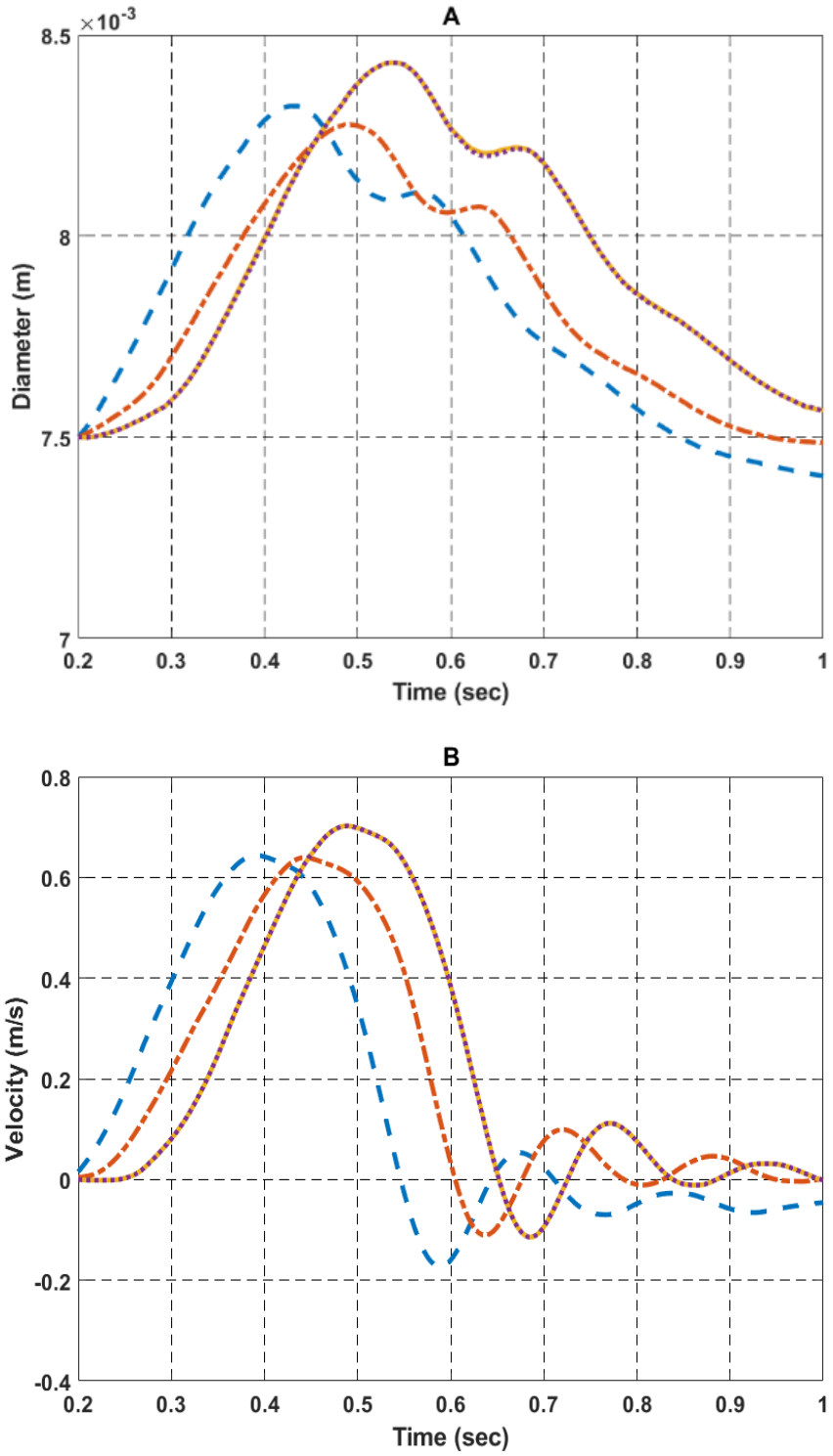

Figure 6.3 – (A) measured diameters and (B) measured velocities for FC stable plaque, dashed blue line, FA stable plaque, central orange line, TCFA vulnerable plaque, solid yellow line, and PR unstable plaque, dotted purple line. The shape and magnitude of the diameter waveforms with PR plaque were similar to those for TCFA plaque (B). This is because the composition of TCFA and PR plaque are nearly similar and soft part for both of them were facing the flow direction.

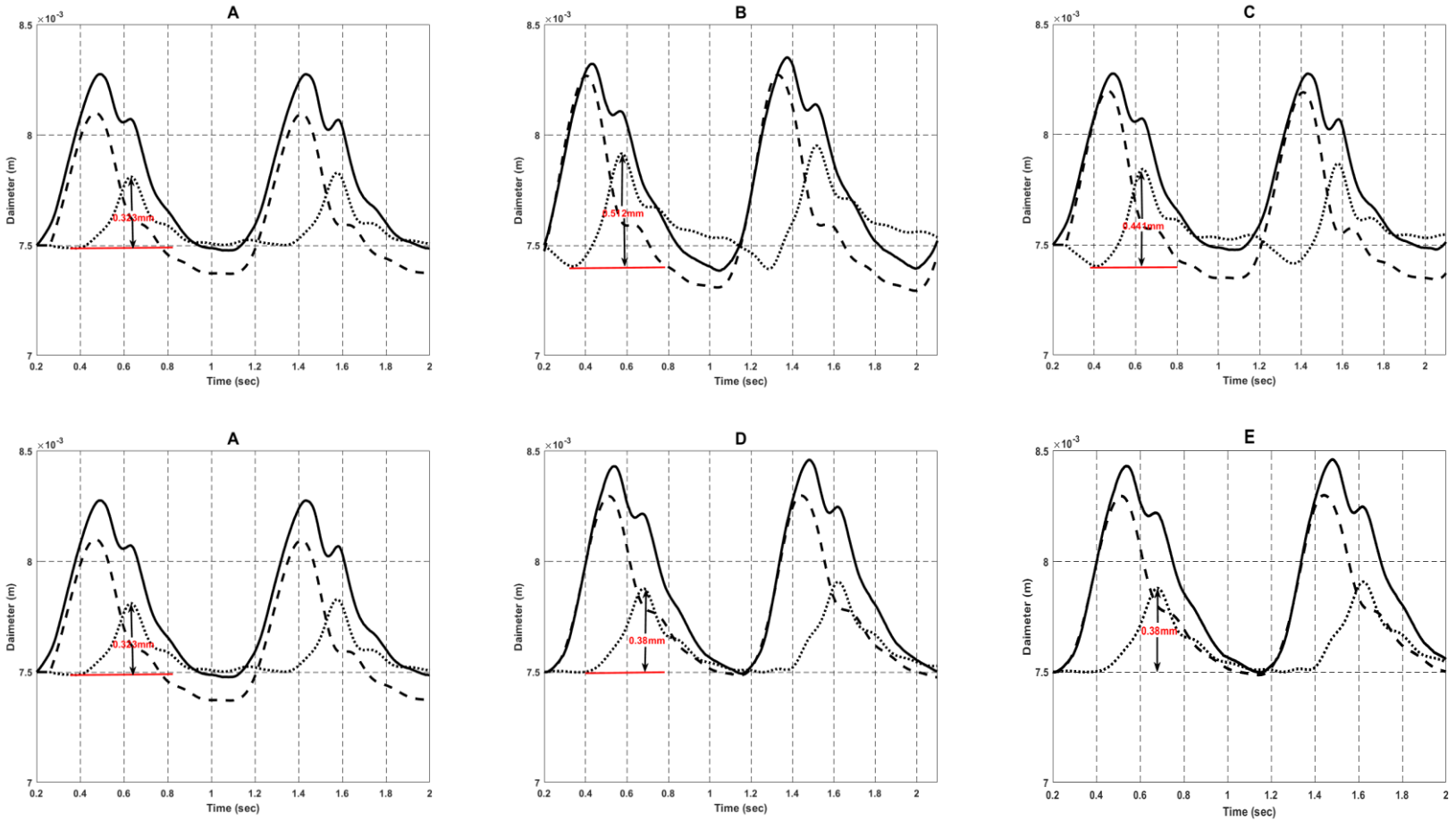

Figure 6.4 - The measured diameter (solid line), forward diameter (dashed line), and backward diameter (dotted line) for (A) healthy vessel, (B) vessel with FC plaque, (C) vessel with FA plaque, (D) vessel with TCFA plaque, and (E) vessel with PR plaque. The backward diameter of stable plaques FC&FA generate higher amplitude than PR unstable and TCFA vulnerable plaques because the stable plaques was facing the stable part of plaque, whereas the unstable and vulnerable plaque was facing the soft part of the plaque. The backward of PR and TCFA plaque (D&E) amplitude is similar because their compositions were nearly the same.

Table 6.1 - shows the increase in measured (D) and backward (D_-) wall diameter for all four types of plaque compared with no plaque case.

Plaque type	**Increase in amplitude diameter %**	
	D %	D_- %
FC (Stable)	14	58.5
FA (Stable)	1.3	36.5
PR (Unstable)	19	18
TCFA (Vulnerable)	18	18

6.3.4.2.Non-invasive Wave Intensity ($_nWI$) Separation

The forward and backward components of $_nWI_{\pm}$ in the healthy vessel (no plaque), and the diseased vessel with stable and unstable plaques are illustrated in Figure 6.5A-E. It was observed that for both the healthy vessel and vessels with attached unstable PR and vulnerable TCFA plaques, no significant backward wave intensity, $_nWI_-$ was observes during the early systolic period (Figure 6.5A, D & E). In contrast, the vessels with attached stable plaques, FA and FC, the backward wave intensity, $_nWI_-$, was clearly noticeable in the early systolic period (Figure.6.5B & C). These findings indicate that unstable and vulnerable plaques, PR and TCFA, generated lower amplitude reflected waves in comparison with the stable plaques, FA and FC.

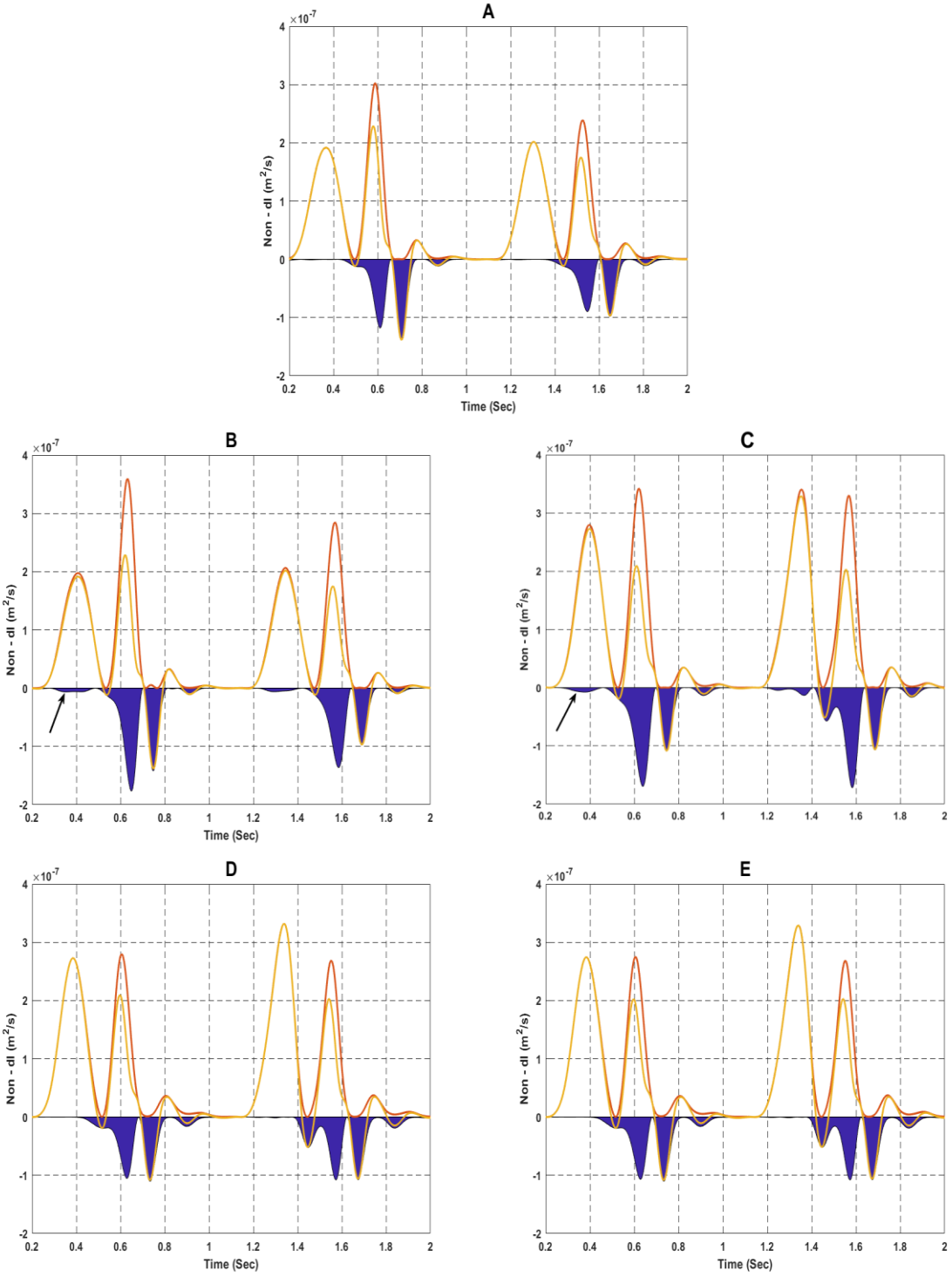

Figure 6.5 - The separation of WI into its forward and backward components: (A) healthy condition, (B) with stable plaque FA, (C) with stable plaque FC, (D) unstable plaque PR, and (E) unstable plaque TCFA. The yellow line represents the measured wave intensity, the orange line the forward wave intensity and the blue area the backward wave intensity. These results indicate that the stable plaques generate significant backward reflections in the early systolic period with the FA plaque producing greater reflection than FC plaque (B&C). This might be again from their fibrous cap thickness. However, no reflection in the early systolic period was detected in PR and TCFA plaques, which could be from their fibrous cap thickness as their fibrous cap thicknesses were too thin.

6.3.5. Statistical Analysis Results

Figure 6.6 shows the correlations between backward diameter amplitude with Col and LC. A strong positive correlation with R = 0.76 was found between backward diameter amplitude and LC (Figure 6.6A). Moreover, Figure 6.6B reveals that there is a strong negative correlation with R = -0.85 between backward diameter and Col. These results indicate that the higher the percentage of Col in the 75% stenosis plaque the lower the backward diameter reflection, whereas the higher the percentage of LC the higher the backward diameter reflection. However, these results is contrary with correlation results in Chapter 5 because the correlation between backward diameter amplitude and LC was significant negative, while a significant positive correlation was found between backward diameter amplitude and Col.

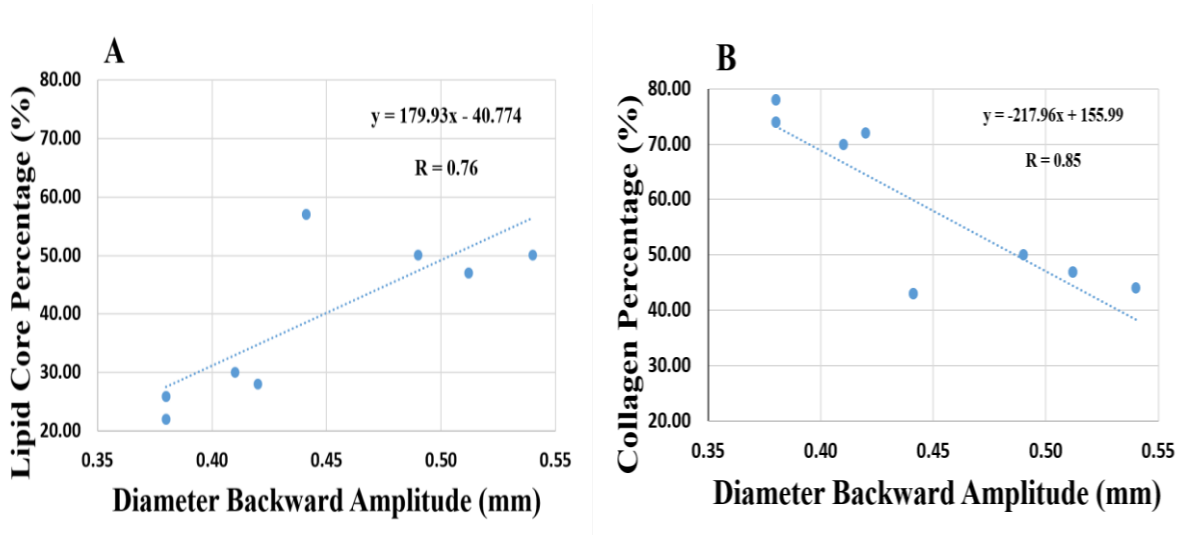

Figure 6.6 - The effect of arterial plaque, Col and LC on arterial backward wall movement. (A) Shows a significant positive correlation (R=0.76) between Lipid Core % and backward diameter amplitude. (B) illustrates a negative correlation (R=-0.85) between the LC% and amplitude of the backward diameter. This result indicate that 75% blockage plaques with higher percentage of collagen generate lower backward reflection, while plaques with higher percentage of lipid core generate higher backward reflection. The results here is contrary with the results of previous Chapter (30% stenosis), which need further investigations.

6.4. Discussion

As discussed in Chapter 5, if the arterial plaque composition could be identified by its arterial waveform, that might allow characterisation of plaque vulnerability (Abdulsalam and Feng, 2021). This study aims to investigate the effect of plaque composition on arterial waveform with severe stenosis (75% blockage, ± 5). Two stable plaques (FA, FC), one unstable (PR) and vulnerable plaques (TCFA) were used in in vitro experiments. The diameters of the artery and flow velocities with and without the presence of the plaques were measured simultaneously at the same position, 5 mm proximal to the plaque. To ensure reproducibility, measurements were made three times, and the each set of date was collected five minutes after starting the experiment.

6.4.1. Measured Diameters and Velocities

The observations of this study indicate that measured movement of the arterial wall in the presence of unstable plaques has a higher amplitude than with stable plaques, (Figure 6.3). This finding is consistent with observations made by Takano *et al.,* (2001), which found that unstable plaques were more extendable than stable plaques. They also found that at the severe stage of stenosis unstable plaque is related to a greater amplitude of the artery diameter while for stable plaques a lower amplitude of diameter was observed. These interesting results were observed with unstable and vulnerable plaques, PR and TCFA and it was also noticed that the shape and magnitude of the diameter waveforms with PR plaque were similar to those for TCFA plaque (Figure 6.3A).

A possible explanation of this result is the composition of PR plaque which contains 22% LC, 0% Ca and 78% Col, was very similar to the composition of TCFA, 26% LC, 0% Ca, and 74% Col. These similar compositions generated similar waveforms. In addition, the lipid core for both plaques was positioned to face the flow, which would be expected to generate similar

reflections leading to similar waveforms. However, although the stable plaques are stiffer and their fibrous caps are thicker than unstable plaques, the measured arterial diameters were lower than for unstable plaques. It would be expected that the measured artery diameters of stable plaques should be higher than unstable plaques because of stronger reflections. Therefore, to investigate reflections at stable and unstable plaques it is necessary to separate the measured waveforms into their forward and backward components.

6.4.2. The Separation of Diameters

Figure 6.4 and Figure 6.5 show that the 75% blockage increases the amplitude of the backward arterial diameter in comparison with the healthy case. Looking at Figure 6.4, the backward amplitude for stable plaques was greater than for unstable plaques. For example, the backward amplitude of FC stable plaque was the highest and FA stable plaque was the second highest, while the amplitudes of backward diameter for PR and TCFA vulnerable plaques had similar values. As explained in Chapter 5, the stiffness of the stable plaques was higher than for unstable plaques, which increased the backward amplitude of the wave reflected from the stable plaques. In addition, the fibrous cap thickness of stable plaques (FA = 0.35 mm and FC = 0.27 mm, Table 3.1) was thicker than for unstable and vulnerable plaques (PR = 0.017 mm and TCFA = 0.022 mm), which should produce a greater backward reflection. However, while the backward diameter amplitude for PR plaque was the highest in the 30% blockage study (0.69 mm), it was the lowest in this study (0.38 mm). A possible explanation is that the tube diameter for the 30% blockage (9.50 mm) was larger than for this study (6.35 mm). Also, in the presence of the 30% blockage there was a greater wall movement than with the 75% blockage because a greater surface area of the artery wall was free to move. Thirdly, the LC area of this plaque was positioned facing towards the incident flow and the position where the measurements were being taken. The fibrous cap covering the LC area was thin (0.017 mm). These factors meant that the incoming wave hit the soft part of the plaque first, generating less reflection than

occurred with the 30% blockage area. Hence, the stable plaques generate a higher backward diameter than unstable plaques because of their stiffness.

6.4.3. Non-invasive Wave Intensity (WI)

The WI pattern in this artificial artery (Figure 6.5A) has three peaks starting with a large forward compression wave then the backward compression wave and ending with the forward expansion wave. The difference in time between the start of the forward compression wave and the arrival of the backward compression wave is the time taken for the wave to travel downstream and be reflected back to the measurement location, proximal the artificial carotid artery. This pattern is similar to the normal carotid artery as obtained by (Feng and Khir, 2010; Pomella *et al.,* 2017).

With the stable plaques, however, there are four main waves in the early systolic period. Two of them appears in the early systole including the first positive peak of the forward compression wave and the first backward negative peak. The other two peaks are the second backward negative peak (backward compression wave) and the second positive peak (forward expansion wave). The first positive peak was initiated from the contraction of the Pulsatile Blood Pump and which travels downstream. This wave meets the stable plaque and some of its energy is reflected causing the first negative peak (BCPW) in the early systolic period, while the mid-systolic backward compression wave is produced by the distal reflection of this wave in the arterial system. Afterwards, the forward expansion wave was generated by the deceleration of the left ventricle contraction causing the second positive peak in the late systole. However, the presence of unstable and vulnerable plaques showed no significant (BCPW) in the early systolic period. This may be because of the fibrous cap thickness, which need further investigations.

Moreover, Figure 6.6A&B show that the 75% stenosis plaque with higher percentage of LC generates higher backward diameter amplitude, whilst plaques with higher proportion of Col produce lower backward diameter amplitude. This result is not consistent with the Chapter 5 results. The reason behind these unexpected results could be either from the location of the soft or the hard part plaque facing the measurements or the stenosis degree of the plaque, which need further investigations.

6.5. Conclusion

This chapter studied the effect of severe artificial plaque compositions on arterial waveform. The results show that the measured peak diameter and velocity amplitudes for unstable plaques are higher than for stable plaques due to area compliance. However, the separated backward diameters for stable plaques are higher than those for unstable plaques. In addition, stable plaques caused a significant backward wave intensity, which was not observed with unstable plaques. Finally, the possibility of plaque rupture and stroke risk at severe stenosis could be detected by effect of plaque compositions on arterial measured and separated waveform amplitudes.

Thus, it is concluded that identification of plaque vulnerability could be determined by using non-WI, which may open the door to a potentially novel non-invasive clinical tool to define the compositions of plaques and distinguish the vulnerability at severe stenosis. The major limitations of this study are that the outer shapes of the plaque were not the same as those observed in clinical studies.

It is strongly recommended that the effect of percentages of calcium and collagen in the plaque on the arterial waveform be investigated because it has been observed in all studies that these two components of the plaque have given what appear to be inconsistent results. Further

investigations conducted into this phenomenon will help give a clearer picture of the effect of the plaque composition on arterial waveform.

CHAPTER 7
Discussion and Conclusions

7.1. Discussion

As explained in Chapter 1 cardiovascular diseases, including strokes, are the leading cause of mortality in the world (Roth *et al.,* 2017). Of the 100,000 stroke events recorded each year in the UK, two thirds of the survivors suffer some form of disability (Stroke Association, 2018). The main cause of strokes is the accumulation of atherosclerosis plaque. There are three main types of plaques: stable, unstable, and vulnerable. Its composition and structure are key features characterising vulnerable plaque which contains a large area of LC within a thin fibrous cap but a reliable approach to determine the composition of this arterial plaque is still lacking. Thus, this study aimed to determine the relationship between plaque composition and arterial waveform non-invasively. Such a relationship could lead to identifying the differences between stable, unstable, and vulnerable plaques from their associated arterial waveforms. The key contributions of this study can be summarized as:

7.1.1. Construction of Artificial Plaque

Three types of plaques were fabricated: stable (FA, FC), unstable (CN, PE, PR) and vulnerable (TCFA) plaques. The characteristics of these plaques can be found in the histological study of the human carotid arterial plaque (Butcovan *et al.,* 2016). In this study, artificial plaques with identical characteristics to that of human carotid atherosclerosis were fabricated by the researcher in the laboratory, see Figure 3.4 and Table 3.1. The components of all the artificial plaques are: (i) calcium chloride hexahydrate, (ii) collagen type III, (iii) lipid core-soybean oil, and (iv) gelatine from bovine skin, type B. The fibrous cap was fabricated by either mixing gelatine and collagen with deionized water (Guo *et al.,* 2013) shaped into a mould in various thicknesses or by bovine skin, then left for 24 hours to dry, after which they were removed

from the mould. The calcium and collagen were prepared after the fibrous cap and placed in the fibrous cap after which the bottom of the plaque was covered by the same material as the artificial artery. These plaques were tested in three experiments and they gave similar results.

7.1.2. Pilot Study of the Effect of Types of Plaque on the Arterial Waveforms

In this study, we hypothesised that the stable and vulnerable plaques can be distinguished from each other through arterial waveform analysis. In Chapter 4, a pilot in vitro study was conducted to verify this hypothesis. This pilot study investigated two types of plaque: FC and TCFA, as representative of stable and unstable plaques, respectively. The configuration of these two artificial plaques were derived from those used in previous studies regarding plaque characteristics and properties (Guo *et al.,* 2013; Teng *et al.,* 2014; Butcovan *et al.,* 2016). It was expected that the presence of stable plaques with the higher proportions of Ca would result in a higher amplitude of the measured diameter, whereas the vulnerable plaques with the higher percentage of lipid core would be related to a lower amplitude of the measured diameter. It was observed that the waveform with the lower measured velocity for the two types of plaques occurred for the arterial system with stable plaque. This means that stable plaques generate stronger reflected waves, leading to a greater amplitude of the arterial diameter and lower amplitude of the velocity waveform.

The observations also showed that the forward velocity in the case of stable plaque was slightly greater than for vulnerable plaque. This observation could be explained as due to a further reflection of the reflected wave occurring at the inlet of the system, which led to the increase of its velocity. Likewise, the amplitude of the forward diameter for stable plaque is slightly higher than for vulnerable plaque with the same reason.

The amplitude of the backward travelling waveform in the arterial system with stable plaque is expected to be greater than for vulneable plaque because the stiffness of arterial stable plaque is greater than for vulnerable plaque and thus would be expected to have a higher reflection

coefficient. It has been observed that the backward reflection amplitude of vulnerable plaque for both velocity and diameter is higher than for stable plaque. These results were not expected and could be due to re-reflections from the inlet tube, or because the material properties of the artificial artery used with stable plaque was different from the one that used with vulnerable plaque. A further investigation was demonstrated in Chapter 5.

7.1.3. The Correlation of the Composition of Plaques at Early Stage with the Arterial Waveform

This study attempted to avoid reflections from the inlet tube by mounting the artificial plaque 26.6 cm away from the inlet of the tube, which is two-thirds of the length of the tube. Six types of plaque (FA, FC, PR, PE, CN and TCFA) were used to investigate the effect of plaque compositions on arterial diameter waveform. The CN plaque was tested several times, but its fibrous cap did not bear the load of calcium and each time it ruptured before data could be collected and so this type of plaque was not analysed.

The correlation between the plaque composition and reflected waveforms was quantitatively analysed. The experimental results indicate that the reflected waveforms are strongly correlated with the plaque composition, with the percentages of collagen positively correlated with the amplitude of the backward diameter (correlation coefficient, $r = 0.74$). The lipid content has a strong negative correlation with the backward diameter ($r = -0.82$). A weak negative correlation exists between the reflected waveform and the percentage of calcium ($r = -0.30$). In addition, stable plaques generated a significant backward wave intensity, while no significant backward wave intensity was observed with unstable and vulnerable plaques. These findings might lead to a potentially novel non-invasive clinical tool to determine the compositions of the plaque and distinguish stable and vulnerable arterial plaques at an early stage.

7.1.4. The Effect of Severe Stenosis of Stable, Unstable and Vulnerable Plaque on the Arterial Waveform

Chapter 6 investigated the correlation of the compositions of the arterial plaques with the arterial waveforms under conditions of severe stenosis, with 75% of vessel lumen occluded. Two types each of stable (FA and FC) unstable (PR) and vulnerable (TCFA) plaques were fabricated and introduced into the artificial arterial blood vessels. The results of this study show that the measured peak diameter and velocity amplitudes for unstable plaques were greater than for stable plaques due to area compliance. However, the separated backward diameter with stable plaques was higher than for unstable plaques, most likely, because stable plaques caused a significantly greater backward (reflected) wave intensity than was observed for unstable plaques.

7.2. Conclusions

The conclusions of this research are:

1- The compositions of arterial plaque, the key factors to distinguish the stable and vulnerable plaque, have the strong effects on the arterial diameter and velocity waveforms.

2- Plaques with a high percentage of collagen and calcium and only a small amount of lipid core generate higher reflections than those plaques with a large lipid core and small amounts of collagen and calcium.

3- In both the early (30% blockage) and later (75% blockage) stage of stenosis, the plaques, composed with higher percentage of collagen and calcium and lower amount of lipid core, generate higher backward diameter; whereas the plaques, characterised as large lipid core and thin fibrous cap, are associated with the lower backward diameter waveform. In particular, at the early stage of stenosis, a strong positive correlation was found between collagen percentage and backward diameter amplitude, while a

significant negative correlation was observed between lipid core and backward diameter amplitude.

4- In both the early and advanced stage of the stenosis (30% and 75% of blockage), the stable plaques generates a significant backward wave intensity in the early systolic period, while no significant backward wave intensity was observed with unstable plaques during the same period slot.

5- The findings from this study provide novel knowledge regarding the nature of the types of plaques related to arterial waveform propagation, providing important information to distinguish between stable, unstable and vulnerable plaques. The findings from this study, combined with the feasibility of using Non-WIA to analyse arterial waveforms in a clinical setting, offer a potential novel medical diagnosis approach to distinguish between the vulnerable and stable plaques.

7.3. Future Perspective

Possible future work related directly to the presented study is suggested below:

1- This study used non-WIA to detect the composition of the plaque using the arterial waveform. The effect of collagen, lipid core and calcium are obvious on the arterial waveform. An investigation of the effect of calcium and collagen combined in various percentage on the arterial waveform is strongly recommended because it was observed that these two factors together sometimes gave expected results. Therefore, groups of plaques with different percentages of collagen and calcium with a fixed percentage of lipid core and fibrous cap should be used to study the effects of the mix on the arterial waveform.

2- The outer shape of the artificial plaque used in this study was uniform, which is not similar to the real situation. Using 3D-printing to fabricate the shape of real plaque

could be achieved by inserting the image of real plaque via the associated CAD software to replicate 30% and 75% blockages. When the model plaques are ready, it would be used in the 30% and 75% studies to increase the relevance of the findings.

3- The effect of the fibrous cap on the arterial waveform is another factor which should be tested by fabricating one particular plaque and use this with fibrous caps of different thicknesses and shapes in order to detect plaque vulnerability.

4- The investigations that have been completed in this thesis would be combined with the results of further investigations using the technique proposed above.

5- The approach used in this study is suggested to be employed for in vivo clinical study in future. Data can be collected by echo-tracking ultrasound to collect the measured wall movement and blood flow. The non-invasive WIA can be used to analyse the waveform, where the forward and backward wave components can be used to link with the features of human plaques recognized by the advanced imaging techniques such as 3-dimensional (3D) ultrasound technique.

References

Abdulsalam, M., and Feng, J. (2019) 'Distinguish the stable and unstable plaques based on arterial waveform analysis.' *Procedia Structural Integrity*, *15*, 2–7. https://doi.org/10.1016/j.prostr.2019.07.002

Abdulsalam, M., and Feng, J. (2021) 'The composition of vulnerable plaque and its effect on arterial waveforms.' *Journal of the Mechanical Behavior of Biomedical Materials*, *119*(February), 104491. https://doi.org/10.1016/j.jmbbm.2021.104491

Akbari, M., Tamayol, A., Laforte, V., Annabi, N., Najafabadi, H., Khademhosseini, A., and Juncker, D. (2014) 'Composite Living Fibers for Creating Tissue Constructs Using Textile Techniques.' *Weinheim*, *11*(24), 4060–4067. https://doi.org/10.1002/adfm.201303655

Alastruey, J., Hunt, A., Weinberg, P. (2013) 'Novel wave intensity analysis of arterial pulse wave propagation accounting for peripheral reflection.' *International Journal for Numerical Methods in Biomedical Engineering*, *26*(1), 807–827. https://doi.org/10.1002/cnm

Alastruey, J. (2011) 'Numerical assessment of time-domain methods for the estimation of local arterial pulse wave speed.' *Journal of Biomechanics*, *44*(5), 885–891. https://doi.org/10.1016/j.jbiomech.2010.12.002

Almuhanna, K., Hossain, M., Zhao, L., Fischell, J., Kowalewski, G., Dux, M., Sikdar, S., and Lal, K. (2015) 'Carotid plaque morphometric assessment with three-dimensional ultrasound imaging.' *Journal of Vascular Surgery*, *61*(3), 690–697. https://doi.org/10.1016/j.jvs.2014.10.003

Ammirati, E., Moroni, F., Norata, D., Magnoni, M., and Camici, G. (2015) 'Markers of inflammation associated with plaque progression and instability in patients with carotid atherosclerosis.' *Mediators of Inflammation*, *2015*. https://doi.org/10.1155/2015/718329

Andrae, J., Gallini, R., and Betsholtz, C. (2008). 'Role of platelet-derived growth factors in physiology and medicine.' *Genes and Development*, *22*(10), 1276–1312. https://doi.org/10.1101/gad.1653708

Anlamlert, W., Lenbury, Y., & Bell, J. (2017). 'Modeling fibrous cap formation in atherosclerotic plaque development: stability and oscillatory behavior.' *Advances in Difference Equations*, *2017*(1). https://doi.org/10.1186/s13662-017-1252-9

Arroyo-olarte, D., Brouwers, F., Kuchipudi, A., and Helms, B. (2015) 'Phosphatidylthreonine and Lipid-Mediated Control of Parasite Virulence.' *Biology Journal*, *13*(11), 1–24. https://doi.org/10.5061/dryad.564sc

Arroyo, L. H., and Lee, R. T. (1999). 'Mechanisms of plaque rupture: Mechanical and biologic interactions.' *Cardiovascular Research*, *41*(2), 369–375. https://doi.org/10.1016/S0008-6363(98)00308-3

Ayadi, A., Sahtout, W., and Balédent, O. (2020) 'A Non-invasive Method for Determining Biomechanical Properties of the Internal Carotid Artery.' *Irbm*, *41*(3), 125–132. https://doi.org/10.1016/j.irbm.2019.10.008

Bentzon, F., Otsuka, F., Virmani, R., and Falk, E. (2014) 'Mechanisms of plaque formation and rupture.' *Circulation Research*, *114*(12), 1852–1866. https://doi.org/10.1161/CIRCRESAHA.114.302721

Biglino, G., Steeden, A., Baker, C., Schievano, S., Taylor, M., and Parker, K. (2012) 'A non-invasive clinical application of wave intensity analysis based on ultrahigh temporal resolution phase-contrast cardiovascular magnetic resonance.' *Journal of Cardiovascular Magnetic Resonance*,

14(1), 2–9. https://doi.org/10.1186/1532-429X-14-57

Bogatu, I., Turco, S., Mischi, M., Woerlee, P., Bouwman, A., Korsten, M., and Muehlsteff, J. (2020) 'A modelling framework for assessment of arterial compliance by fusion of oscillometry and pulse wave velocity information.' *Computer Methods and Programs in Biomedicine*, *196*, 105492. https://doi.org/10.1016/j.cmpb.2020.105492

Borlotti, A., Li, Y., Parker, K., and Khir, W. (2014a) 'Experimental evaluation of local wave speed in the presence of reflected waves.' *Journal of Biomechanics*, *47*(1), 87–95. https://doi.org/10.1016/j.jbiomech.2013.10.007

Borlotti, A., Li, Y., Parker, K., and Khir, W. (2014b) 'Experimental evaluation of local wave speed in the presence of reflected waves.' *Journal of Biomechanics*, *47*(1), 87–95. https://doi.org/10.1016/j.jbiomech.2013.10.007

Brugaletta, S., Giacchi, G., Ortega-Paz, L., Garcia-Garcia, H., and Sabaté, M. (2016) 'Stable coronary artery disease. Is it really stable? Lesion morphology interpretation by Grayscale and VH-IVUS in patients with coronary artery disease.' *Continuing Cardiology Education*, *2*(2), 66–76. https://doi.org/10.1002/cce2.24

Butcovan, D., Mocanu, V., Baran, D., Ciurescu, D., and Tinica, G. (2016) 'Assessment of vulnerable and unstable carotid atherosclerotic plaques on endarterectomy specimens.' *Experimental and Therapeutic Medicine*, *11*(5), 2028–2032. https://doi.org/10.3892/etm.2016.3096

Camici, P., Rimoldi, E., Gaemperli, O., and Libby, P. (2012) 'Non-invasive anatomic and functional imaging of vascular inflammation and unstable plaque.' *European Heart Journal*, *33*(11), 1309–1317. https://doi.org/10.1093/eurheartj/ehs067

Cassar, A., Matsuo, Y., Herrmann, J., Li, J., Lennon, R. J., Gulati, R., and Lerman, A. (2013). 'Coronary atherosclerosis with vulnerable plaque and complicated lesions in transplant recipients: New insight into cardiac allograft vasculopathy by optical coherence tomography.' *European Heart Journal*, *34*(33), 2610–2617. https://doi.org/10.1093/eurheartj/eht236

Chan, S., Monaco, C., Wylezinska-Arridge, M., Tremoleda, L., and Gibbs, J. (2014a) 'Imaging of the vulnerable carotid plaque: Biological targeting of inflammation in atherosclerosis using iron oxide particles and MRI.' *European Journal of Vascular and Endovascular Surgery*, *47*(5), 462–469. https://doi.org/10.1016/j.ejvs.2014.01.017

Chan, S., Monaco, C., Wylezinska-Arridge, M., Tremoleda, L., and Gibbs, J. (2014b) 'Imaging of the vulnerable carotid plaque: Biological targeting of inflammation in atherosclerosis using iron oxide particles and MRI.' *European Journal of Vascular and Endovascular Surgery*, *47*(5), 462–469. https://doi.org/10.1016/j.ejvs.2014.01.017

Cuadrado, I., Saura, M., Castejón, B., Martin, M., Herruzo, I., Balatsos, N., Zamorano, L., and Zaragoza, C. (2016) 'Preclinical models of atherosclerosis. The future of Hybrid PET/MR technology for the early detection of vulnerable plaque.' *Expert Reviews in Molecular Medicine*, *18*, e6. https://doi.org/10.1017/erm.2016.5

Cunnane, M., Mulvihill, E., Barrett, E., Hennessy, M., Kavanagh, G., and Walsh, T. (2016) 'Mechanical properties and composition of carotid and femoral atherosclerotic plaques: A comparative study.' *Journal of Biomechanics*, *49*(15), 3697–3704. https://doi.org/10.1016/j.jbiomech.2016.09.036

D'Oria, M., Chiarandini, S., Pipitone, D., Fisicaro, M., Calvagna, C., Bussani, R., Rotelli, A and Ziani, B. (2018) 'Contrast Enhanced Ultrasound (CEUS) Is Not Able to Identify Vulnerable Plaques in Asymptomatic Carotid Atherosclerotic Disease.' *European Journal of Vascular and Endovascular*

Surgery, *56*(5), 632–642. https://doi.org/10.1016/j.ejvs.2018.07.024

Davies, E., Whinnett, I., Francis, P., Willson, K., Foale, A., Malik, S., Hughe, D., Parker, K., and Mayet, J. (2006) 'Use of simultaneous pressure and velocity measurements to estimate arterial wave speed at a single site in humans.' *American Journal of Physiology - Heart and Circulatory Physiology*, *290*(2), 59–61. https://doi.org/10.1152/ajpheart.00751.2005

De Weert, T., Ouhlous, M., Meijering, E., Zondervan, E., Hendriks, M., Van Sambeek, M., Dippel, J., and Van Der Lugt, A. (2006) 'In vivo characterization and quantification of atherosclerotic carotid plaque components with multidetector computed tomography and histopathological correlation.' *Arteriosclerosis, Thrombosis, and Vascular Biology*, *26*(10), 2366–2372. https://doi.org/10.1161/01.ATV.0000240518.90124.57

Denzel, C., Lell, M., Maak, M., Höcki, M., Balzer, K., Müller, K. M., and Lang, W. (2004). 'Carotid artery calcium: Accuracy of a calcium score by computed tomography - An in vitro study with comparison to sonography and histology.' *European Journal of Vascular and Endovascular Surgery*, *28*(2), 214–220. https://doi.org/10.1016/j.ejvs.2004.05.004

Di Lascio, N., Kusmic, C., Stea, F., and Faita, F. (2017) 'Wave intensity analysis in mice: age-related changes in WIA peaks and correlation with cardiac indexes.' *Heart and Vessels*, *32*(4), 474–483. https://doi.org/10.1007/s00380-016-0914-y

Doherty, T. M., Asotra, K., Fitzpatrick, L. A., Qiao, J. H., Wilkin, D. J., Detrano, R. C., and Rajavashisth, T. B. (2003). 'Calcification in atherosclerosis: Bone biology and chronic inflammation at the arterial crossroads.' *Proceedings of the National Academy of Sciences of the United States of America*, *100*(20), 11201–11206. https://doi.org/10.1073/pnas.1932554100

Fatkhullina, A. ., Peshkova, I. O., and Koltsova, E. K. (2016). 'The Role of Cytokines in the Development of Atherosclerosis.' *Biochemistry*, *81*(11), 139–148. https://doi.org/10.1134/S0006297916110134.The

Fayad, A., and Fuster, V. (2001) 'Clinical imaging of the high-risk or vulnerable atherosclerotic plaque.' *Circulation Research*, *89*(4), 305–316. https://doi.org/10.1161/hh1601.095596

Feng, J., and Khir, W. (2005) 'A new approach to investigate wave dissipation in viscoelastic tubes: Application of Wave Intensity Analysis.' *Annual International Conference of the IEEE Engineering in Medicine and Biology - Proceedings*, *7 VOLS*(4), 2260–2263. https://doi.org/10.1109/iembs.2005.1616914

Feng, J., and Khir, W. (2007) 'The compression and expansion waves of the forward and backward flows: An in-vitro arterial model.' *Proceedings of the Institution of Mechanical Engineers, Part H: Journal of Engineering in Medicine*, *222*(4), 531–542. https://doi.org/10.1243/09544119JEIM339

Feng, J., and Khir, W. (2010) 'Determination of wave speed and wave separation in the arteries using diameter and velocity.' *Journal of Biomechanics*, *43*(3), 455–462. https://doi.org/10.1016/j.jbiomech.2009.09.046

Feng, J., Long, Q., and Khir, W. (2007) 'Wave dissipation in flexible tubes in the time domain : In vitro model of arterial waves.' Journal of Biomechanics, *40*, 2130–2138. https://doi.org/10.1016/j.jbiomech.2006.10.034

Feng, J., Rajeswaran, T., He, S., Wilkinson, L., Serracino-Inglott, F., Azzawi, M., Parikh, V., Miraftab, M., and Alexander, Y. (2015) 'Investigation of the composition of arterial plaques based on arterial waveforms and material properties.' *Proceedings of the Annual International Conference of the IEEE Engineering in Medicine and Biology Society, EMBS*, *2015–Novem*, 993–

996. https://doi.org/10.1109/EMBC.2015.7318531

Finn, V., Nakano, M., Narula, J., Kolodgie, D., and Virmani, R. (2010) 'Concept of vulnerable/unstable plaque.' *Arteriosclerosis, Thrombosis, and Vascular Biology*, *30*(7), 1282–1292. https://doi.org/10.1161/ATVBAHA.108.179739

Gaziano, A., Bitton, A., Anand, S., Abrahams-Gessel, S., and Murphy, A. (2010) 'Growing Epidemic of Coronary Heart Disease in Low- and Middle-Income Countries.' *Current Problems in Cardiology*, *35*(2), 72–115. https://doi.org/10.1016/j.cpcardiol.2009.10.002

Gomez, D., and Owens, G. K. (2012). 'Smooth muscle cell phenotypic switching in atherosclerosis.' *Cardiovascular Research*, *95*(2), 156–164. https://doi.org/10.1093/cvr/cvs115

Guo, I., Saylor, M., Glaser, P., and Patwardhan, V. (2013) 'Impact of Artificial Plaque Composition on Drug Transport.' *JOURNAL OF PHARMACEUTICAL SCIENCES*, *102*(6), 1905–1914. https://doi.org/10.1002/jps

Hacham, S., and Khir, W. (2019) 'The speed, reflection and intensity of waves propagating in flexible tubes with aneurysm and stenosis: Experimental investigation. *Proceedings of the Institution of Mechanical Engineers, Part H:, Journal of Engineering in Medicine*, *233*(10), 979–988. https://doi.org/10.1177/0954411919859994

Hamada, S., Kashiwazaki, D., Yamamoto, S., Akioka, N., Kuwayama, N., and Kuroda, S. (2018) 'Impact of Plaque Composition on Risk of Coronary Artery Diseases in Patients with Carotid Artery Stenosis.' *Journal of Stroke and Cerebrovascular Diseases*, *27*(12), 3599–3604. https://doi.org/10.1016/j.jstrokecerebrovasdis.2018.08.031

Holdt, L. M., and Teupser, D. (2013). 'From genotype to phenotype in human atherosclerosis - Recent findings.' *Current Opinion in Lipidology*, *24*(5), 410–418. https://doi.org/10.1097/MOL.0b013e3283654e7c

Huang, C., He, Q., Huang, M., Huang, L., Zhao, X., Yuan, C., and Luo, J. (2017) 'Non-Invasive Identification of Vulnerable Atherosclerotic Plaques Using Texture Analysis in Ultrasound Carotid Elastography: An In Vivo Feasibility Study Validated by Magnetic Resonance Imaging.' *Ultrasound in Medicine and Biology*, *43*(4), 817–830. https://doi.org/10.1016/j.ultrasmedbio.2016.12.003

Ibrahimi, P., Jashari, F., Nicoll, R., Bajraktari, G., Wester, P., and Henein, M. Y. (2013). 'Coronary and carotid atherosclerosis: How useful is the imaging?' *Atherosclerosis*, *231*(2), 323–333. https://doi.org/10.1016/j.atherosclerosis.2013.09.035

Jashari, F., Ibrahimi, P., Johansson, E., Ahlqvist, J., Arnerlöv, C., Garoff, M., Jäghagen, L., Wester, P., and Henein, Y. (2015) 'Atherosclerotic Calcification Detection : A Comparative Study of Carotid Ultrasound and Cone Beam CT.' *International Journal of Molecular Sciences*, 19978–19988. https://doi.org/10.3390/ijms160819978

Johri, M., Herr, E., Li, Y., Yau, O., and Nambi, V. (2017) 'Novel Ultrasound Methods to Investigate Carotid Artery Plaque Vulnerability.' *Journal of the American Society of Echocardiography*, *30*(2), 139–148. https://doi.org/10.1016/j.echo.2016.11.003

Joshi, R., Lindsay, C., Obaid, R., Falk, E., and Rudd, F. (2012) 'Non-invasive imaging of atherosclerosis.' *European Heart Journal Cardiovascular Imaging*, *13*(3), 205–218. https://doi.org/10.1093/ejechocard/jer319

Karimi, M. (2012) 'Detection and Quantification of Coronary Atherosclerotic Plaque Using Different Imaging Modalities.' *American Journal of Biomedical Engineering*, *2*(2), 1–6. https://doi.org/10.5923/j.ajbe.20120202.01

Kerwin, W., Hatsukami, T., Yuan, C., and Zhao, Q. (2013) 'MRI of Carotid Atherosclerosis.' *Physiology & Behavior*, *176*(1), 139–148. https://doi.org/10.1016/j.physbeh.2017.03.040

Khir, W., Brien, O., Gibbs, R., and Parker, K. (2001) 'Determination of wave speed and wave separation in the arteries.' *Journal of Biomechanics 34*, *34*, 1145–1155.

Khir, W., and Parker, K. (2002) 'Measurements of wave speed and reflected waves in elastic tubes and bifurcations.' *Journal of Biomechanics*, *35*, 775–783.

Khir, W., and Parker, K. (2005) 'Wave intensity in the ascending aorta: Effects of arterial occlusion.' *Journal of Biomechanics*, *38*(4), 647–655. https://doi.org/10.1016/j.jbiomech.2004.05.039

Klem, I., Heitner, F., Shah, J., Sketch, H., Behar, V., Weinsaft, J., Cawley, P., Parker, M.' Elliott, M., Judd, R., and M. Kim, J. (2006) 'Improved Detection of Coronary Artery Disease by Stress Perfusion Cardiovascular Magnetic Resonance With the Use of Delayed Enhancement Infarction Imaging.' *Journal of the American College of Cardiology*, 47(8), 1630–1638. https://doi.org/10.1016/j.jacc.2005.10.074

Kobielarz, M., Kozuń, M., Gąsior-Głogowska, M., and Chwiłkowska, A. (2020) 'Mechanical and structural properties of different types of human aortic atherosclerotic plaques.' *Journal of the Mechanical Behavior of Biomedical Materials*, *109*(May). https://doi.org/10.1016/j.jmbbm.2020.103837

Krejza, J., Arkuszewski, M., Kasner, E., Weigele, J., Ustymowicz, A., Hurst, W., Cucchiara, L., and Messe, R. (2006) 'Carotid artery diameter in men and women and the relation to body and neck size.' *Stroke*, *37*(4), 1103–1105. https://doi.org/10.1161/01.STR.0000206440.48756.f7

Lafont, A. (2003). *VULNERABILITY*. (fig 1).

Li, X., Apostolakis, Z., Kemper, P., McGarry, J., Ip, A., Connolly, S., McKinsey, F., and Konofagou, E. (2019) 'Pulse Wave Imaging in Carotid Artery Stenosis Human Patients in Vivo.' *Ultrasound in Medicine and Biology*, *45*(2), 353–366. https://doi.org/10.1016/j.ultrasmedbio.2018.07.013

Li, Y., Parker, K., and Khir, W. (2016) 'Using wave intensity analysis to determine local reflection coefficient in flexible tubes.' *Journal of Biomechanics*, *49*(13), 2709–2717. https://doi.org/10.1016/j.jbiomech.2016.06.004

Libby, P. (2013). 'Collagenases and cracks in the plaque.' *Journal of Clinical Investigation*, *123*(8), 3201–3203. https://doi.org/10.1172/JCI67526

Libby, P., Ridker, M., and Hansson, K. (2011) 'Progress and challenges in translating the biology of atherosclerosis.' *Nature*, *473*(7347), 317–325. https://doi.org/10.1038/nature10146

Lindsay, C., Biasiolli, L., Knight, S., Cunnington, C., Robson, D., Neubauer, S., Kennedy, J., Handa, A., and Choudhury, P. (2014) 'Non-invasive imaging of carotid arterial restenosis using 3T cardiovascular magnetic resonance.' *Journal of Cardiovascular Magnetic Resonance : Official Journal of the Society for Cardiovascular Magnetic Resonance*, *16*(1), 5. https://doi.org/10.1186/1532-429X-16-5

Liu, Q., Huang, J., Zhao, L., Wang, W., Liu, S., He, P., Liao, Li., and Zeng, Y. (2020) 'Association between knowledge and risk for cardiovascular disease among older adults: A cross-sectional study in China.' *International Journal of Nursing Sciences*, (xxxx), 4–10. https://doi.org/10.1016/j.ijnss.2020.03.008

Lu, J., Yang, J., Wu, Y., Hung, H., Chan, Y., and Hsu, C. (2011) 'Wave energy patterns of counterpulsation: A novel approach with wave intensity analysis.' *Journal of Thoracic and Cardiovascular Surgery*, *142*(5), 1205–1213. https://doi.org/10.1016/j.jtcvs.2011.02.018

Macharzina, R., Kocher, S., Hoffmann, F., Becher, H., Kammerer, T., Vogt, M., Vach, W., Fan, N., Rastan, A., Neumann, J., and Zeller, T. (2020) 'Accuracy of Carotid Artery Stenosis Quantification with 4-D-Supported 3-D Power-Doppler versus Color-Doppler and 2-D Blood Velocity-Based Duplex Ultrasonography.' *Ultrasound in Medicine and Biology*, *46*(5), 1082–1091. https://doi.org/10.1016/j.ultrasmedbio.2019.12.022

Madamanchi, R., Vendrov, A., and Runge, S. (2005) 'Oxidative stress and vascular disease.' *Arteriosclerosis, Thrombosis, and Vascular Biology*, *25*(1), 29–38. https://doi.org/10.1161/01.ATV.0000150649.39934.13

Majmudar, D., Yoo, J., Keliher, J., Truelove, J., Iwamoto, Y., Sena, B., Dutta, P., Borodovsky, A., Fitzgerald, K., Di Carli, F., Libby, P., Anderson, G., Swirski, K., Weissleder, R and Nahrendorf, M. (2013) 'Polymeric nanoparticle PET/MR imaging allows macrophage detection in atherosclerotic plaques.' *Circulation Research*, *112*(5), 755–761. https://doi.org/10.1161/CIRCRESAHA.111.300576

Martinet, W., Schrijvers, D. M., and Meyer, G. R. Y. De. (2011). 'Necrotic cell death in atherosclerosis.' *Basic Res Cardiol*, 749–760. https://doi.org/10.1007/s00395-011-0192-x

Masuda, M., Emoto, T., Suzuki, A., Akutagawa, M., Kitawaki, T., and Kitaoka, K. (2013) 'Biomedical Signal Processing and Control Evaluation of blood flow velocity waveform in common carotid artery using multi-branched arterial segment model of human arteries.' *Biomedical Signal Processing and Control*, *8*(6), 509–519. https://doi.org/10.1016/j.bspc.2013.05.005

Meletta, R., Slavik, R., Mu, L., Rancic, Z., Borel, N., Schibli, R., Ametamey, M., Krämer, D and Müller, A. (2017) 'Cannabinoid receptor type 2 (CB2) as one of the candidate genes in human carotid plaque imaging : Evaluation of the novel radiotracer [11 C] RS-016 targeting CB2 in atherosclerosis.' *Nuclear Medicine and Biology*, *47*, 31–43. https://doi.org/10.1016/j.nucmedbio.2017.01.001

Meyer, De. (2011) 'Necrotic cell death in atherosclerosis.' *Basic Res Cardiol*, 749–760. https://doi.org/10.1007/s00395-011-0192-x

Moll, L. (2008) 'After Carotid Endarterectomy.' *The Journal of the American Medical Association*, *299*(5), 547–554.

Moradi, M., Mahdavi, B., and Nogourani, K. (2020) 'The Relation of Calcium Volume Score and Stenosis of Carotid Artery.' *Journal of Stroke and Cerebrovascular Diseases*, *29*(1), 104493. https://doi.org/10.1016/j.jstrokecerebrovasdis.2019.104493

Motoyama, R., Saito, K., Tonomura, S., Ishibashi-Ueda, H., Yamagami, H., Kataoka, H., Sugie, K., Toyoda, K., and Nagatsuka, K. (2019) 'Utility of Complementary Magnetic Resonance Plaque Imaging and Contrast-Enhanced Ultrasound to Detect Carotid Vulnerable Plaques.' *Journal of the American Heart Association*, *8*(8), 1–8. https://doi.org/10.1161/JAHA.118.011302

Naghavi, M., Libby, P., Falk, E., Casscells, W., Litovsky, S., Rumberger, J., Badimon, J. J., Stefanadis, C., Moreno, P., Pasterkamp, G., Fayad, Z., Stone, H., Waxman, S., Raggi, P., Madjid, M., Zarrabi, A., Burke, A., Yuan, C., Fitzgerald, J., Siscovick, S., De Korte, L., Aikawa, M., Airaksinen, J., Assmann, G., Becker, R., Chesebro, H., Farb, A., Galis, S., Jackson, C., Jang, K., Koenig, W., Lodder, A., March, K., Demirovic, J., Navab, M., Priori, G., Rekhter, D., Bahr, R., Grundy, M., Mehran, R., Colombo, A., Boerwinkle, E., Ballantyne, C., Insull, W., Schwartz, S., Vogel, R., Serruys, W., Hansson, K., Faxon, P., Kaul, S., Drexler, H., Greenland, P., Muller, J. E.,Virmani, R., Ridker, M., Zipes, P., Shah, K. and Willerson, T. (2003) 'From vulnerable plaque to vulnerable patient: A call for new definitions and risk assessment strategies: Part I.' *Circulation*, *108*(14), 1664–1672. https://doi.org/10.1161/01.CIR.0000087480.94275.97

Naim, C., Cloutier, G., Mercure, E., Destrempes, F., Qin, Z., El-Abyad, W., Lanthier, S., Giroux, Marie F., and Soulez, G. (2013) 'Characterisation of carotid plaques with ultrasound elastography: Feasibility and correlation with high-resolution magnetic resonance imaging.' *European Radiology*, *23*(7), 2030–2041. https://doi.org/10.1007/s00330-013-2772-7

Naim, C., Douziech, M., Therasse, É., Robillard, P., Giroux, F., Arsenault, F., Cloutier, G., and Soulez, G. (2014) 'Vulnerable atherosclerotic carotid plaque evaluation by ultrasound, computed tomography angiography, and magnetic resonance imaging: An overview.' *Canadian Association of Radiologists Journal*, *65*(3), 275–286. https://doi.org/10.1016/j.carj.2013.05.003

Narula, J., Nakano, M., Virmani, R., Kolodgie, D., Petersen, R., Newcomb, R., Malik, S., Fuster, V., and Finn, V. (2013) 'Histopathologic characteristics of atherosclerotic coronary disease and implications of the findings for the invasive and noninvasive detection of vulnerable plaques.' *Journal of the American College of Cardiology*, *61*(10), 1041–1051. https://doi.org/10.1016/j.jacc.2012.10.054

Negoita, M., Hughes, D., Parker, K., and Khir, W. (2018) 'A Method for Determining Local Pulse Wave Velocity in Human Ascending 7 8 9 Aorta from Sequential Ultrasound Measurements of Diameter and Velocity.' *Institue of Physics and Engineering in Medicine*, *10*, 22408–22418.

Nichols, M., Townsend, N., Scarborough, P., and Rayner, M. (2013) 'Cardiovascular disease in Europe : epidemiological update.' *European Heart Journal*, (34), 3028–3034. https://doi.org/10.1093/eurheartj/eht356

Niki, K., Sugawara, M., Kayanuma, H., Takamisawa, I., Watanabe, H., Mahara, K., Sumiyoshi, T., Ida, T., Takanashi, S., and Tomoike, H. (2017) 'Associations of increased arterial stiffness with left ventricular ejection performance and right ventricular systolic pressure in mitral regurgitation before and after surgery: Wave intensity analysis.' *IJC Heart and Vasculature*, 0–6. https://doi.org/10.1016/j.ijcha.2017.06.002

Niki, K., Sugawara, M., Uchida, K., Tanaka, R., Tanimoto, K., Imamura, H., Sakomura, Y., Ishizuka, N., Koyanagi, H., and Kasanuki, H. (1999) 'A noninvasive method of measuring wave intensity, a new hemodynamic index: Application to the carotid artery in patients with mitral regurgitation before and after surgery.' *Heart and Vessels*, *14*(6), 263–271. https://doi.org/10.1007/BF03257237

Otsuka, F., Yasuda, S., Noguchi, T., and Ishibashi-Ueda, H. (2016). 'Pathology of coronary atherosclerosis and thrombosis.' *Cardiovascular Diagnosis and Therapy*, *6*(4), 396–408. https://doi.org/10.21037/cdt.2016.06.01

Ozawa, H., Ohki, T., Kanaoka, Y., Shukuzawa, K., and Maeda, K. (2016) 'Routine completion angiography and intraoperative stent placement for the management of distal intimal flap during eversion carotid endarterectomy.' *Journal of Vascular Surgery Cases and Innovative Techniques*, *2*(3), 63–65. https://doi.org/10.1016/j.jvsc.2016.01.003

Park, M., Hughes, D., Henein, Y., and Khir, W. (2020) 'Mechanisms of Aortic Flow Deceleration and the Effect of Wave Reflection on Left Ventricular Function.' *Frontiers in Physiology*, *11*(November), 1–10. https://doi.org/10.3389/fphys.2020.578701

Park, S., Chung, J., Lee, J., Han, M., and Park, J. (2001) 'Carotid artery involvement in Takayasu's arteritis: evaluation of the activity by ultrasonography.' *Journal of Ultrasound in Medicine*, *20*(4), 371–378. https://doi.org/10.7863/jum.2001.20.4.371

Parker, K. (2009) 'An introduction to wave intensity analysis.' *Medical and Biological Engineering and Computing*, *47*(2), 175–188. https://doi.org/10.1007/s11517-009-0439-y

Parker, K., and Jones, C. (1990) ' Forward and Backward Running Waves in the Arteries : Analysis Using the Method of Characteristics' *Brodland J Biomech Eng 1990.pdf* (pp. 322–326). pp. 322–326.

Partovi, S., Loebe, M., Aschwanden, M., Baldi, T., Jäger, K., Feinstein, B., and Staub, D. (2012) 'Contrast-enhanced ultrasound for assessing carotid atherosclerotic plaque lesions.' *American Journal of Roentgenology*, *198*(1), 13–19. https://doi.org/10.2214/AJR.11.7312

Pereira, T., Maldonado, J., Pereira, L., and Conde, J. (2001) 'Aortic stiffness is an independent predictor of stroke in hypertensive patients.' *Arquivos Brasileiros de Cardiologia*, *37*(5), 437–443. https://doi.org/10.5935/abc.20130079

Pomella, N., Wilhelm, N., Kolyva, C., González-Alonso, J., Rakobowchuk, M., and Khir, W. (2017a) 'Common Carotid Artery Diameter, Blood Flow Velocity and Wave Intensity Responses at Rest and during Exercise in Young Healthy Humans: A Reproducibility Study.' *Ultrasound in Medicine and Biology*, *43*(5), 943–957. https://doi.org/10.1016/j.ultrasmedbio.2016.12.018

Pomella, N., Wilhelm, N., Kolyva, C., González-Alonso, J., Rakobowchuk, M., and Khir, W. (2017b) 'Common Carotid Artery Diameter, Blood Flow Velocity and Wave Intensity Responses at Rest and during Exercise in Young Healthy Humans: A Reproducibility Study.' *Ultrasound in Medicine & Biology*, *43*(5), 943–957. https://doi.org/10.1016/j.ultrasmedbio.2016.12.018

Quail, A., Knight, S., Steeden, A., Taelman, L., Moledina, S., Taylor, M., Segers, P., Coghlan, J., and Muthurangu, V. (2015) 'Noninvasive pulmonary artery wave intensity analysis in pulmonary hypertension.' *American Journal of Physiology - Heart and Circulatory Physiology*, *308*(12), H1603–H1611. https://doi.org/10.1152/ajpheart.00480.2014

Rabben, I., Stergiopulos, N., Hellevik, R., Smiseth, A., Slørdahl, S., Urheim, S., and Angelsen, B. (2004) 'An ultrasound-based method for determining pulse wave velocity in superficial arteries.' *Journal of Biomechanics*, *37*(10), 1615–1622. https://doi.org/10.1016/j.jbiomech.2003.12.031

Raphael, E., Cooper, R., Parker, K., Collinson, J., Vassiliou, V., Pennell, J., De Silva, R., Hsu, Y., Greve, M., Nijjer, S., Broyd, C., Ali, A., Keegan, J., Francis, P., Davies, E., Hughes, D., Arai, A., Frenneaux, M., Stables, H., Di Mario, C., and Prasad, K. (2016) 'Mechanisms of Myocardial Ischemia in Hypertrophic Cardiomyopathy: Insights From Wave Intensity Analysis and Magnetic Resonance.' *Journal of the American College of Cardiology*, *68*(15), 1651–1660. https://doi.org/10.1016/j.jacc.2016.07.751

Raphael, E., Keegan, J., Parker, K., Simpson, R., Collinson, J., Vassiliou, V., Wage, R., Drivas, P., Strain, S., Cooper, R., de Silva, R., Stables, R., Di Mario, C., Frenneaux, M., Pennell, J., Davies, E., Hughes, D., Firmin, D., and Prasad, K. (2017) 'Feasibility of cardiovascular magnetic resonance derived coronary wave intensity analysis.' *Journal of Cardiovascular Magnetic Resonance*, *18*(1), 93. https://doi.org/10.1186/s12968-016-0312-8

Razavi, A., Shirani, E., and Sadeghi, R. (2011) 'Numerical simulation of blood pulsatile flow in a stenosed carotid artery using different rheological models.' *Journal of Biomechanics*, *44*(11), 2021–2030. https://doi.org/10.1016/j.jbiomech.2011.04.023

ROSS, R. (1999) 'Atherosclerosis: An inflammatory disease.' *The New England Journal of Medicine.*, *340*(2), 115–126. https://doi.org/10.2174/138161212802481237

Roth, A., Johnson, C., Abajobir, A., Abd-Allah, F., Abera, F., Abyu, G., Ahmed, M., Aksut, B., Alam, T., Alam, K., Alla, F., Alvis-Guzman, N., Amrock, S., Ansari, H., Ärnlöv, J., Asayesh, H., Atey, M., Avila-Burgos, L., Awasthi, A., Banerjee, A., Barac, A., Bärnighausen, T., Barregard, L., Bedi, N., Belay Ketema, E., Bennett, D., Berhe, G., Bhutta, Z., Bitew, S., Carapetis, J., Carrero, J., Malta, C., Castañeda-Orjuela, A., Castillo-Rivas, J., Catalá-López, F., Choi, Y., Christensen, H., Cirillo, M.,

Cooper, L., Criqui, M., Cundiff, D., Damasceno, A., Dandona, L., Dandona, R., Davletov, K., Dharmaratne, S., Dorairaj, P., Dubey, M., Ehrenkranz, R., El Sayed, M., Faraon, A., Esteghamati, A., Farid, T., Farvid, M., Feigin, V., Ding, L., Fowkes, G., Gebrehiwot, T., Gillum, R., Gold, A., Gona, P., Gupta, R., Habtewold, D., Hafezi-Nejad, N., Hailu, T., Hailu, B., Hankey, G., Hassen, Y., Abate, H., Havmoeller, R., Hay, I., Horino, M., Hotez, J., Jacobsen, K., James, S., Javanbakht, M., Jeemon, P., John, D., Jonas, J., Kalkonde, Y., Karimkhani, C., Kasaeian, A., Khader, Y., Khan, A., Khang, H., Khera, S., Khoja, T., Khubchandani, J., Kim, D., Kolte, D., Kosen, S., Krohn, J., Kumar, A., Kwan, F., Lal, K., Larsson, A., Linn, S., Lopez, A., Lotufo, A., El Razek, A., Malekzadeh, R., Mazidi, M., Meier, T., Meles, G., Mensah, G., Meretoja, A., Mezgebe, H., Miller, T., Mirrakhimov, E., Mohammed, A., Moran, E., Musa, I., Narula, J., Neal, B., Ngalesoni, F., Nguyen, G., Obermeyer, M., Owolabi, M., Patton, G., Pedro, J., Qato, D., Qorbani, M., Rahimi, K., Rai, K., Rawaf, S., Ribeiro, A., Safiri, S., Salomon, A., Santos, I., Santric Milicevic, M., Sartorius, B., Schutte, A., Sepanlou., Shaikh, A., Shin, J., Shishehbor, M., Shore, H., Silva, S., Sobngwi, E., Stranges, S., Swaminathan, S., Tabarés-Seisdedos, R., Tadele Atnafu, N., Tesfay, F., Thakur, S., Thrift, A., Topor-Madry, R., Truelsen, T., Tyrovolas, S., Ukwaja, N., Uthman, O., Vasankari, T., Vlassov, V., Vollset, E., Wakayo, T., Watkins, D., Weintraub, R., Werdecker, A., Westerman, R., Wiysonge, S., Wolfe, C., Workicho, A., Xu, G., Yano, Y., Yip, P., Yonemoto, N., Younis, M., Yu, C., Vos, T., and Naghavi, C. (2017) 'Global, Regional, and National Burden of Cardiovascular Diseases for 10 Causes, 1990 to 2015.' *Journal of the American College of Cardiology*, *70*(1), 1–25. https://doi.org/10.1016/j.jacc.2017.04.052

Saba, L., Anzidei, M., Marincola, C., Piga, M., Raz, E., Bassareo, P., Napoli, A., Mannelli, L., Catalano, C., and Wintermark, M. (2014) 'Imaging of the carotid artery vulnerable plaque.' *CardioVascular and Interventional Radiology*, *37*(3), 572–585. https://doi.org/10.1007/s00270-013-0711-2

Sage, H., and Bornstein, P. (1979) 'Characterization of a Novel Collagen Chain in Human Placenta and Its Relation to AB Collagen.' AB AND COLLAGEN, *18*(17), 3815–3822.

Saremi, A., Anderson, R. J., Luo, P., Moritz, T. E., Schwenke, D. C., Allison, M., and Reaven, P. D. (2009). 'Association between IL-6 and the extent of coronary atherosclerosis in the veterans affairs diabetes trial (VADT).' *Atherosclerosis*, *203*(2), 610–614. https://doi.org/10.1016/j.atherosclerosis.2008.07.031

Sasu, C., Ciutan, M., Scîntee, G., Muşat, S., and Diaconescu, R. (2016) 'Potentially Life-threatening Vascular Events (Myocardial and Cerebral Infarction) - Geographical Distribution and Temporal Evolution in Romania.' *Procedia Environmental Sciences*, *32*, 327–336. https://doi.org/10.1016/j.proenv.2016.03.038

Schindler, A., Schinner, R., Altaf, N., Hosseini, A., Simpson, J., Esposito-Bauer, L., Singh, N., Kwee, M., Kurosaki, Y., Yamagata, S., Yoshida, K., Miyamoto, S., Maggisano, R., Moody, R., Poppert, H., Kooi, E., Auer, P., Bonati, H., and Saam, T. (2020) 'Prediction of Stroke Risk by Detection of Hemorrhage in Carotid Plaques: Meta-Analysis of Individual Patient Data.' *JACC: Cardiovascular Imaging*, *13*(2), 395–406. https://doi.org/10.1016/j.jcmg.2019.03.028

Schinkel, L., Bosch, G., Staub, D., Adam, D., and Feinstein, B. (2020) 'Contrast-Enhanced Ultrasound to Assess Carotid Intraplaque Neovascularization.' *Ultrasound in Medicine and Biology*, *46*(3), 466–478. https://doi.org/10.1016/j.ultrasmedbio.2019.10.020

Shimada, H., Ogata, T., Takano, K., Abe, H., Higashi, T., Yamashita, T., Matsunaga, A., and Inoue, T. (2018) 'Evaluation of the Time-Dependent Changes and the Vulnerability of Carotid Plaques Using Contrast-Enhanced Carotid Ultrasonography.' *Journal of Stroke and Cerebrovascular Diseases*, *27*(2), 321–325. https://doi.org/10.1016/j.jstrokecerebrovasdis.2017.09.010

Silverman-Gavrila, R., Silverman-Gavrila, L., and Bendeck, M. P. (2013). 'Cell division fidelity is altered during the vascular response to injury: Its novel role in atherosclerosis progression.' *American*

Journal of Pathology, *182*(3), 628–639. https://doi.org/10.1016/j.ajpath.2012.11.007

Stroke Association. State of the nation: Stroke statistics. , Stroke Association 40 (2018).

Sugawara, M., Niki, K., Ohte, N., Okada, T., and Harada, A. (2009) 'Clinical usefulness of wave intensity analysis.' *Medical and Biological Engineering and Computing*, *47*(2), 197–206. https://doi.org/10.1007/s11517-008-0388-x

Sun, J., Zhao, Q., Balu, N., Neradilek, B., Isquith, A., Yamada, K., Cantón, G., Crouse, R., Anderson, J., Huston, J., O'Brien, K., Hippe, S., Polissar, L., Yuan, C., and Hatsukami, S. (2017) 'Carotid Plaque Lipid Content and Fibrous Cap Status Predict Systemic CV Outcomes: The MRI Substudy in AIM-HIGH.' *JACC: Cardiovascular Imaging*, *10*(3), 241–249. https://doi.org/10.1016/j.jcmg.2016.06.017

Sun, Y., Anderson, T. J., Parker, K. I. M. H., Tyberg, J. V, Anderson, T. J., Parker, K. H., and Tyberg, J. V. (2000). 'cutting-edge report.' *J Appl Physiol*, *1*(89), 1636–1644.

Takano, M., Mizuno, K., Okamatsu, K., Yokoyama, S., Ohba, T., and Sakai, S. (2001) 'Mechanical and structural characteristics of vulnerable plaques: Analysis by coronary angioscopy and intravascular ultrasound.' *Journal of the American College of Cardiology*, *38*(1), 99–104. https://doi.org/10.1016/S0735-1097(01)01315-8

Tamaru, H., Fujii, K., Fukunaga, M., Imanaka, T., Kawai, K., Miki, K., Horimatsu, T., Nishimura, M., Saita, T., Sumiyoshi, A., Shibuya, M., Masuyama, T., and Ishihara, M. (2021) 'Mechanisms of gradual pressure drop in angiographically normal left anterior descending and right coronary artery: Insights from wave intensity analysis.' *Journal of Cardiology*, (xxxx), 1–7. https://doi.org/10.1016/j.jjcc.2021.01.006

Taylor, A., and Figueroa, A. (2009) 'Patient-specific modeling of cardiovascular mechanics.' *Annual Review of Biomedical Engineering*, *11*, 109–134. https://doi.org/10.1146/annurev.bioeng.10.061807.160521

Teng, Z., Zhang, Y., Huang, Y., Feng, J., Yuan, J., Lu, Q., Sutcliffe, F., Brown, J., Jing, Z., and Gillard, J. H. (2014) 'Material properties of components in human carotid atherosclerotic plaques: A uniaxial extension study.' *Acta Biomaterialia*, *10*(12), 5055–5063. https://doi.org/10.1016/j.actbio.2014.09.001

Tuenter, A., Selwaness, M., Lorza, A., Schuurbiers, H., Speelman, L., Vernooij, W., and Wentzel, J. (2016) 'High shear stress relates to intraplaque haemorrhage in asymptomatic carotid plaques.' *Atherosclerosis*, 1–7. https://doi.org/10.1016/j.atherosclerosis.2016.05.018

Underhill, R., Hatsukami, S., Cai, J., Yu, W., DeMarco, K., Polissar, L., Ota, H., Zhao, X., Dong, L., Oikawa, M., and Yuan, C. (2010) 'A noninvasive imaging approach to assess plaque severity: The carotid atherosclerosis score.' *American Journal of Neuroradiology*, *31*(6), 1068–1075. https://doi.org/10.3174/ajnr.A2007

Van Den Oord, H., Akkus, Z., Renaud, G., Bosch, G., Van Der Steen, W., Sijbrands, G., and Schinkel, L. (2014) 'Assessment of carotid atherosclerosis, intraplaque neovascularization, and plaque ulceration using quantitative contrast-enhanced ultrasound in asymptomatic patients with diabetes mellitus.' *European Heart Journal Cardiovascular Imaging*, *15*(11), 1213–1218. https://doi.org/10.1093/ehjci/jeu127

Van Der Giessen, A. G., Gijsen, F. J. H., Wentzel, J. J., Jairam, P. M., Van Walsum, T., Neefjes, L. A. E., and Van Der Steen, A. F. W. (2011). 'Small coronary calcifications are not detectable by 64-slice contrast enhanced computed tomography.' *International Journal of Cardiovascular Imaging*, *27*(1), 143–152. https://doi.org/10.1007/s10554-010-9662-8

van der Wal, A. (1999) 'Atherosclerotic plaque rupture – pathologic basis of plaque stability and instability.' *Cardiovascular Research*, *41*(2), 334–344. https://doi.org/10.1016/S0008-6363(98)00276-4

Virmani, R., Kolodgie, D., Burke, P., Farb, A., and Schwartz, M. (2000) 'Lessons from sudden coronary death: A comprehensive morphological classification scheme for atherosclerotic lesions.' *Arteriosclerosis & Thrombosis*, 1262–1275. https://doi.org/10.1161/01.ATV.20.5.1262

Vulliémoz, S., Stergiopulos, N., and Meuli, R. (2002) 'Estimation of local aortic elastic properties with MRI.' *Magnetic Resonance in Medicine*, *47*(4), 649–654. https://doi.org/10.1002/mrm.10100

Wasserman, A., Wityk, J., Trout, H., and Virmani, R. (2005) 'Low-grade carotid stenosis: Looking beyond the lumen with MRI.' *Stroke*, *36*(11), 2504–2513. https://doi.org/10.1161/01.STR.0000185726.83152.00

Weber, C., and Noels, H. (2011) 'Atherosclerosis: current pathogenesis and therapeutic option.' *nature medicine, 17*(11), 1410–1422.

Xiao, H., Qi, L., Xu, L., Li, D., Hu, B., Zhao, P., Ren, H., and Huang, J. (2019) 'Estimation of wave reflection in aorta from radial pulse waveform by artificial neural network: a numerical study.' *Computer Methods and Programs in Biomedicine*, *182*. https://doi.org/10.1016/j.cmpb.2019.105064

Xu, D., Hippe, S., Underhill, R., Oikawa-Wakayama, M., Dong, L., Yamada, K., Yuan, C., and Hatsukami, S. (2014) 'Prediction of high-risk plaque development and plaque progression with the carotid atherosclerosis score.' *JACC: Cardiovascular Imaging*, *7*(4), 366–373. https://doi.org/10.1016/j.jcmg.2013.09.022

Yi-Hui, S., Anderson, T., Parker, K., and Tyberg, J. (2000) ' Wave-intensity analysis: a new approach to coronary hemodynamics.' *J Appl Physiol*, *1*(89), 1636–1644.

Zhang, Q., Qiao, H., Dou, J., Sui, B., Zhao, X., Chen, Z., Wang, Y., Chen, S., Lin, M., Chiu, B., Yuan, C., Li, R., and Chen, H. (2019) 'Plaque components segmentation in carotid artery on simultaneous non-contrast angiography and intraplaque hemorrhage imaging using machine learning.' *Magnetic Resonance Imaging*, *60*(December 2018), 93–100. https://doi.org/10.1016/j.mri.2019.04.001

Ziegler, M., Good, E., Engvall, J., Warntjes, M., de Muinck, E., and Dyverfeldt, P. (2020) 'Towards Automated Quantification of Vessel Wall Composition Using MRI.' *Journal of Magnetic Resonance Imaging*, *52*(3), 710–719. https://doi.org/10.1002/jmri.27116

Publications & Presentations

Publications

- Abdulsalam, M., and J. Feng. 2019 'Distinguish the Stable and Unstable Plaques Based on Arterial Waveform Analysis.' Procedia Structural Integrity, 15: 2–7. https://doi.org/10.1016/j.prostr.2019.07.002. **(Chapter 4)**
- Abdulsalam, M. and Feng, J. (2021) 'The composition of vulnerable plaque and its effect on arterial waveforms.' Journal of the Mechanical Behavior of Biomedical Materials. Elsevier Ltd, 119(February), p. 104491. doi: 10.1016/j.jmbbm.2021.104491. **(Part of Chapter 5)**

Presentations

- Biomedical Engineering Research Seminar Manchester Metropolitan University - Online (Jan 2021)
- The 1st Virtual European Conference on Fracture (VECF1) - Online (Jun 2020)
- The 5th European Stroke Organisation Conference ESOC – Italy (April 2019)
- The International Conference on Stents: Materials, Mechanics and Manufacturing ICS3M – London (July 2019)
- Manchester Metropolitan University Post-Graduate Research Conference 2017